UNIVERSITÀ DEGLI STUDI DI MODENA E REGGIO EMILIA

DIPARTIMENTO DI SCIENZE BIOMEDICHE, METABOLICHE E NEUROSCIENZE

DOTTORATO DI RICERCA IN NEUROSCIENZE

in convenzione con l'Università degli Studi di Parma

Settore scientifico disciplinare BIO 09/ Fisiologia

Tesi per il conseguimento del titolo

Generation and characterization of human mesencephalic dopaminergic neurons derived from induced pluripotent stem cells as a tool to develop new therapeutics for Parkinson's-related disorders

Coordinatore:
Chiar.mo Prof. Michele Zoli

Relatore:
Chiar.mo Prof. Michele Zoli

Dottoranda:
Dott.ssa Laura Cavalleri

Matricola:
136791

XXXIV Ciclo
2018-2021

Index

Abstract in English

The degeneration of dopaminergic (DA) neurons of the ventral mesencephalon is considered one of the hallmarks in Parkinson's disease (PD) and Parkinsonism. Their susceptibility to damage and their adaptability and plasticity were initially studied in animal models in order to understand the cellular and molecular mechanisms and the action of pharmacological therapeutics. The recent introduction of human inducible pluripotent stem cells (iPSCs) technology and the development of protocols for their differentiation into neurons with a DA phenotype has permitted the direct evaluation of cellular mechanisms of PD and Parkinsonism, the mechanism of action of anti-parkinsonian drugs and the exploratory applications of various aspects of cell therapy.

The aim of this thesis was the generation and phenotypic characterization of human DA neurons amenable to be used as a tool for the development of a variety of therapeutic devices based on cell therapy. In order to achieve high quality and reproducible human DA neuron precursors that are able to differentiate and mature into functional DA neurons, this work was subdivided in four main subprojects.

The first subproject was dedicated to the optimization of the methods of differentiation of human iPSCs into mesencephalic DA neuron precursors using a previously published protocol (Fedele et al. 2017). This protocol offers the advantage of generating a large number of homogeneous midbrain floor plate progenitors (mFPPs) that can be expanded for several passages and stored in liquid nitrogen for any future use. For the optimization of this protocol, one hiPSC clone generated from a healthy donor (Collo et al. 2018), was differentiated into mFPPs. Cells were passaged for at least 4 passages and were stored in liquid nitrogen at each passage for the future uses. mFPPs were characterized by the expression of two typical markers of midbrain differentiation: the floor plate marker FOXA2 and the roof plate marker LMX1α. mFPPs were induced to differentiate into mature DA neurons up to 70 days *in vitro* in order to reach a complete maturation. At this stage, a full phenotypic and molecular characterization was performed. DA neurons co-expressed the tyrosine hydroxylase (TH) and the dopamine transporter (DAT) markers and formed a functional network with GABAergic and glutamatergic neurons, as stated by immunofluorescence. The DA neuronal maturity was confirmed by electrophysiology, studying the spontaneous action potentials, and by HPLC analysis, studying the release of DA.

The second subproject was dedicated to the investigation of the pharmacological response to two dopaminergic agonists (i.e., pramipexole and piribedil) currently used for the treatment of PD.

Recent data have demonstrated a neurotrophic effect produced by an anti-parkinsonian DA D2/D3 receptor (D2R/D3R) agonist, ropinirole (Collo et al. 2018). Based on these findings, the cellular and molecular effects of pramipexole and piribedil on human DA neurons were evaluated by studying morphological changes related to structural plasticity and the activation of intracellular pathways. DA neurons derived from hiPSCs were exposed to piribedil and pramipexole for 72 hours. Piribedil and pramipexole (0.01-20 μM) produced a dose-dependent effect on structural plasticity 72 hrs after the beginning of treatment when measured on three structural plasticity parameters (maximal length of dendrites, number of primary dendrites and soma area). The effect of piribedil (10 μM) on hiPSC-derived DA neurons was studied on the phosphorylation of p70S6K, one of the main substrates of the activated mammalian target of rapamycin complex 1 (mTORC1), by western blot and immunofluorescence analysis. Piribedil significantly increased phosphorylated p70S6K (p-p70S6K) after 2 min. The involvement of MEK-ERK, PI3K-Akt and mTOR pathways in mediating the effects of piribedil on p-p70S6K was studied using the MEK inhibitor PD98059, the PI3-K inhibitor LY294002 and the mTORC1 inhibitor rapamycin. Pretreatments (20 minutes) with each inhibitor separately blocked the effects of piribedil. The role of intracellular signaling leading to mTOR pathway activation in structural plasticity of DA neurons induced by piribedil and pramipexole was investigated using the same kinase inhibitors of the intracellular pathways. Pretreatments with PD98059, LY294002 and rapamycin significantly counteracted the effects of piribedil and pramipexole on all three structural plasticity parameters. The role of D3R in mediating p-p70S6K and structural plasticity of DA neurons induced by piribedil was investigated by pretreatments with two selective D3R antagonists SB277011-A and S33084. Both antagonists significantly attenuated the increase of p-p70S6K produced by piribedil as measured by western blot and immunofluorescence analysis in DA neuronal cultures 2 min after exposure. The role of D3R-dependent signaling in structural plasticity produced by piribedil and pramipexole was assessed 72 hrs after the pharmacological blockade of D3R. Pretreatments with SB277011-A and S33084 significantly counteracted the effects of piribedil and pramipexole on all three structural plasticity parameters. The blockade of BDNF-TrkB signaling in DA neurons prevented structural plasticity induced by piribedil and pramipexole. The BDNF-TrkB signaling inhibitors used were an anti-BDNF blocking antibody (α-BDNF), a TrkB-Fc Chimera, a TrkB receptor blocker K252a and a Src phosphorylation inhibitor PP2. DA neurons were pretreated with the BDNF-TrkB signaling inhibitors before exposing to piribedil or pramipexole. All the inhibitors antagonized the effects of piribedil and pramipexole on all three structural plasticity parameters. The neuroprotective and neuroregenerative properties of these two pharmacological agents were also studied. In a first set

of experiments, DA neurons were pretreated with piribedil or pramipexole for 48 hrs before exposing to 6-OHDA for 24 hrs. Both piribedil and pramipexole significantly counteracted the effects of 6-OHDA on all three structural plasticity parameters. In a second set of experiments, DA neurons were pretreated with 6-OHDA before exposing to piribedil or pramipexole. Both piribedil and pramipexole significantly counteracted the effects of 6-OHDA on all three structural plasticity parameters.

The third subproject was dedicated to the study of the effects of the electrical stimulation on the structural plasticity of DA neurons derived from hiPSCs. Several reports have shown that electrical stimulation can promote neuronal differentiation and neurite growth of various neuronal cell types *in vitro*, including rat pheochromocytoma cells PC12 (Jing et al. 2019), murine neuroblastoma cells N2 (Pelletier SJ et al. 2014) and human neural stem cells (Stewart et al. 2015). The structural plasticity effects of electrical stimulation were studied on hiPSC-derived DA neurons. DA neurons were exposed to a current with amplitude of respectively 0 mA, 1 mA, 2 mA or 4 mA, 2 hours/day for 3 days. This repeated electric stimulation produced a dose-dependent structural plasticity effect on DA neurons. This effect was characterized by a significant increase of the maximal length of dendrites, number of primary dendrites and soma area.

The fourth subproject was dedicated to the generation of human iPSCs from peripheral blood mononuclear cells (PBMCs) donated from a novel set of healthy controls and patients affected by a Parkinsonism, i.e., the multiple system atrophy (MSA). The iPSC clones obtained from the control and the patient underwent a phenotypic characterization to examine the presence of pluripotency markers by immunofluorescence and quantitative PCR analysis, karyotype analysis, pluripotency and trilineage differentiation potential. The iPSCs were subsequently differentiated into mesencephalic DA neurons and assessed for their pharmacological response to dopaminergic agonists. PBMCs from healthy subjects and MSA patients were isolated from peripheral blood and were reprogrammed using the Cytotune reprogramming kit. After the reprogramming period, numerous emerging colonies were identified, picked, dissociated, transferred and expanded. After several passages, four clones for MSA1, two clones from MSA2 and four clones for MSAC1 were selected, further expanded and cryobanked. One representative clone for MSAC1 (MSAC1-12) and one representative clone for MSA1 (MSA1-8) were used in this study. MSAC1-12 and MSA1-8 hiPSC clones exhibit a hESC-like morphology. Both hiPSC clones expressed the pluripotency markers Oct3/4, Sox2 and Nanog by immunofluorescence. Real-time PCR confirmed the expression of the pluripotency genes Oct4, Sox2 and Nanog. Analysis of the karyotype of the two hiPSC clones showed

a normal karyotype with no chromosomal aberrations. The pluripotency potential of the two hiPSC clones was examined *in vitro* by embryoid body formation and differentiation into cells of the three germ layers. Immunofluorescence analysis showed endodermal cells expressing α-fetoprotein (AFP), mesodermal cells expressing smooth muscle actin (SMA) and brachyury, and ectodermal cells expressing PAX6 and βIII Tubulin. Real-time PCR confirmed the expression of markers of the three germ layers. MSAC1-12 and MSA1-8 were induced to generate mFPPs. mFPPs were passaged for at least 4 passages and stored in liquid nitrogen at each passage. MSAC1-12 and MSA1-8 mFPPs showed the co-expression of FOXA2 and LMX1α as confirmed by immunofluorescence analysis. mFPPs were then induced to differentiate into DA neurons. In a preliminary experiment, the structural plasticity effects produced by D2R/D3R agonists ropinirole and pramipexole in DA neurons differentiated from MSAC1-12 and MSA1-8 iPSCs were evaluated by studying morphological changes. MSAC1-12 and MSA1-8 DA neurons were exposed to ropinirole and pramipexole for 72 hrs. Ropinirole and pramipexole produced a significant effect on structural plasticity when measured on all three structural plasticity parameters.

Abstract in Italian

La degenerazione dei neuroni dopaminergici (DA) del mesencefalo ventrale è considerata uno dei segni distintivi della malattia di Parkinson (PD) e del parkinsonismo. La loro suscettibilità al danno e la loro adattabilità e plasticità sono state inizialmente studiate in modelli animali per comprendere i meccanismi cellulari e molecolari e l'azione delle terapie farmacologiche. La recente introduzione della tecnologia delle cellule staminali pluripotenti indotte umane (iPSCs) e lo sviluppo di protocolli per la loro differenziazione in neuroni con un fenotipo DA ha permesso la valutazione diretta dei meccanismi cellulari della malattia di Parkinson e del parkinsonismo, il meccanismo d'azione dei farmaci antiparkinsoniani e le applicazioni esplorative di vari aspetti della terapia cellulare.

Lo scopo di questa tesi è la generazione e la caratterizzazione fenotipica di neuroni DA umani utilizzabili come strumento per lo sviluppo di una varietà di dispositivi terapeutici basati sulla terapia cellulare. Al fine di ottenere precursori di neuroni DA umani di alta qualità e riproducibili, in grado di differenziarsi e maturare in neuroni DA funzionali, questo lavoro è stato suddiviso in quattro sottoprogetti principali.

Il primo sottoprogetto è stato dedicato all'ottimizzazione dei metodi di differenziamento delle iPSCs umane in precursori di neuroni DA mesencefalici utilizzando un protocollo precedentemente pubblicato (Fedele et al. 2017). Questo protocollo offre il vantaggio di generare un gran numero di progenitori mesencefalici (mFPPs) che possono essere espansi per diversi passaggi e crioconservati in azoto liquido per qualsiasi uso futuro. Per l'ottimizzazione di questo protocollo, un clone di hiPSCs generato da un donatore sano è stato differenziato in mFPPs (Collo et al. 2018). Le cellule sono state passate per almeno 4 passaggi e ad ogni passaggio sono state congelate in azoto liquido per usi futuri. I mFPPs sono caratterizzati dall'espressione di due marker tipici del differenziamento del mesencefalo: il floor plate marker FOXA2 e il roof plate marker LMX1α. I mFPPs sono stati indotti a differenziare in neuroni DA maturi fino a 70 giorni *in vitro* per raggiungere una maturazione completa. In questa fase, è stata eseguita una caratterizzazione fenotipica e molecolare completa. I neuroni DA co-esprimevano i marcatori della tirosina idrossilasi (TH) e del trasportatore della dopamina (DAT) e formavano una rete funzionale con i neuroni GABAergici e glutamatergici, come dimostrato dall'immunofluorescenza. La maturità neuronale DA è stata confermata mediante elettrofisiologia, studiando i potenziali d'azione spontanei, e dall'analisi HPLC, studiando il rilascio di DA.

Il secondo sottoprogetto è stato dedicato allo studio della risposta farmacologica a due agonisti dopaminergici (pramipexolo e piribedil) attualmente utilizzati per il trattamento del PD. Dati recenti hanno dimostrato un effetto neurotrofico prodotto da un agonista antiparkinsoniano del recettore DA D2/D3 (D2R/D3R), il ropinirolo (Collo et al. 2018). Sulla base di questi risultati, sono stati valutati gli effetti cellulari e molecolari di pramipexolo e piribedil sui neuroni DA umani studiando i cambiamenti morfologici legati alla plasticità strutturale e all'attivazione delle vie intracellulari. I neuroni DA derivati dalle hiPSCs sono stati esposti a piribedil e pramipexolo per 72 ore. Piribedil e pramipexolo (0,01-20 μM) hanno prodotto un effetto dose-dipendente sulla plasticità strutturale 72 ore dopo l'inizio del trattamento, effetto valutato su tre parametri di plasticità strutturale (lunghezza massima dei dendriti, numero di dendriti primari e area del soma). L'effetto del piribedil (10 μM) sui neuroni DA derivati dalle hiPSCs è stato studiato sulla fosforilazione di p70S6K, uno dei principali substrati del mammalian target of rapamycin complex 1 (mTORC1), mediante western blot e analisi in immunofluorescenza. Il piribedil ha aumentato significativamente la p70S6K fosforilata (p-p70S6K) dopo 2 min. Il coinvolgimento dei pathway di MEK-ERK, PI3K-Akt e mTOR nella mediazione degli effetti del piribedil sulla p-p70S6K è stato studiato utilizzando l'inibitore di MEK PD98059, l'inibitore di PI3-K LY294002 e l'inibitore di mTORC1 rapamicina. I pretrattamenti (20 minuti) con ciascun inibitore utilizzato separatamente hanno bloccato gli effetti del piribedil. Il ruolo del signalling intracellulare che porta all'attivazione del pathway di mTOR nella plasticità strutturale dei neuroni DA indotta dal piribedil e dal pramipexolo è stato studiato utilizzando gli stessi inibitori. I pretrattamenti con PD98059, LY294002 e rapamicina hanno contrastato significativamente gli effetti del piribedil e del pramipexolo su tutti e tre i parametri di plasticità strutturale. Il ruolo del D3R nella mediazione della p-p70S6K e della plasticità strutturale dei neuroni DA indotti dal piribedil è stato studiato mediante pretrattamenti con due antagonisti selettivi del D3R SB277011-A e S33084. Entrambi gli antagonisti hanno attenuato significativamente l'aumento della p-p70S6K prodotto dal piribedil in colture neuronali DA 2 minuti dopo l'esposizione, effetto valutato mediante western blot e analisi in immunofluorescenza. Il ruolo del signalling D3R-dipendente nella plasticità strutturale prodotta dal piribedil e dal pramipexolo è stato valutato 72 ore dopo il blocco del D3R. I pretrattamenti con SB277011-A e S33084 hanno contrastato significativamente gli effetti del piribedil e del pramipexolo su tutti e tre i parametri di plasticità strutturale. Il blocco del signalling di BDNF-TrkB nei neuroni DA ha inibito la plasticità strutturale indotta dal piribedil e dal pramipexolo. Gli inibitori del signalling di BDNF-TrkB utilizzati sono un anticorpo bloccante anti-BDNF (α-BDNF), una chimera TrkB-Fc, un bloccante del recettore TrkB K252a e un inibitore della fosforilazione di Src PP2. I neuroni DA sono stati pretrattati con gli inibitori del signaling di BDNF-

TrkB prima dell'esposizione al piribedil o al pramipexolo. Tutti gli inibitori hanno antagonizzato gli effetti del piribedil e del pramipexolo su tutti e tre i parametri di plasticità strutturale. Sono state inoltre studiate le proprietà neuroprotettive e neurorigenerative di questi due agenti farmacologici. In una prima serie di esperimenti, i neuroni DA sono stati pretrattati con il piribedil o con il pramipexolo per 48 ore prima di essere esposti a 6-OHDA per 24 ore. Sia il piribedil che il pramipexolo hanno contrastato significativamente gli effetti della 6-OHDA su tutti e tre i parametri di plasticità strutturale. In una seconda serie di esperimenti, i neuroni DA sono stati pretrattati con 6-OHDA prima dell'esposizione al piribedil o al pramipexolo. Sia il piribedil che il pramipexolo hanno contrastato significativamente gli effetti della 6-OHDA su tutti e tre i parametri di plasticità strutturale.

Il terzo sottoprogetto è stato dedicato allo studio degli effetti della stimolazione elettrica sulla plasticità strutturale dei neuroni DA derivati dalle hiPSCs. Diversi lavori hanno dimostrato che la stimolazione elettrica può promuovere la differenziazione neuronale e la crescita dei neuriti di vari tipi di cellule neuronali *in vitro*, comprese le cellule di feocromocitoma di ratto PC12 (Jing et al. 2019), le cellule di neuroblastoma murino N2 (Pelletier SJ et al. 2014) e le cellule neurali staminali umane (Stewart et al. 2015). Gli effetti sulla plasticità strutturale della stimolazione elettrica sono stati studiati sui neuroni DA derivati dalle hiPSCs. I neuroni DA sono stati esposti a una corrente rispettivamente di 0 mA, 1 mA, 2 mA o 4 mA, 2 ore/giorno per 3 giorni. Questa stimolazione elettrica ripetuta ha prodotto un effetto sulla plasticità strutturale dose-dipendente sui neuroni DA. Questo effetto era caratterizzato da un aumento significativo della lunghezza massima dei dendriti, del numero dei dendriti primari e dell'area del soma.

Il quarto sottoprogetto è stato dedicato alla generazione di iPSCs umane da cellule mononucleate del sangue periferico (PBMCs) donate da un nuovo set di controlli sani e pazienti affetti da un parkinsonismo, ovvero l'atrofia multisistemica (MSA). I cloni iPSCs ottenuti dal controllo e dal paziente sono stati sottoposti a una caratterizzazione fenotipica per esaminare la presenza di marcatori di pluripotenza mediante immunofluorescenza, PCR quantitativa, analisi del cariotipo, pluripotenza e capacità di differenziazione nei tre foglietti embrionali. Le iPSCs sono state successivamente differenziate in neuroni DA mesencefalici e valutate per la loro risposta farmacologica agli agonisti dopaminergici. I PBMCs di soggetti sani e pazienti affetti da MSA sono stati isolati dal sangue periferico e sono stati riprogrammati utilizzando il kit di riprogrammazione Cytotune. Dopo il periodo di riprogrammazione, numerose colonie sono state identificate, raccolte, dissociate, trasferite ed espanse. Dopo diversi passaggi, sono stati selezionati quattro cloni per

MSA1, due cloni per MSA2 e quattro cloni per MSAC1, ulteriormente espansi e crioconservati. In questo studio sono stati utilizzati un clone rappresentativo per MSAC1 (MSAC1-12) e un clone rappresentativo per MSA1 (MSA1-8). I cloni hiPSCs MSAC1-12 e MSA1-8 mostrano una morfologia simile alle hESCs. Entrambi i cloni hanno espresso i marcatori di pluripotenza Oct3/4, Sox2 e Nanog mediante immunofluorescenza. La real-time PCR ha confermato l'espressione dei geni di pluripotenza Oct4, Sox2 e Nanog. L'analisi del cariotipo dei due cloni ha mostrato un cariotipo normale senza aberrazioni cromosomiche. La pluripotenza dei due cloni è stata esaminata *in vitro* mediante formazione di corpi embrionali e loro differenziamento in cellule dei tre foglietti embrionali. L'analisi in immunofluorescenza ha mostrato cellule endodermiche che esprimono l'α-fetoproteina (AFP), cellule mesodermiche che esprimono l'actina muscolare liscia (SMA) e brachyury, e cellule ectodermiche che esprimono PAX6 e βIII tubulina. La real-time PCR ha confermato l'espressione dei marcatori dei tre foglietti embrionali. MSAC1-12 e MSA1-8 sono stati indotti a generare i mFFPs. I mFFPs sono stati passati per almeno 4 passaggi e crioconservati in azoto liquido ad ogni passaggio. I mFFPs MSAC1-12 e MSA1-8 hanno mostrato la coespressione di FOXA2 e LMX1α come confermato dall'analisi in immunofluorescenza. I mFFPs sono stati quindi indotti a differenziare in neuroni DA. In un esperimento preliminare, sono stati valutati gli effetti sulla plasticità strutturale prodotti dagli agonisti D2R/D3R ropinirolo e pramipexolo in neuroni DA differenziati dalle iPSCs di MSAC1-12 e MSA1-8 studiando i cambiamenti morfologici. I neuroni DA MSAC1-12 e MSA1-8 sono stati esposti a ropinirolo e pramipexolo per 72 ore. Ropinirolo e pramipexolo hanno prodotto un effetto significativo su tutti e tre i parametri di plasticità strutturale.

1 Introduction

1.1 Pluripotent stem cells

Pluripotent stem cells (PSCs) are stem cells derived from the inner cell mass of the blastocyst, they retain the ability to undergo unlimited self-renewal and to differentiate into cells of the three germ layers, namely mesoderm, endoderm and ectoderm. They were first isolated from the inner cell mass of mouse blastocyst in 1981 (Evans MJ and Kaufman MH 1981, Martin GR 1981). This achievement was followed in 1998 by the first report of human blastocyst-derived pluripotent cell lines (ESCs) (Thomson JA et al. 1998). These cells were capable of continuous proliferation without showing signs of mutations, retained the normal karyotype, had high telomerase activity and expressed surface markers typical of primates ESCs. Despite the substantial potential of ESCs as tool to study human development, to understand mechanisms of diseases, to investigate drug's efficacy and safety and to treat patients, the use of human ESCs raised ethical controversies because they were derived from human embryos. These concerns were settled in 2006 when the laboratory of professor Shinya Yamanaka published a novel approach to induce the pluripotent status into adult somatic cells of the mouse by a reprogramming technology. The newly generated cells were named induced pluripotent stem cells (iPSCs) (Takahashi K and Yamanaka S 2006).

1.2 Induced pluripotent stem cells

Induced pluripotent stem cells (iPSCs) are a type of pluripotent stem cells derived from adult somatic cells that have been genetically reprogrammed to an ESC-like state through the forced expression of genes and factors important for maintaining the defining properties of ESCs.

The publication in 2006 of the generation of mouse iPSCs from mouse embryonic and adult fibroblasts (Takahashi K and Yamanaka S 2006) was followed in 2007 by the publication of the first human iPSCs lines independently produced by the Yamanaka's and the Thomson's groups from human fibroblasts (Takahashi K et al. 2007, Yu J et al. 2007).

iPSCs are similar to ESCs in many aspects, such as the expression of ESCs markers, chromatin methylation patterns, embryoid body formation, teratoma formation, viable chimera formation, pluripotency and the ability to contribute to many different tissues *in vitro.*

iPSCs are morphologically similar to ESCs since they express markers of pluripotency such as alkaline phosphatase (AP), nuclear transcription factors Oct3/4, Sox2 and Nanog, keratin sulfate antigens Tra-1-60 and Tra-1-81 and glycolipid antigens SSEA3 and SSEA4, in levels comparable to ESCs.
They also have the ability to differentiate into tissues derived from the three embryonic germ layers i.e., ectoderm, mesoderm and endoderm (Robinton DA and Daley GQ 2013, Marti M et al. 2013).
iPSCs were first established from fibroblast, which are easy to culture and highly proliferative.
However, the access to human primary fibroblasts requires skin biopsies, which involve invasive surgical operation and professional expertise.
More accessible somatic cells are being used lately to reduce or avoid discomfort and stress for the patients. These include: peripheral blood mononuclear cells (PBMCs), T cells (Seki T et al. 2010) or B cells (Hanna J et al. 2008), hematopoietic stem cells (Loh YH et al. 2009), hair derived keratinocytes (Re S et al. 2018), hair follicles (Petiti I et al. 2012) and urine cells (Zhou T et al. 2012, Sun H et al. 2018).
Several approaches have been used to reprogram somatic cells into iPSCs. The first method used was the retrovirus-mediated transfection of the four transcription factors that contribute to the maintenance of pluripotency of ESCs and to their rapid proliferation *in vitro*. These transcription factors are octamer-binding transcription factor 3/4 (Oct3/4) (Nichols J et al. 1998), SRY (sex determining region Y)-box 2 (Sox2) (Avilion AA et al. 2003), Kruppel-like factor 4 (Klf4) and cellular-Myelocytomatosis (c-Myc) (Cartwright P et al. 2005). They are collectively called OSKM. The transcription factor-mediated reprogramming of somatic cells into the pluripotency state begins with the ectopic expression of OSKM and the consequent changes in the transcriptome and chromatin structure typical of a differentiated state into that of a pluripotent-like state (Al Abbar A et al. 2020). The induction of pluripotency is established by two consecutive transcriptional waves. The first transcriptional wave is characterized by the binding of c-Myc to a large region of somatic genome with methylated H3K4me2 and H3K4me3, causing the opening of the chromatin (Stadtfeld M and Hochedlinger K 2010). This allows Oct4 and Sox2 to access the reprogramming genes and to ultimately silence the somatic related genes (Al Abbar A et al. 2020). The second transcriptional wave is more restricted to the reprogrammed cells; OSKM access the enhancers and promoters of early pluripotency associated genes, triggering their transcription and expression. During this wave, somatic cells are enforced to alter their morphology, increase proliferation rate, and undergo mesenchymal-to-epithelial transition (MET) (Takahashi K and Yamanaka S 2016). This transition leads to the upregulation of epithelial genes (Papp B and Plath K 2013) and to the establishment of the basic state of epithelial character forming larger ESC-like clusters. Simultaneously, the cells start

expressing pluripotency genes, including alkaline phosphatase (AP) and stage specific embryonic antigen-1 (SSEA1) for mouse cells or the surface gene TRA-1-60 for human cells. Klf4 plays contradicting roles in both phases. In the first phase, it restricts differentiated genes as it binds and activates epithelial genes, such as E-cadherin (Plath K and Lowry W 2011). In the second phase, it accelerates the essential endogenous Oct4 and Sox2 expression, which establishes the autoregulatory loop that maintains the pluripotent state (Nakatake Y et al. 2006, Karagiannis P et al. 2019).

The retrovirus vectors used by Takahashi and Yamanaka (2006) attach to the cell surface and introduce the reprogramming genes into the infected cells allowing them to integrate into the host genome. Inevitably, they have a significant risk that limits their clinical application.

Lentivirus-based vectors have similar properties of retrovirus, higher reprogramming efficiency and less variability (Wernig M et al. 2008, Yu J et al. 2007), while adenovirus vectors have low reprogramming efficiency (Stadtfeld M et al. 2008).

Viral induction is useful for cell reprogramming in basic research, but it is incompatible with cell transplantation therapy because there is a risk of the spontaneous reactivation of the viral transgenes and tumor formation. Of all the viral methods tested, the safest appears to be Sendai viruses, non-integrative single strand RNAs that replicate outside the nucleus (Fusaki N et al. 2009, Nishimura K et al. 2011).

There are also DNA-based approaches: episomal vectors that incorporates two components from Epstein-Barr virus, EBNA-1 and OriP sequences. This method allows the generation of human iPSCs completely free of vector and transgene sequences (Yu J et al. 2009). Finally, another non integrative strategy is based on the direct delivery of synthetic messenger RNAs, capable of reprogramming somatic cells to pluripotency with high efficiency (Warren L et al. 2010).

1.3 The midbrain

The midbrain is the second of three vesicles that arise from the neural tube during the embryonic development; it joins caudally to the metencephalon and rostrally to the diencephalon and it is considered to belong to the brain stem. The midbrain forms the upper part of the brain stem and carries the quadrigemini bodies on the dorsal surface and the cerebral peduncles on the ventral surface of the cerebral aqueduct. The midbrain contains two major neuronal subtypes: the dopaminergic (DA) neurons of the substantia nigra (SN) (A9) and the dopaminergic neurons of the ventral tegmental area (VTA) (A10), both containing the neurotransmitter dopamine. In the rat

brain, DA cells consist of approximately 45,000 neurons; in humans, in the first two decades of life, dopaminergic neurons are about 590,000 (Prakash N et al. 2006). The dopaminergic neurons that send projections from the substantia nigra to the dorsolateral striatum and the caudate putamen form the nigrostriatal pathway and control the posture and the beginning of the movement; the degeneration of these neurons causes the Parkinson's disease (PD). The dopaminergic neurons in the ventral tegmental area send projections to the ventral striatum, which is composed of nucleus accumbens (NAc), amygdala and olfactory tubercle, forming the mesolimbic pathway and establishing connections with the prefrontal cortex forming the mesocortical pathway (Prakash N et al. 2006); the dysfunction of these neurons can cause psychiatric diseases (Yan Y et al. 2005). The mesencephalic dopaminergic system, through the mesolimbic pathway, that connects the VTA with the NAc, is considered the main area in which act many neuroactive substances in the reward mechanism (Fibiger HC et al. 1986, Wise RA et al. 1987, McBride WJ et al. 1999, Pierce RC et al. 2006).

1.3.1 The substantia nigra

The substantia nigra (SN) is found in an intermediate position between the midbrain and the diencephalon. The functionality of the substantia nigra differs according to the two parts in which is consist of, according to a frontal plane: the pars reticulata or reticulated portion, ventral, and the pars compacta or compact portion, dorsal. The substantia nigra pars reticulata (SNr) has the task of spreading the depressants impulses on the thalamic motor activity performing an inhibition of the movement. Projections from the pars compacta (SNc) stimulate striatal GABAergic neurons through the D1 receptor, resulting in disinhibition of the thalamus and activation of the cortex.

1.3.2 The ventral tegmental area

Dopaminergic neurons of the ventral tegmental area (VTA) are not related to the movement, they are located above the substantia nigra, forming two bundles: the mesolimbic bundle, facing the nucleus accumbens, and the mesocortical bundle, directed to the prefrontal cortex and the cingulate cortex. The mesolimbic bundle mediates the effects of acute positive reinforcement (gratification) and the effects of negative reinforcement (punishment). The mesocortical bundle is involved in cognitive control, motivation and emotional response and in the regulation of executive functions.

1.4 The development of the mesencephalic dopaminergic system

The generation of mesencephalic dopaminergic neurons from a neural progenitor cell can be divided into distinct phases. Molecular markers allow the distinction of three sequential cell populations in the mesencephalic DA lineage: progenitors, immature neurons and mature neurons. These populations are generated during three developmental steps: regional specification, early differentiation and late differentiation (Ang SL 2006).

1.4.1 Regional specification

The first key steps in ventral mesencephalon (VM) DA generation are the early patterning events which lead to the formation of the VM region. During gastrulation, the dorsal ectoderm is restricted towards a neural fate in response to signals arising from the Speamann organizer (Harland R 2000, Hemmati-Brivanlou A and Melton D 1997, Liu A and Niswander LA 2005). The resulting neural plate is then subdivided into restricted domains and subsequently closes to form the neural tube, which is specified by graded signals along the anterior-posterior (A/P) and dorsoventral (D/V) axes (Puelles L 2001, Simon H et al. 1995, Ulloa F and Briscoe J 2007). The development of the VM region relies on appropriate A/P and D/V patterns of gene expression which are regulated by signals arising from two key structures in the early embryo: the floor plate (FP) of the midbrain and the isthmus organizer (Hegarty SV et al. 2013). The correct positioning of the isthmus organiser at the midbrain-hindbrain boundary (MHB) is dependent on the mutual repression of two opposing homeodomain transcription factors: Otx2 and Gbx2 (Martinez-Barbera JP et al. 2001). Otx2 is expressed in the forebrain and midbrain of the developing anterior neural tube (Acampora D et al. 1997, Matsuo I et al. 1995, Simeone A et al. 1992) while Gbx2 is expressed more posteriorly in the anterior hindbrain (Wassarman KM et al. 1997). The formation of the isthmus, which produces fibroblast growth factor 8 (FGF8), together with sonic hedgehog (SHH) signalling from the notochord designates the region in which mesodiencephalic dopaminergic (mdDA) neurons are born (Hynes M et al. 1995, Hynes M and Rosenthal A 1999, Hynes M et al. 2000). Midbrain morphogenesis is regulated by Wnt signaling, it has a central role in the patterning of the midbrain-hindbrain boundary region (Thomas KR and Capecchi MR 1990, McMahon AP and Bradley A 1990, Chilov D et al. 2010, Brault V et al. 2001). Finally, retinoic acid (RA) is required for the proper positioning of the MHB and is therefore indirectly needed for the correct organization of the midbrain (Avantaggiato V et al. 1996, Clotman F et al. 1997, Holder N and Hill J 1991). The floor plate-derived signal SHH and FGF8 from the MHB are required for the induction of DA neurons before embryonic day (E) 9.5 (Ye W et al. 1998).

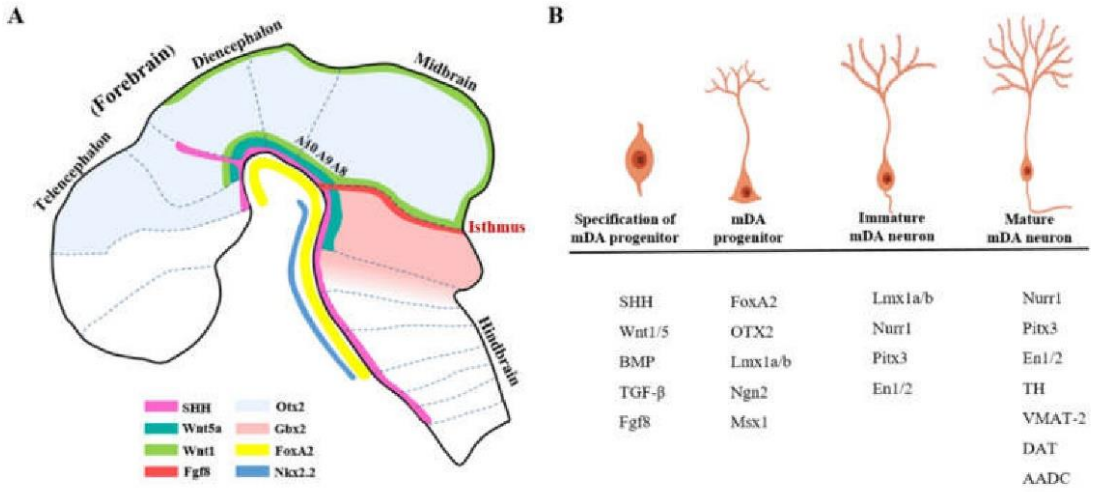

Figure 1. *Signaling and morphogens involved in midbrain and mesencephalic DA neuron development.* (**A**) Sagittal plane of the brain, which illustrates the expression of the morphogens and transcription factors located in the midbrain and hindbrain, and (**B**) the main transcription factors expressed in the different stages of mesencephalic DA progenitor or DA neuron (Wang M et al. 2020).

1.4.2 Early differentiation

A developmental program involving a sequential pattern of gene expression establishes the identity of VM DA neural precursors (Kim HJ 2011, Morizane A et al. 2008, Toulouse A and Sullivan AM 2008). The floor plate and isthmus organiser are also crucial for the induction of a VM DA phenotype. Their role in induction of a DA phenotype is dependent upon the interaction of isthmus secreted FGF8 and floor plate-secreted SHH (Hynes M et al. 1997, Ye W et al. 1998). The mechanism by which FGF8 regulates VM DA development is still under investigation, however a recent study suggested that FGF8 is required to induce the correct patterning of VM DA neural precursors (NPs) (Lahti L et al. 2012). SHH induces the expression of Lmx1a, which subsequently induces the expression of its downstream effector Msx1 (Andersson E et al. 2006). Msx1 contributes to DA neurogenesis by inducing the expression of the proneural gene, neurogenin (Ngn) 2, and thus neuronal differentiation (Vernay B et al. 2005). Ngn2 activates Sox2-positive progenitors that later develop into Nurr1-positive post-mitotic neurons, which differentiate into tyrosine hydroxylase (TH)-positive mdDA neurons (Kele J et al. 2006). SHH has also been shown to play a key role in induction of a DA phenotype by modulating the expression of the transcriptional regulator FoxA2 (Hynes M et al. 1997). FoxA1/2 are key regulators for mesencephalic DA neurogenesis and specification (Ferri AL et al. 2007). Recent data on the Wnt1 gene indicate that it contributes to the mdDA neuronal phenotype by activating Otx2, which suppresses expression of Nkx2.2, a transcription factor that is

important in inducing the serotonergic neuronal lineage (Prakash N et al. 2006). It seems that activation of the Wnt/β-catenin pathway contributes to increased DA neurogenesis during development: β-catenin promotes midbrain dopaminergic neurogenesis *in vivo* (Joksimovic M et al. 2009) and the stabilization of β-catenin in ventral mesencephalic precursors, by GSK3β inhibition, leads to an increase in DA differentiation (Castelo-Branco G et al. 2004, Tang M et al. 2009). Wnt signaling via β-catenin enhances the transcriptional activity of Nurr1 in cells, leading to TH promoter activation (Alves dos Santos MTM and Smidt MP 2011).

1.4.3 Late differentiation

Once NPs of the VM floor plate are specified towards a DA phenotype, the DA NPs gradually become post-mitotic (Lauder JM and Bloom FE 1974, Lumsden A and Krumlauf R 1996). The induction of TH expression is the first sign of the acquisition of the DA phenotype and occurs shortly after the final mitosis of VM DA NPs while they are actively migrating to their final positions (Puelles L and Verney C 1998, Specht LA et al. 1981a, Specht LA et al. 1981b). Several transcription factors have been identified which are essential for the differentiation and subsequent long-term survival of VM DA neurons. These include Lmx1b, Nurr1, Pitx3, En1 and En2. Each of these factors are not individually capable of inducing a complete DA phenotype, suggesting that they function as part of a network (Hegarty SV et al. 2013).

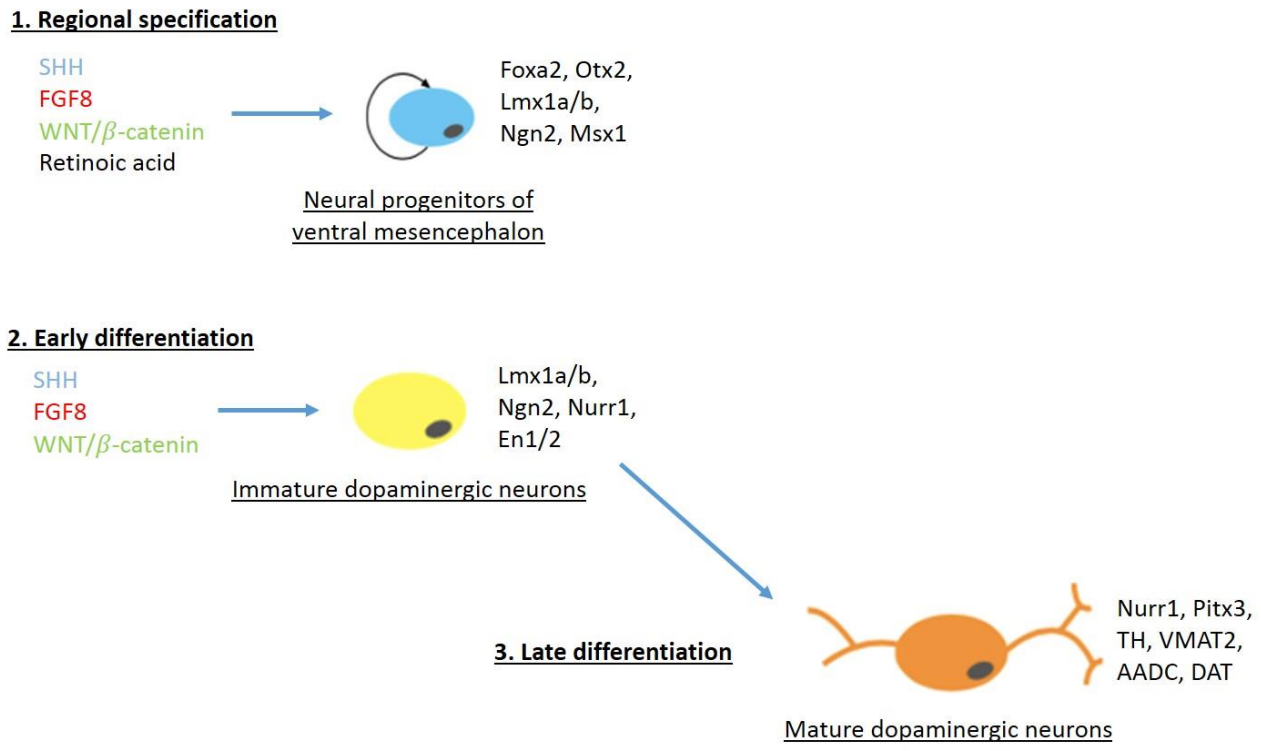

Figure 2. *Overview of the developmental process of the mesencephalic DA neurons* (Ang SL 2006, modified).

1.5 The dopaminergic neurons

Catecholaminergic neurons in the brain were discovered in 1962 by Arvid Carlsson e colleagues through the use of immunofluorescence methods that identified the two major catecholamines in the nervous system, norepinephrine (NA) and dopamine (DA) (Carlsson A et al. 1962). In 1964 Annica Dahlström and Kjell Fuxe analyzed the distribution of catecholamines in the rat brain by identifying 12 groups of catecholaminergic cells, named from A1 to A12 and distributed by the medulla oblongata to the hypothalamus. Subsequently 5 other groups were added, from A13 to A17, located in diencephalon, olfactory bulb and retina (Dahlström A et al. 1964, Hökfelt T 1984).
Since 1970 catecholaminergic systems have been mapped in a detailed manner and the different catecholamines have been differentiated: noradrenaline, adrenaline and dopamine, thanks to the introduction of immunohistochemical techniques aimed at recognition of enzymes synthesized by catecholaminergic neurons, such as tyrosine hydroxylase (Bjorklund A et al. 1984). Dopaminergic neurons reside in several areas of the brain, including the midbrain, the hypothalamus, the olfactory bulbs and the retina.

1.6 The dopamine

Dopamine is a catecholaminergic neurotransmitter present in the extrapyramidal system. Dopamine is important in the modulation of psychic and motor activity, in mood tone, in the secretion of certain hormones, in some components of cognitive processes and in reward mechanisms (Ikemoto S 2007). The starting point for the dopamine synthesis is represented by the amino acids tyrosine and phenylalanine, which are obtained through the diet; phenylalanine is transformed into tyrosine by the enzyme phenylalanine hydroxylase. Tyrosine is exposed to hydroxylation in position 3 of the phenolic ring through tyrosine hydroxylase with the formation of dihydroxyphenylalanine (DOPA). DOPA is the limiting factor of synthesis, because it forms slowly and is rapidly converted into dopamine by the DOPA decarboxylase, so it is not accumulated in the catecholaminergic nerves. The degradation of dopamine is carried out by monoamine oxidase (MAO) and by catecholmethyltransferase (COMT). MAOs are located on the outer membrane of mitochondria and present in two isoforms: MAO-A, ubiquitous, and MAO-B, expressed only in the

central nervous system (CNS). Dopamine is a good substrate for the B isoform and it is deaminated at the level of the phenylethylamine nucleus. COMTs are ubiquitous enzymes, they are positioned post-synaptically and act as donors of methyl groups to allow the inactivation of catecholamines.

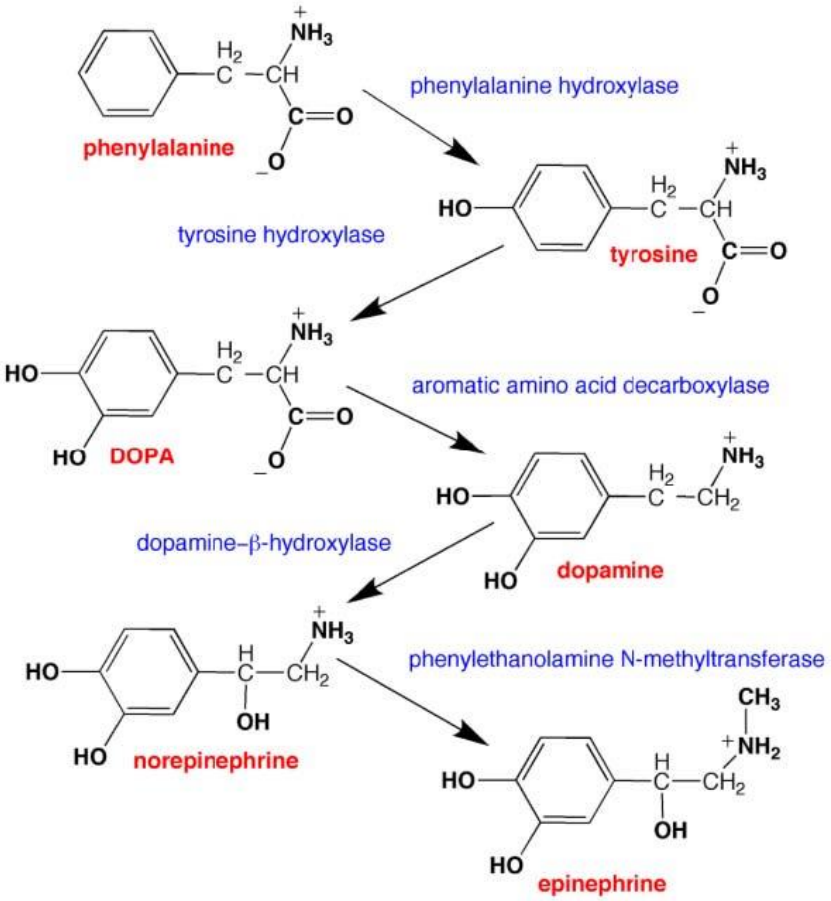

Figure 3. *The biosynthetic pathway for the catecholamine neurotransmitters.* Phenylalanine hydroxylase converts phenylalanine to tyrosine, tyrosine hydroxylase hydroxylates tyrosine to L-DOPA. DOPA is converted to dopamine by aromatic amino acid decarboxylase. Dopamine-β-hydroxylase hydroxylates dopamine to norepinephrine, which is methylated to epinephrine by phenylethanolamine N-methyltransferase. Tyrosine hydroxylase is the rate-limiting enzyme of the pathway (Daubner SC et al. 2011).

1.7 The nigrostriatal system

The nigrostriatal dopaminergic system is represented by the DA neurons of the substantia nigra, whose axons project to the caudate nucleus and to the putamen, that together constitute the corpus striatum. The striatum belongs to the basal ganglia, a subcortical circuit that carries out an important activity in the modulation and planning of motors memory. The striatum is divided into two parts: dorsal and ventral; the dorsal striatum is characterized by the dorsolateral part of the

caudate putamen nucleus, while the ventral striatum is formed by the ventromedial caudate putamen, the nucleus accumbens and the olfactory tubercle (Gerfen CR et al. 1996, Heimer L et al. 1995). The activity of the striatum depends on the integration of two neuronal afferents: the dopaminergic fibers that originate from the SN, and the glutamatergic fibers, that are generated from the cortex (Smith AD et al. 1990, Graybiel AM 1990). These fibers converge on the GABAergic neurons (Smith AD et al. 1990) and make two main efferent pathways of the striatum: the direct and indirect pathways. The direct pathway, called the strio-pale-thalamus-cortical pathway, projects to the interior segment of the pale globe and the SNr; the indirect pathway, called the strio-subthalamo-pale-thalamus-cortical pathway, projects to the outer segment of the pale globe and the subthalamic nucleus (Gerfen CR et al. 1995). The nigrostriatal system belongs to the extrapyramidal system and is responsible for control of motor functions, muscle tone and posture. In Parkinson's disease, due to the degeneration of the nigrostriatal dopaminergic system resulting in dopamine depletion at the striatal level, the activity of the direct and indirect pathways is unbalanced, with hyperactivity of the indirect pathway and consequent onset of akinesia (Obeso JA et al. 2000).

1.8 The mesolimbic system

The mesolimbic system is characterized by DA neurons with cell bodies in the ventral tegmental area that innervate the nucleus accumbens, the amygdala and the olfactory tubercle playing an important role in the addiction to drugs. The NAc is an integral part of the circuits of the limbic and extrapyramidal areas, it mediates the effects of acute positive reinforcement (gratification) of many substances of abuse and the effects of negative reinforcement (punishment). From a functional and histological point of view, the NAc can be divided into two sub-portions: the core that represents the most ventral portion of the striatum with direct connections to the ventral pale and a role in the initiation of movement; the shell that is the most rostral part of the amygdala with limbic functions, such as the integration of emotions, motivation and autonomic functions.

1.9 The mesocortical system

The mesocortical system projects from the ventral tegmental area to the prefrontal cortex. It is essential to the normal cognitive function of the dorsolateral prefrontal cortex and it is thought to be involved in cognitive control, motivation and emotional response and in the regulation of executive functions, i.e., attention, working memory, inhibitory control, planning, etc. (Malenka

EJ et al. 2009). This pathway appears to be abnormal or functioning abnormally in some psychoses, such as schizophrenia. In particular, it is thought to be associated with the negative symptoms of schizophrenia. In the mesocortical system, some dopaminergic fibers innervate the nucleus of the lateral septum, the hippocampus, the amygdala and the cortex. Some dopaminergic fibers also innervate some regions of the neocortex such as the visual and association areas.

1.10 The tubero-infundibular and tubero-pituitary systems

The tubero-infundibular and tubero-pituitary systems originate from the dopaminergic cell bodies of the arcuate and periarchial nuclei of the hypothalamus. The tubero-pituitary system innervates the intermediate and posterior part of the pituitary, where inhibits the secretion of melanocytostimulating hormone (α-MSH). In the intermediate pituitary, it inhibits the release of β-endorphin and in the posterior pituitary, it inhibits the hormones oxytocin and vasopressin. The neurons of the tubero-infundibular system innervate the outer layer of the median eminence, where they are in contact with the capillaries of the pituitary portal system and with the neurons that produce the luteinizing releasing hormone (LRH) and the liberator of the thyrotropic hormone (TRH), which regulate the activity. Dopamine is secreted as a neurormone and carried by the blood hypothalamus-pituitary portal to the lactotropic cells of the pituitary, where it interacts with high affinity of type D2 DA receptors by inhibiting the prolactin secretion (Missale C et al. 1998).

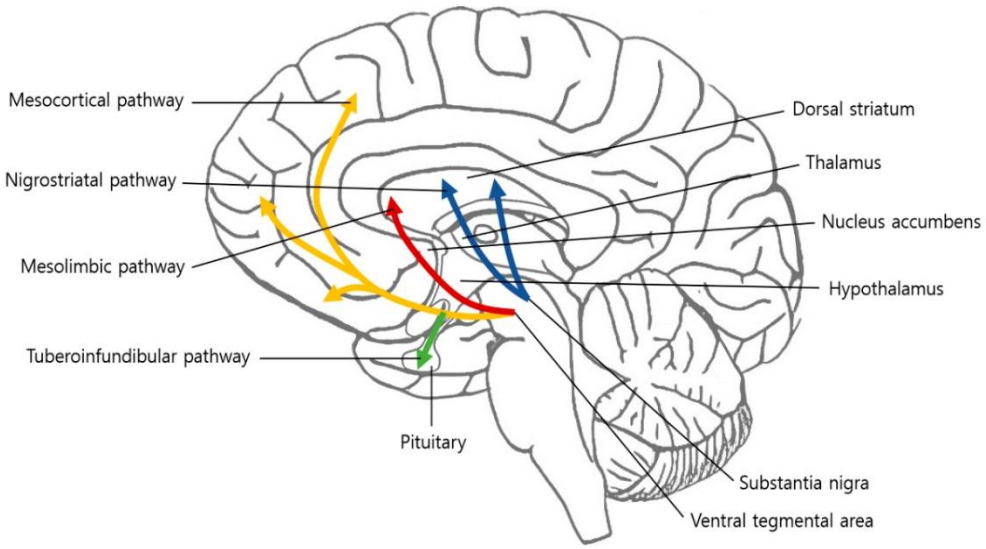

Figure 4. *Four major dopaminergic pathways in the brain: the nigrostriatal, mesolimbic, mesocortical, and tubero-infundibular pathways* (Yang S et al. 2020).

1.11 The dopaminergic receptors

Dopaminergic receptors were discovered in 1970 and were divided into two families: D1 and D2. These families differ from a pharmacological, biochemical and physiological point of view and for anatomical localization. The activation of the receptors belonging to the two families determines a different signal transduction: the activation of receptors belonging to the D1 family causes the formation of cyclic adenyl monophosphate (cAMP) and the increase in the activity of phospholipase C (PLC); the activation of receptors belonging to the active D2 family activates the efflux of K^+ and inhibits the influx of Ca^{2+}, inhibiting adenylate cyclase (AC). The two receptor families differ in their sensitivity to different agonists and antagonists: receptors belonging to the D1 family are sensitive to apomorphine and fenoldopam and are blocked by neuroleptics, while the receptors belonging to the D2 family are activated by bromocriptine and lisuride and blocked by sulpiride. Thanks to the introduction of the gene cloning, other three new central receptor subtypes have been characterized: the D3 (D3R), D4 (D4R) and D5 (D5R) receptors who belong to the two previous families (Sokoloff P et al. 1990, Van Tol HHM et al. 1991, Sunahara RK et al. 1991, Tiberi M et al. 1991). In fact, the D1R and D5R share a high homology in their transmembrane domains and are called D1-like, while the sequences of D3R and D4R are highly shared with the D2R and are called D2-like. After dopamine is released in the synaptic space, about 80% of it is reuptaken by an active, saturable and Na^+-dependent transporter named dopamine transporter (DAT); thereafter, the reuptaken dopamine can undergo to the degradation or be reused.

1.12 The structure of dopaminergic receptors

Dopaminergic receptors belong to the 7-domain transmembrane receptor family coupled to G proteins (GPCR). They share many structural characteristics with other GPCRs (Probst WC et al. 1992). GPCRs are composed of a single polypeptide chain, whose structural feature is represented by 7 α-transmembrane helices, with a N-terminal extracellular domain and a C-terminal intracellular domain. Through the activation of different signal transduction mechanisms, GPCRs control various aspects of cellular function. The connection between the receptor and the first step of signal transduction is established by G proteins which consist of three subunits: α, β and γ. Guanine nucleotides bind to the α subunit, which with its enzymatic activity, catalyzes the conversion of GTP into GDP. The β and γ subunits remain associated and form a single βγ complex. All three subunits are anchored to the plasma membrane linked to G proteins. In the resting state, the G protein is found free in the αβγ trimer form with the GDP linked to the specific site of the α subunit. The

occupation of a GPCR by an agonist molecule activates a conformational change with the acquisition of a state of high affinity for the αβγ trimer. The association of the αβγ trimer with the receptor causes the release of the GDP and its replacement with GTP; this modification causes the dissociation of the trimer with the release of α-GTP and βγ subunits: these represent the active protein forms of G protein, which spread in the membrane and can bind to enzymes and ion channels, causing their activation or inactivation. The process ends with the hydrolysis of GTP to GDP by the α subunit. The α-GDP dissociates from the effector and combines with βγ, completing the cycle. The mechanism leads to an amplification of the signal, because a single complex agonist-receptor can activate several G proteins at each cycle and each of these can remain associated with the effector enzyme for quite long periods to determine the formation of many product molecules.

1.13 The structure of the different receptor subtypes

The receptors belonging to the same family have a high homology: the D1R and the D5R share 80% of the transmembrane domain, while the D2R and D3R share 75% (Jackson DM et al. 1994, O'Dowd BF 1993). The amino termination (-NH2) possesses a number of aminoacids similar in all receptor subtypes and a variable number of N-glycosylation sites (Civelli O et al. 1993, Gingrich JA et al. 1993). The carboxy termination (-COOH) is 7 times longer in D1-like receptors, it is rich in serine and threonine residues, it contains one residue of cysteine which has the role in anchoring the cytoplasmic tail to the membrane (O'Dowd BF et al. 1989, Ovchinnikov Y et al. 1988): in the D1-like receptors the cysteine residue is located near the -COOH termination, while in the D2-like receptors the amino acid represents the last residue. D2-like receptors have a long third intracellular loop, while D1-like receptors have a short third intracellular loop (O'Dowd BF 1993).

1.14 The pharmacological profile of the receptors

The two receptor families have a different pharmacological profile. Within the same family there is a greater or lesser affinity for agonists and for antagonists (Seeman P et al. 1994, Tiberi M et al. 1991). Within the D1-like family, some antagonists are effective on D1R, but not on D5R, suggesting that the latter may show constitutive activity (Sunahara RK et al. 1991, Tiberi M et al. 1991). Within the D2-like family the different response to some agonists and antagonists allows to differentiate the D2R from the D3R. The apomorphine and bromocriptine agonists have similar affinities for the two receptors, while pergolide, quinpirole and 7-hydroxy-dipropylaminotetralin (7-OH-DPAT) have a greater affinity for D3R than for D2R. Among the antagonists, haloperidol and spiperone show a

greater affinity for D2R, while sulpiride, clozapine and raclopride do not discriminate between the two receptors (Sokoloff P et al. 1990, Robinson SW et al. 1994); among the antagonists introduced recently, the SB277011-A and the S33084 have a hundred-fold affinity for D3R higher than for D2R (Reavill C et al. 2000, Millan MJ et al. 2000). The pharmacological profile of D4R is very similar to the other receptors in the class D2-like; the most important difference is the high affinity for clozapine, as opposed to a low affinity for raclopride and chlorpromazine (Seeman P et al. 1994, Van Tol HHM et al. 1991).

Table 2. Dissociation constants (K_i) for ligands at dopamine receptors

Ligand	K_i values (nM)				
	D_1-like		D_2-like		
	D_1	D_5	D_2	D_3	D_4
Antagonists					
Chlorpromazine	~90	~130	3	4	35
Clozapine	~170	~330	~230	~170	21
Haloperidol	~80	~100	1.2	~7	2.3
Nemonapride			0.06	0.3	0.15
Olanzapine			45		27
Raclopride	18000		1.8	3.5	2400
Remoxipride			~300	~1600	~2800
Risperidone			~5	6.7	7
SCH23390	~0.2	0.3	~1100	~800	~3000
Spiperone	~350	~3500	0.06	0.6	0.08
S-Sulpiride	~45000	77000	~15	~13	1000
R-Sulpiride	~19000	29000	~900	~400	970
Agonists[a]					
(−)-Apomorphine	~0.7		~0.7	~32	~4
(+)-Apomorphine			~75		~15
Dopamine[b]	0.9	<0.9	~7	~4	~30
7-OH-DPAT	~5000		10	~1	650
Bromocriptine	~440	~450	~8	~5	~290
R-Fenoldopam	0.8	0.6	3		~150
Pergolide	0.8		~0.8	~1.5	
Naxagolide	80		~1.5		~20
Quinpirole	1900		4.8	~24	~30
SKF38393	1	~0.5	~150	~5000	~1000

[a] K_i values for agonists were determined at the high-affinity state for all receptors, except for D_3 receptors. [b] The K_i value for dopamine was determined at the high-affinity state of the D_3 receptor.

Figure 5. *Dissociation constants (K_i) for ligands at dopamine receptors* (Seeman P et al. 1994).

1.15 The distribution of the receptors in the mesolimbic circuit

Dopaminergic neurons are located in the midbrain in the SNc and in the VTA, in the diencephalon in the hypothalamus; a small group of dopaminergic cells was also identified in the olfactory bulb and in the telencephalon (Prakash N et al. 2006). The D1R is widespread in the caudate nucleus, in the putamen and in the NAc, where it is expressed in the GABAergic neurons projecting to the inner segment of the pale globe and to the SNr (Aubert I et al. 2000, Le Moine C et al. 1995). The D2R is located pre-synaptically on the terminations of the dopaminergic neurons in the striatum; elevated levels are found in the caudate nucleus, putamen, NAc and on the dendrites of GABAergic neurons of the striatum and pituitary. The D3R is localized in the mesolimbic-mesocortical and nigrostriatal systems, in particular in the shell of NAc, in the amygdala, in the olfactory tubercle, in the hippocampus, in the ventral striatum, and in Calleja islands; it is also present on the DA neurons in SN and VTA (Sokoloff P et al. 1990). This receptor is found in the mesolimbic dopaminergic system where it modulates cognitive processes, the reward mechanisms and the emotional processes (Zahm DS 1992); it is also present in neurons of the dorsal striatum, in the caudate and putamen nuclei, indicating that the D3R may be involved in non-limbic functions such as the processing of motor and sensitive information (Hillefors M et al. 2001, Levant B et al. 1998, Morissette M et al. 1998); in the ventral striatum, this receptor is found in the GABAergic neurons, where it is also present the D1R (Ridray S et al. 1998, Schwartz JC et al. 1998, Curran EJ et al. 1995, Le Moine C et al. 1996). Furthermore, it has been shown that the D3 receptor, expressed in striatal neurons, it is strongly induced in the dorsal striatum of rats injured with 6-hydroxydopamine (6-OHDA) and chronically treated with levodopa (L-DOPA) (Bezard E et al. 2003, Bordet R et al. 2000). The D4R was found in the lateral septal nucleus and in the dorsomedial thalamus (Murray AM et al. 1995). The D5R is located in the ventral striatum, in the Calleja islands, in the olfactory tubercle and in the septal area (Khan ZU et al. 2000).

1.16 The signal transduction

In vitro and *in vivo* evidence suggests that pharmacological agents cause changes of neuronal morphology and that this effect is at least partly due to the increase of the dopamine release by dopaminergic neurons and the subsequent activation of the dopaminergic receptors. These phenomena of structural plasticity involve the activation of multiple signal transduction pathways including the mitogen-activated protein kinases / extracellular signal-regulated kinases (MAPK-ERK)

pathway and the phosphatidyl-inositol-3-kinase / thymoma viral proto-oncogene (PI3K-Akt) pathway.

1.16.1 MAPK-ERK pathway

The mitogen-activated protein kinases (MAP kinases) cascade consists of protein kinases that play an important role in signaling transduction in all eukaryotic cells. The central elements in the cascade are a family of serine- / threonine- kinase proteins called MAP kinases, which are activated in response to a variety of growth factors or other signal molecules that allow to regulate growth and cell differentiation. MAP kinase molecules include the extracellular signal regulated family kinases (ERK): their activation plays a central role in the proliferative signal induced by growth factors. Furthermore, the increase in intracellular Ca^{2+} and cAMP can modify ERK phosphorylation, stimulating or inhibiting it, depending on the cell type (Garrington TP et al. 1999). ERK activation is mediated by two protein kinases that are coupled to the receptors by a protein bound to GTP (Ras). The activation of this protein leads to the activation of a serine- / threonine- kinase protein (Raf), which phosphorylates and activates another protein kinase called MAP kinase / ERK-kinase (MEK). The latter activates the members of the ERK family through the phosphorylation of two residues, one of threonine and the other of tyrosine, separated by only one amino acid. Most of the activated ERK molecules translocates to the nucleus where it regulates the transcription by phosphorylation; the first response to stimulation by growth factors is the rapid transcriptional induction of one hundred genes, called immediate-early genes.

1.16.2 PI3K-Akt pathway

The phosphatidyl-inositol 3 kinase (PI3K) / Akt pathway is involved in the regulation of many cellular processes including transcription, migration, angiogenesis, growth and cell proliferation, apoptosis and glucose metabolism. The activation of PI3K is due to various hormones, including insulin, to growth factors such as EGF, to signals derived from receptors for molecules of the extracellular matrix, such as integrins, and various forms of cellular stress. Following the activation of a tyrosine kinase receptor by a ligand through the recruitment of the p85 regulatory subunit of PI3K, the catalytic subunit p110 of PI3K phosphorylates the phosphatidylinositols present on the cell membrane generating phosphatidylinositol-triphosphate (PIP3) starting from phosphatidylinositol-bisphosphate (PIP2). Phosphatidylinositol-triphosphate activated on the cell membrane recruits numerous targets that contain PH domains capable of binding phosphatidylinositols. A serine-

treonine-cytosolic kinase Akt, also called protein kinase B (PKB), is activated directly by phosphatidylinositol-3,4-diphosphate and by phosphorylation by one constitutive membrane threonine kinase PDK1, which is activated by the phosphatidylinositol-3,4,5-triphosphate. Subsequently, Akt and PDK1 move to membrane binding with their PH domains to PIP3 (Clementi F et al. 1999). Complete activation of Akt requires phosphorylation by kinase PDK2 on a serine in position 473 within the regulatory carboxyterminal region and by PDK1 on a threonine in position 308. Subsequently, Akt and PDK1 migrate from the cytoplasm to the nucleus by phosphorylating and by regulating the activity of a huge variety of target proteins including kinases, transcription and other regulatory molecules involved in different cellular processes important for the regulation of cell growth and survival, the cycle and cell proliferation, including GSK3β, mTOR and p70S6K.

1.16.3 mTOR pathway

The mammalian target of rapamycin (mTOR) is a kinase that is encoded by the MTOR gene. mTOR is a member of the phosphatidylinositol 3 kinase-related family of protein kinases. mTOR links with other proteins and serves as a core component of two distinct protein complexes, mTOR complex 1 and mTOR complex 2, which regulate different cellular processes. In particular, as a core component of both complexes, mTOR functions as a serine/threonine protein kinase that regulates cell growth, cell proliferation, cell motility, cell survival, protein synthesis, autophagy, and transcription (Hay N and Sonenberg N 2004). As a core component of mTORC2, mTOR also functions as a tyrosine protein kinase that promotes the activation of insulin receptors and insulin-like growth factor 1 receptors (Yin Y et al. 2016). mTOR integrates the input from upstream pathways, including insulin, growth factors (such as IGF-1 and IGF-2), and amino acids (Hay N and Sonenberg N 2004). The mTOR pathway is a central regulator of mammalian metabolism and physiology, with important roles in the function of tissues including the brain, and is dysregulated in human diseases, such as depression. Rapamycin inhibits mTOR by associating with its intracellular receptor FKBP12. The FKBP12–rapamycin complex binds directly to the FKBP12-Rapamycin Binding (FRB) domain of mTOR, inhibiting its activity (Huang S et al. 2003).

mTOR is the catalytic subunit of two structurally distinct complexes: mTORC1 and mTORC2. The two complexes localize to different subcellular compartments, thus affecting their activation and function. mTOR Complex 1 (mTORC1) is composed of mTOR, regulatory-associated protein of mTOR (Raptor), mammalian lethal with SEC13 protein 8 (mLST8) and the non-core components PRAS40 and DEPTOR. This complex controls protein synthesis. The activity of mTORC1 is regulated by

rapamycin, insulin, growth factors, phosphatidic acid, certain amino acids and their derivatives, mechanical stimuli and oxidative stress (Kim DH et al. 2002). mTOR Complex 2 (mTORC2) is composed of MTOR, rapamycin-insensitive companion of MTOR (RICTOR), MLST8, and mammalian stress-activated protein kinase interacting protein 1 (mSIN1). mTORC2 has been shown to function as an important regulator of the actin cytoskeleton through its stimulation of F-actin stress fibers, paxillin, RhoA, Rac1, Cdc42, and protein kinase C α (PKCα) (Sarbassov DD et al. 2004).

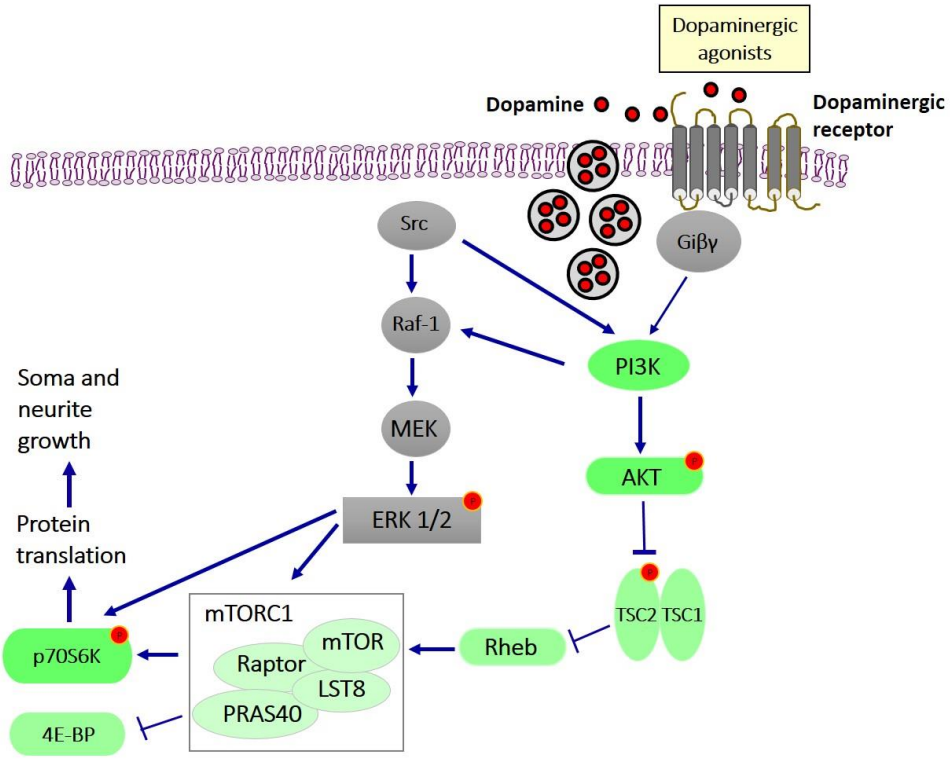

Figure 6. *Signaling pathways involved in structural plasticity of dopaminergic neurons.*

1.17 The neuronal structural plasticity

Several studies have shown that exposure to substances of abuse causes changes in the morphology of neurons located in the areas of the mesolimbic and mesocortical circuits (Nestler EJ et al. 1993). These morphological changes can also be defined as phenomena of structural plasticity. Structural plasticity induced by substances of abuse is a long-term event, which suggests that these substances can produce a specific reorganization of synaptic connectivity in affected the brain regions.

Alterations in structural plasticity may contribute to the maintenance of some behaviors associated with drugs of abuse. They can be the basis of disorders related to motivation and cognitive

alterations which constitute the key points of addiction (Robinson TE and Berridge KC 2003). In fact, it has been demonstrated that the treatment with amphetamine or cocaine produces modifications of the dendritic spines in the striatum and prefrontal cortex of rats (Robinson TE and Kolb B 1999, Robinson TE and Kolb B 2004, Lee KW et al. 2005). The density of dendritic spines in the NAc shell is increased after a single treatment with amphetamine (Kolb B et al. 2003). A repeated exposure to amphetamine in young rats causes an increase of the dendritic tree in dopaminergic neurons of the VTA that send projections to the NAc (Mueller D et al. 2006). In addition, an increase in dendritic spines was observed in VTA of rats that received a single cocaine treatment (Sarti F et al. 2007). Finally, *in vivo* studies have shown that morphine treatments induce changes in the size of the soma of dopaminergic neurons of the VTA (Russo SJ et al. 2007).

1.18 Methodological approaches to study structural plasticity of mesencephalic dopaminergic neurons

Studies aiming to clarify the pathogenesis of human neurological diseases have utilized transgenic animal models and postmortem tissues. The development of murine models has contributed to understand human disease, but they do not fully recapitulate the human cellular phenotype. Animal models can mimic genetic form of human neurological disease. However, they are limited to monogenic disorders and inadequate due to species difference and genetic backgrounds. Moreover, postmortem tissues are not always available and often represent the end stage of the disease. This situation indicates that an advancement towards more human relevant models is definitely needed to study neurogenetic disorders (Wang H and Doering LC, 2012). The first and most fundamental step to construct cellular models of neurological disease is to generate the relevant cell types, neurons and glia, from the patient's own cells. Induced pluripotent stem cell lines from patient's somatic cells could provide the opportunities. In the last years, the generation of iPSCs by ectopic expression of a defined set of factors (Takahashi K et al. 2007, Yu J et al. 2007) has enabled the derivation of patient-specific pluripotent cells, providing a valid support to model human diseases (Park IH et al. 2008, Soldner F et al. 2009) and opening the possibility of implementing patient-specific cell therapy applications.

1.19 Structural plasticity of dopaminergic neurons: role of D3 receptor

The involvement of the dopaminergic receptor D3 in neuronal structural plasticity-related phenomena is been suggested by multiple authors in *in vitro* and *in vivo* study models. The

involvement of the D3 receptor in cellular modifications has also been demonstrated *in vitro*. *In vivo* experiments on rats injured with 6-hydroxydopamine (6-OHDA) and treated by intraventricular infusion with the D3 preferential agonist, 7-hydroxy-dipropilamminotetraline (7-OH-DPAT), demonstrated a neurogenic effect induced by this dopaminergic agonist for the D3 receptor characterized by a significant increase in the number of dopaminergic neurons of the SN (Van Kampen JM et al. 2006). Results from Collo and colleagues suggest the involvement of the D3 receptor in the phenomena of structural plasticity concerning mesencephalic dopaminergic neurons, after administration of 7-OH-DPAT (Collo G et al. 2008a). Such effects of structural plasticity characterized by an increase in the length and number of dendrites and an increase in the soma area are associated with a rapid activation of the intracellular pathway of ERK (Collo G et al. 2008b). The effect on ERK phosphorylation following activation of the D3 receptor by dopaminergic agonists was also highlighted in the works by Cussac (1999) and Beom (2004) through experiments performed on transfected cell lines that overexpress the D3 receptor (Cussac D et al. 1999, Beom SR et al. 2004). Both the effects on the morphology of neurons and the effects on the activation of the MAPK pathway are inhibited by selective blockade of the D3 receptor by the selective D3R antagonist SB277011-A (Collo G et al. 2008 a and b). Other authors also have suggested the involvement of the D3 receptor in neurotrophic phenomena induced by dopaminergic agonists. Du and colleagues (2005) have suggested that the *in vitro* treatment of mesencephalic dopaminergic cultures with quinpirole induces an increase in the number of dopaminergic neurons through D3 receptor activation thus inducing an increase in the release of trophic factors such as BDNF and GDNF (Du F et al. 2005).

1.20 Role of the activation of signaling pathways in the phenomena of neuronal plasticity

Studies have shown that the activation of the MAPK-ERK pathway regulates the development of new dendritic spines in hippocampal neurons (Alonso M et al. 2004). Furthermore, psychostimulants have been observed to induce an increase in ERK phosphorylation in various brain areas including the VTA (Valjent E et al. 2004, Dietz DM et al. 2009). Variable effects on PI3K activation were observed depending on the areas studied, for example an increase of PI3K was appreciated in the shell of the nucleus accumbens, but a decrease in the core (Zhang X et al. 2006). Activation of the PI3K-Akt pathway plays an important role in the genesis of new dendrites and their growth as it has been shown in experiments conducted on hippocampal neurons (Jaworski J et al.

2005). It has also been shown that the size of the neuronal soma is also influenced by the activation of the PI3K-Akt pathway. In particular, exposure to morphine induces a decrease in the soma area of the dopaminergic neurons of the VTA. Such effect is mediated by the inhibition of the PI3K-Akt pathway (Russo SJ et al. 2007). Furthermore, pharmacological agents and substances of abuse have been observed to produce an increase of the phosphorylation of ERK and Akt in *in vitro* mouse cultures of mesencephalic dopaminergic neurons (Collo G et al. 2008, 2012, 2013). The activation of mTOR pathway induced by the dopaminergic agonist ropinirole has also been identified both in mouse primary cultures and in hiPSC-derived dopaminergic neurons (Collo G et al. 2018).

1.21 Brain disorders associated with dopaminergic system

Several important diseases of the central nervous system (CNS) are associated with dysfunctions of the dopaminergic system, ranging from Parkinson's disease (PD), schizophrenia (SCZ) and autism (Kostrzewa RM 2014). The substantia nigra is involved in the control of voluntary movement and body posture, and the selective degeneration of DA neurons together to the loss of DA innervations of the striatum leads to the characteristic symptoms of PD (Hirsch E et al. 1988, Barzilai A and Melamed E 2003, Klockegether T 2004). The mesocortical and the mesolimbic systems are involved in the modulation and control of cognitive and emotional/rewarding behaviors, and the dysregulation of DA synaptic transmission in the mesolimbic system has been linked to the development of depression (Dailly E et al. 2004), while an exaggerated mesocorticolimbic DA transmission is thought to contribute to the psychotic symptoms of schizophrenia (Sesack SR and Carr DB 2002).

1.22 Parkinson's disease

Parkinson's disease (PD) is the most common chronic progressive neurodegenerative movement disorder (de Rijk MC et al. 1997). In industrialized countries, the estimated prevalence of PD is 0.3% in the general population (Lee A and Gilbert RM 2016). The age is the most important risk factor and males appear to have a moderate risk comparing with women. Some environmental factors have also been correlated to the risk of PD, including rural living and some pesticides (Balestrino R and Schapira AHV 2020).

Parkinson's disease includes a range of motor and non-motor symptoms. The main motor symptoms are tremor, rigidity, bradykinesia and postural instability, but the clinical picture includes also other

non-motor symptoms such as dysphagia, gastrointestinal, sleep, sensorial, cognitive and neuropsychiatric disturbances (Balestrino R and Schapira AHV 2020).

The main pathological features of PD are the loss of dopaminergic neurons of the SNc which are particularly susceptible to neurodegeneration. This results in the anatomopathological evidence of a subsequent depigmentation of the SNc. Another typical anatomopathological finding are Lewy's bodies (LBs), intraneuronal, round, eosinophilic inclusions with a hyaline core and a pale peripheral halo that are composed of proteins (Wakabayashi K et al. 2013), their main components being α-synuclein and ubiquitin (Spillantini MG et al. 1997).

The familial history is a risk factor for PD and the familial forms of PD account for 5%‑15% of cases. At present, there have been identified 11 genes linked to PD, the most important are: SNCA, PARKIN, PINK1, DJ1 and GBA (Balestrino R and Schapira AHV 2020).

The treatment of PD is mainly symptomatic and is represented by levodopa-preparations designed to replace the dopamine in the depleted striatum. Currently no disease-modifying treatments for PD are available (Balestrino R and Schapira AHV 2020).

Levodopa crosses the blood brain barrier (BBB) and is converted into dopamine by DOPA decarboxylase. Others PD treatments are dopamine receptor agonists that stimulate the activity of the dopamine system by binding to the dopaminergic receptors and, unlike levodopa, do not need to be converted into dopamine (Zahoor I et al. 2018). The commonly used agonists may be categorized into ergot (bromocriptine and pergolide) and non-ergot (pramipexole and ropinirole) derived, based on receptor specificities (Deleu D et al. 2002). Also in use are the MAO-B inhibitors that work by inhibiting the enzymes involved in dopamine metabolism, preserving the levels of endogenous dopamine.

1.23 iPSCs in Parkinson's disease

In recent years, researches attempted to establish PD-specific iPSCs models by reprogramming PD patients' somatic cells. The first successful examples of iPSCs derived from PD patients were reported by Park IH et al. (2008) and Soldner F et al. (2009).

Some of the topics in iPSCs research in PD focused on the establishment of specific iPSCs models of PD patients carrying susceptible genes such as SNCA, PARKIN, PINK1, GBA and others (Ren C et al. 2019).

Several authors propose iPSC technology as a tool to model PD *in vitro* and for drug discovery, but there are still some limitations. The application of CRISPR/Cas9 technique (Calatayud C et al. 2019)

and single cell high content assay (Little D et al. 2018) may provide new technologies to solve these limitations. In addition, other researchers (Brodski C et al. 2019) also believe that a better regulation of the signal transduction pathways of FGF8, SHH, WNT and bone morphogenetic proteins (BMP) is the key to ensure that iPSCs could be used for drug screening.

More recently, cell replacement therapy using iPSCs has been encountered. A pre-clinical study using a clinical-grade iPSC line was performed and a clinical trial to treat Parkinson's disease patients was started (Takahashi J 2020). Some undergoing clinical trials are available at the First People's Hospital of Yunnan Province (China) and at the Royal Melbourne Hospital (Australia).

1.24 Multiple system atrophy

Multiple system atrophy (MSA) is a neurodegenerative disorder characterized by autonomic failure, parkinsonian features, cerebellar and pyramidal signs. It is classified as the parkinsonian subtype if parkinsonism is the main feature and as the cerebellar subtype if cerebellar features predominate.

The mean incidence is 0.6 to 0.7 cases per 100,000 person/years (Bower JH et al. 1997). Cases of the parkinsonian subtype overcome cases of the cerebellar subtype in most countries by 2:1 to 4:1, although the cerebellar subtype is more frequent in Japan. Disease onset is usually in the sixth decade of life, with both sexes equally affected (Ben-Shlomo Y et al. 1997). The mean survival from the onset of symptoms is 6 to 10 years (Petrovic IN et al. 2012).

MSA is considered a sporadic disease although some emerging evidence suggests rare genetic variants may increase the susceptibility to the disease (Multiple System Atrophy Research Collaboration 2014, Katzeff JS et al. 2019, Pérez-Soriano A et al. 2020).

Variable degrees of olivopontocerebellar atrophy and striatonigral degeneration are typically found at postmortem examination of patients with MSA (Ahmed Z et al. 2012). Proteinaceous oligodendroglial cytoplasmic inclusions are the histologic hallmark of MSA (Papp MI et al. 1989). Activated microglia and reactive astrogliosis are other common findings (Ozawa T et al. 2004). The main constituent of glial cytoplasmic inclusions (GCI) is misfolded α-synuclein, a protein normally located in neuronal axons and synapses. Therefore, MSA is classified as an oligodendroglial α-synucleinopathy.

Multiple system atrophy has a premotor phase in 20% to 75% of cases, including orthostatic hypotension, rapid-eye-movement sleep behavior and various degree of sleep disorders months to years before the first motor symptoms appear (Jecmenica-Lukic M et al. 2012). Parkinsonism, with slowness of movements, rigidity and a tendency to fall, characterizes the motor presentation of the

parkinsonian subtype of MSA (Köllensperger M et al. 2010). Progressive degeneration of the striatum explains the poor response or lack of response to levodopa, which is a mandatory diagnostic criterion for probable MSA of the parkinsonian subtype (MSA-P). Cerebellar ataxia predominates in the motor presentation of the cerebellar subtype of MSA (MSA-C) (Bensimon G et al. 2009).

MSA may be misdiagnosed, especially at disease onset. A diagnosis of definite MSA requires postmortem evidence of widespread α-synuclein-positive glial cytoplasmic inclusions with concomitant olivopontocerebellar atrophy or striatonigral degeneration.

Only symptomatic therapy is available at present, including pharmacologic and nonpharmacologic approaches. While levodopa produces a transient beneficial response in about 40% of patients (Köllensperger M et al. 2010), dopamine agonists are less likely to provide a motor benefit. At the moment, no specific therapy is available for the symptoms of MSA-C.

Studies are conducted to identify MSA biomarkers in order to facilitate the identification of patients, at early or even pre-symptomatic disease stages (Laurens B et al. 2015). Preliminary evidence suggests that positron-emission tomography (PET) with 11C-2-(2-[2dimethylaminothiazol-5-yl]ethenyl)-6-(2-[fluoro]ethoxy) benzoxazole, an α-synuclein ligand, may allow visualization of the density of glial cytoplasmic inclusions in regions of the brain *in vivo* (Kikuchi A et al. 2010). Currently are available several MSA preclinical models, i.e., administration of selective toxins in rodents which reproduces striatonigral degeneration, oligodendroglial over-expression of human α-synuclein which replicates GCI-like pathology in mice and oxidative stress in transgenic mice with oligodendroglial α-synucleinopathy which induces MSA-like neuronal and glial pathology (Stefanova N et al. 2005).

1.25 iPSCs in multiple system atrophy

Animal models do not fully recapitulate the pathology of the disease. A valid alternative is represented by the use of human iPSC models.

Recent advances in hiPSC technology allow to study molecular mechanisms of neurological diseases in differentiated neurons and glia harboring specific mutations and showing disease-relevant pathology, thereby providing a new translational approach for better understanding the disease mechanisms. This technology could be useful for investigating the pathogenesis of MSA-P in cultures of DA neurons and oligodendrocytes differentiated from hiPSCs of MSA-P donors explaining the phenomena that precede α-synuclein misfolding and accumulation. Impairment of oligodendroglial

precursors' maturation and myelination was shown to be involved in MSA pathogenesis (Ishizawa K et al. 2004). Thus, studying the various steps of oligodendrocytes generation and maturation through iPSC technology might help clarifying early events in MSA pathogenesis. iPSCs can be differentiated into many cell types and thus it could be possible to study degenerative pathways both in affected neurons and in oligodendrocytes. Moreover, patient-derived iPSCs could generate not only simple oligodendroglial or neuronal cultures, but also mixed oligodendroglial-neuronal cultures, which could then be searched for differential expression of α-synuclein and apoptotic markers. Mixed oligodendroglial and neuronal cultures could also represent a useful tool to study trophic interaction between neurons and oligodendrocytes. Although these techniques have not been used for studying MSA, significant advancements have been made in other fields.

On the other hand, studying a disease such as MSA with iPSCs poses many challenges. The absence of a gene defect means it is extremely difficult to model MSA with stem cells. Likewise, the lack of a precise knowledge about the role of environmental influences in the pathogenesis challenges the validity of *in vitro* results. However, iPSCs still remain the best technique to study MSA at a preclinical level (Abati E et al. 2018).

1.26 CytoTune™-iPS 2.0 reprogramming system

CytoTune™-iPS 2.0 Reprogramming System uses vectors based on a modified, non-transmissible form of Sendai virus (SeV) to safely and effectively deliver and express key genetic factors necessary for reprogramming somatic cells into iPSCs.

In contrast to many available protocols, which rely on viral vectors that integrate into the genome of the host cell, the CytoTune™-iPS 2.0 Reprogramming System uses vectors that are non-integrating and remain in the cytoplasm, without altering the genetic information of the host cell. In addition, the host cell can be cleared of the vectors and reprogramming factor genes by exploiting the cytoplasmic nature of SeV and the functional temperature sensitivity mutations introduced into the key viral proteins. The CytoTune™-iPS 2.0 Sendai Reprogramming Kit has several advantages. Reprogramming vectors do not integrate into chromosomes of the target cells and do not potentially disrupt important genes. Reprogramming vectors are capable of transducing a wide range of cell types in proliferative and quiescent states. The transduction efficiency is high with low multiplicity of infection (MOI), the contact time of virus with target cells is short and sufficient to establish transduction, the level of expression of the transgenes is high and the expression of the transgenes is fast (as early as 6-10 hours after transduction). Furthermore, the vectors and

transgenes can be eliminated from the cells and the transduced cells do not produce infectious particles. Finally, Sendai virus is derived from a virus that is non-pathogenic to humans.

1.27 Sendai virus

Sendai virus (SeV) is a respiratory virus of mouse and rat, classified as mouse parainfluenza virus type I belonging to the Paramyxoviridae family. SeV was first isolated in Japan in the early 1950s and is also called Hemagglutinating Virus of Japan (HVJ). SeV is an enveloped virus of 150-250 nm in diameter whose genome is a single chain RNA (15,384 bases) in the minus sense. Six genes coding for viral proteins are situated sequentially on the genome of the wild-type SeV in the following order (starting from the 3'end): Nucleocapsid protein (NP) forms the core nucleocapsid complex with the genome RNA, Phosphoprotein (P) is the small subunit of the RNA polymerase, Matrix protein (M) supports the envelope structure from the inside, Fusion protein (F) fuses the viral envelope with cell membrane when the virus enters the cell, Hemagglutinin-Neuraminidase (HN) recognizes the cell surface receptor, sialic acid, Large protein (L) is the large subunit of RNA polymerase.

Because SeV infects cells by attaching itself to the sialic acid receptor present on the surface of many different cells, it can infect a wide range of cell types of various animal species. Activation of F protein by a protease is required for the virus-cell fusion process to take place. After infection, the virus goes through genome replication and protein synthesis, and then daughter virus particles are assembled and released.

1.28 Implantable whole-organic electronic devices

Implantable whole-organic electronic devices could be used for loco-regional therapies in neuropathology characterized by a focal brain damage, such as Parkinson's disease.

This type of devices implanted in animal models of diseases such as PD could supply electrical and chemical stimuli, administer neuronal progenitor cells (NPCs) and support their functions. Implantable whole-organic electronic devices could interface living systems, such as cells, organoids, tissues and organs, with organic field effect transistors. Transistors architectures are able to transduce ionic currents and sense molecular signals.

The device could be provided with organic transducers of electrical signals, and electronic sensors of inflammatory biomarkers, neurotransmitters and metabolites. The response of the brain region to therapeutic intervention could be monitored in real time.

Examples of organic transducers of bioelectric signals *in vitro* include: recording of individual action potentials evoked in neuronal populations and collective signals from stem cell-derived neuron population evoked by gate voltage pulses (Khodagholy D et al. 2014, Cramer T et al. 2013). Organic transistors can be operated to modulate behavior and functionality of living systems. Examples include: the modulation of cell adhesion, the precise time delivery of neurotransmitters, drugs and ions and mimicking signals of neural synapses (Bolin MH et al. 2009, Simon DT et al. 2009, Desbief S et al. 2016). Thus, organic transistors are suitable for establishing bidirectional communication with living systems, as they enable the spatio-temporal control of transient currents or chemical gradients.

For what concern PD, pharmacological support to the degenerated dopaminergic system provides motor symptom relief for most patients and for many years. However, this pharmacological approach does not affect the pathogenic mechanisms of PD. As a consequence, several cell therapies have been proposed on both animal models and clinical trials. Current strategies for PD cell therapy aim at recovering the supply of dopamine to the striatal circuits through a direct transplantation of dopamine-producing cells into the striatum. A major contribution of loco-regional device optimization is warranted to maximize the survival and support the functionality of the dopamine-releasing cells with electrical and chemical signals after transplant and to monitor their functional outcome in real time.

1.29 Electrical fields

The protocols presently available for the differentiation of hiPSCs into DA neurons with some degree of maturity requires a very long time, up to 90 days (Kriks et al. 2012). However, often, even long and complex differentiation protocols can result in neurons with immature features (Avior Y et al. 2016). This aspect must be considered when studying diseases that occur at late stages in life, such as PD. Moreover, long and complex protocols are very expensive and they cannot easily be used for pharmacological testing in drug discovery, therefore the need to identify and implement methodologies that accelerate the process of maturation.

Seminal papers have shown the effect of electrical activity on growing axons *in vivo* and *in vitro* (Catalano SM and Shatz CJ 1998, Dantzker JL and Callaway EM 1998, Ming G et al. 2001), effect that was mediated by Ca^{2+} and cyclic AMP. On the path of these works, recently, some publications have demonstrated that a proper electrical stimulation (ES) can significantly promote neuronal differentiation and neurite growth of various cell types *in vitro*. For example, rat

pheochromocytoma cells PC12 (Jing W et al. 2019), murine neuroblastoma cells N2 (Pelletier SJ et al. 2014), human neural stem cells (Stewart E et al. 2015) were shown to accelerate their differentiation and increase the neurite growth in proper conditions. At the moment, no publications are available on hiPSC-derived neurons.

1.30 Pharmacological agents

1.30.1 Dopaminergic agonists

Ropinirole

Ropinirole is a DA agonist of the non-ergoline class of medications. Ropinirole acts as a D2, D3 and D4 DA receptor agonist with highest affinity for D3 (D3 > D2 > D4). It is weakly active at the 5-HT2, and α2 receptors and it has virtually no affinity for the 5-HT1, benzodiazepine, GABA, muscarinic, α1 and β-adrenoreceptors (Eden RJ et al. 1991). Ropinirole is prescribed for mainly Parkinson's disease, restless leg syndrome, and extrapyramidal symptoms. It can also reduce the side effects caused by selective serotonin reuptake inhibitors, including Parkinsonism syndrome as well as sexual dysfunction and erectile dysfunction caused by either SSRIs or antipsychotics. Many authors have showed a potent neuroprotective activity of ropinirole. It was showed that ropinirole may slow the loss of dopaminergic terminals upon long-term administration to patients with PD (Shill HA et al. 2009). This neuroprotective effects seems to be mediated by the activation of D3 receptor via a pathway involving ERK1/2 and Akt activation (Chen S et al. 2008, Joyce JN and Millan MJ 2007, Whone AL et al. 2003, Joyce JN 2001).

Piribedil

Piribedil is a direct DA agonist, in clinical use for treatment of dopaminergic system dysfunction. A work suggests that it is selective for the D3 receptor subtype, for which it has 20 times higher affinity than for D2, and possesses no significant affinity for D1 receptors. It has also α2-adrenergic antagonist properties (Millan MJ et al. 2001). Piribedil is used for the treatment of PD, either in monotherapy or in combination with L-DOPA therapy, in the early stage of the disease as well as in the advanced ones. This drug has been shown to enhance working memory capacities and enhance cognitive skill learning in healthy older adults (Peretti CS et al. 2004).

Pramipexole

Pramipexole is a DA agonist of the non-ergoline class. It is a DA receptor agonist exhibiting selectivity for the D3 receptor (Ki values are 0.5, 3.3, 3.9 and 3.9 nM for D3, D2S, D2L and D4 receptors, respectively). It exhibits negligible affinity for D1 and D5 receptors and displays activity in the treatment of Parkinson's disease. Pramipexole has been used (in combination with D2- and or D3-preferring antagonists) to discover the role of D3 receptor function in rodent models and tasks for neuropsychiatric disorders (Weber M et al. 2008). Pramipexole has shown effects on pilot studies in a placebo-controlled proof of concept study in bipolar disorder (Zarate CA et al. 2004). It is also being investigated for the treatment of clinical depression and fibromyalgia (Cassano P et al. 2004).

6-Hydroxydopamine

6-Hydroxydopamine (6-OHDA) is a neurotoxic synthetic organic compound that selectively destroy dopaminergic neurons in the brain. 6-OHDA enters the neurons via the dopamine reuptake transporters. The main use for 6-OHDA is to induce Parkinsonism in laboratory animals by lesioning the dopaminergic neurons of the substantia nigra pars compacta, in order to develop an *in vivo* model and test new drugs and treatments for Parkinson's disease (Duty S and Jenner P 2011, Tieu K 2011). In order to induce this condition in animals, around 70% of the dopaminergic neurons in the substantia nigra must be destroyed. This agent destroys neurons by generating reactive oxygen species such as superoxide radical.

1.30.2 Dopaminergic antagonists

SB277011-A

SB277011-A is a selective D3 DA receptor antagonist (pKi values are 8.0, 6.0, 5.0 and <5.2 for D3, D2, 5-HT1D and 5-HT1B, respectively). Studies on CHO cells have shown a potent and selective affinity of this compound with DA D3 receptor >100-fold functional selectivity over D2 receptor and other receptors or channels (Reavill C et al. 2000). It is employed *in vitro* for pharmacologic and functional studies of DA receptors (Vorel SR et al. 2002, Di Ciano P et al. 2003, Collo G et al. 2008, 2012, 2013).

S33084

S33084 is a synthetic compound that acts as a potent, competitive and selective DA D3 receptor antagonist, >100-fold functional selectivity over D2 receptor (Cussac D et al. 1999, Millan MJ et al. 2000).

SCH-23390

SCH-23390 is a potent D1 DA receptor antagonist (Ki values are 0.2 nM and 0.3 nM at D1 and D5 receptor subtypes, respectively). It is also an agonist at 5-HT1C and 5-HT2C receptors *in vitro* (Ki values are 6.3 nM and 9.3 nM, respectively).

1.30.3 Intracellular inhibitors

PD-98059

PD-98059 is an inhibitor of mitogen-activated protein kinase kinase (MKK/MEK). It acts by binding to the inactivated form of MEK, thereby preventing its phosphorylation by RAF or MEK kinase (IC50= 2-7 μM).

LY-294002

LY-294002 is a highly selective inhibitor of phosphatidylinositol 3-kinase (IC50 values are 0.31, 0.73, 1.06 and 6.60 μM for PI 3-Kβ, PI 3-Kα, PI 3-Kδ and PI 3-Kγ, respectively).

Rapamycin

Rapamycin is a macrocyclic antibiotic produced by the bacterium Streptomyces hygroscopicus found in the soil of Easter Island. Rapamycin was discovered as a potent antifungal agent, but it was lately showed to be an immunosuppressive leading to its development as a clinically drug to prevent rejection after organ transplantation (Ballou LM and Lin RZ, 2008). Rapamycin acts by inhibiting mTOR autophosphorylation and phosphorylation of 4EBP1 (Jefferies HB et al. 1997, Kumar V et al. 2005, Soliman GA et al. 2010). Clinical trials are ongoing to test rapamycin in the preventive treatment of infants with Tuberous Sclerosis Complex (EudraCT Number: 2020-003231-19), and in children with Tuberous Sclerosis Complex with Intractable Epilepsy (EudraCT Number: 2010-022655-29).

α-Brain Derived Neurotrophic Factor

α-Brain Derived Neurotrophic Factor (α-BDNF) antibody specifically recognizes BDNF and not the other neurotrophins. Furthermore, it is capable of blocking the functional effects of BDNF (Yan Q et al. 1997).

Recombinant Human TrkB Fc Chimera Protein

The Recombinant Human TrkB Fc Chimera Protein (TrkB-Fc Chimera) is an inhibitor of BDNF activity. TrkB is a receptor tyrosine kinase of the Trk family. It is activated by BDNF, neurotrophin-3, -4 and -5 and is involved in the development and maintenance of the nervous system (Klein R et al 1990). TrkB-Fc is a fusion protein combining the extracellular binding domain of TrkB and the Fc domain of human IgG. TrkB-Fc is a tool for studying the biological actions of BDNF (Croll SD et al. 1998).

K252a

K252a is a non-selective protein kinase inhibitor. It inhibits protein kinase C (PKC) (IC50 = 32.9 nM), protein kinase A (PKA) (IC50 = 140 nM), and receptor tyrosine kinases. It prevents autophosphorylation and activation of downstream effectors (MAPK, Akt) (Kase H et al. 1986).

PP2

PP2 is a selective inhibitor of Src-family tyrosine kinases. It inhibits p56lck and p59fynT (IC50 values are 4 and 5 nM, respectively). It displays > 10000-fold selectivity over ZAP-70 and JAK2 (Hanke JH et al. 1996).

2. Aims

The degeneration of dopaminergic (DA) neurons of the ventral mesencephalon is considered one of the hallmarks in Parkinson's disease (PD) and Parkinsonism. Their susceptibility to damage and their adaptability and plasticity were initially studied in animal models in order to understand the cellular and molecular mechanisms and the action of pharmacological therapeutics. The recent introduction of human inducible pluripotent stem cells (iPSCs) technology and the development of protocols for their differentiation into neurons with a DA phenotype has permitted the direct evaluation of cellular mechanisms of PD and Parkinsonism, the mechanism of action of anti-parkinsonian drugs and the exploratory applications of various aspects of cell therapy.

The aim of this thesis was the generation and phenotypic characterization of human DA neurons amenable to be used as a tool for the development of a variety of therapeutic devices based on cell therapy, in particular implantable whole-organic electronic devices. These devices were designed to be implanted in animal models of PD for a loco-regional therapy driven by electrical and chemical stimuli to support the engraftment of DA neuron precursors, maximizing their differentiation and function.

In order to achieve high quality and reproducible human DA neuron precursors that are able to differentiate and mature into functional DA neurons that respond to electrical and chemical stimuli, therefore amenable to the above described use, this work was organized in four main subprojects.

The first subproject was dedicated to the optimization of the methods of differentiation of human iPSCs into mesencephalic DA neuron precursors using a previously published protocol (Fedele S et al. 2017). These DA neuron precursors can be expanded for several passages and stored in liquid nitrogen for any future use.

The second subproject was dedicated to the differentiation of mesencephalic DA precursors into mature DA neurons that were characterized by immunofluorescence, quantitative PCR, HPLC and electrophysiological analyses. The DA phenotype of the neurons was investigated by testing their response to two dopaminergic agonists (i.e., pramipexole and piribedil) currently used for the treatment of PD. Recent data have demonstrated a neurotrophic effect produced by an anti-parkinsonian DA D2/D3 receptor (D2R/D3R) agonist, ropinirole (Collo G et al. 2018). Based on these findings, the cellular and molecular effects of pramipexole and piribedil on human DA neurons were evaluated by studying morphological changes related to structural plasticity and the activation of

intracellular pathways. The neuroprotective and neuroregenerative properties of these two pharmacological agents were also studied.

The third subproject was dedicated to the study of the effects of the electrical stimulation on the structural plasticity of human DA neurons. Several reports have shown that electrical stimulation can promote neuronal differentiation and neurite growth of various neuronal cell types *in vitro*, including PC12 (Jing W et al. 2019) and human neural stem cells (Stewart E et al. 2015).

The fourth subproject was dedicated to the generation of human iPSCs from peripheral blood mononuclear cells (PBMCs) donated from a novel set of healthy controls and patients affected by a Parkinsonism, i.e., the multiple system atrophy (MSA). The iPSC clones obtained from the control and the patient underwent a phenotypic characterization to examine the presence of pluripotency markers by immunofluorescence and quantitative PCR analysis, karyotype analysis, pluripotency and trilineage differentiation potential. The iPSCs were subsequently differentiated into mesencephalic DA neurons and assessed for their pharmacological response to dopaminergic agonists.

3. Materials and methods

3.1 Chemicals

Ascorbic acid (AA) and Adenosine-3',5'-cyclic monophosphate (cAMP) were purchased from Sigma-Aldrich; LDN193189 (LDN) and CHIR99021 (CHIR) were purchased from Stemgent (Cambridge, MA); Y27632 dihydrochloride (ROCK inhibitor) and SB431542 were purchased from Tocris Bioscience; Shh C25II (Shh), fibroblast growth factor 8 (FGF8), brain-derived neurotrophic factor (BDNF), glial cell line-derived neurotrophic factor (GDNF) and transforming growth factor type β3 (TGFβ3) were purchased from R&D Systems (Minneapolis, MN, USA).

3.2 Pharmacological agents

Ropinirole, piribedil dihydrochloride, pramipexole dihydrochloride, PD98059, LY294002, rapamycin, SB277011-A, SCH23390, K252a, PP2, 6-hydroxydopamine hydrobromide (6OHDA) (Tocris Bioscience, Bristol, UK), S33084 (Institut de Recherches Servier, Croissy-sur-Seine, France), α-BDNF (Merck Millipore, Milan, Italy), TrkB-Fc Chimera (R&D Systems, Minneapolis, MN) were used in the present study. For each vehicle treatment, solvents required by specific drugs were used at the same dilution used for the active treatment.

3.3 Human peripheral blood mononuclear cells

Human peripheral blood mononuclear cells (PBMCs) were obtained from blood samples of healthy donors (in collaboration with Professor Paolo Barone and Professor Maria Teresa Pellecchia, University of Salerno) following the approval of the local ethics committee and informed consent for use in research applications. PBMCs were isolated through density gradient centrifugation via Ficoll-Paque and frozen in FBS and DMSO-containing medium. PBMCs were cultured in StemPro™-34 medium with the following cytokines: SCF (C-Kit Ligand) Recombinant Human (100 ng/mL), FLT-3 Ligand Recombinant Human (100 ng/mL), IL-3 Recombinant Human (20 ng/mL) and IL-6 Recombinant Human (20 ng/mL).

3.4 Human PBMCs reprogramming and iPSC culture

Human PBMCs reprogramming was performed using the CytoTune™-iPS 2.0 Sendai Reprogramming Kit (Thermo Fisher Scientific) to generate hiPSCs cultured in feeder-free conditions on matrigel-coated culture dishes.

At day –4, four days before transduction, thaw PBMCs from liquid nitrogen, centrifuge the cell suspension at 200 × g for 10 minutes, discard the supernatant, and resuspend the cells in complete StemPro™-34 medium with the cytokines to 5×10^5 cells/mL, add 1 mL per well to the middle section of a 24-well plate and incubate the cells in a 37°C incubator with a humidified atmosphere of 5% CO_2.

From day –3 to –1 add fresh medium by removing 0.5 mL of the medium from each well, and replace it with 0.5 mL of fresh complete PBMC medium.

At day 0, count the cells and calculate the volume of each virus needed to reach the target MOI.

Volume of virus (µL) = MOI (CIU/cell) × number of cells / titer of virus (CIU/mL) × 10^{-3} (mL/µL)

For each transduction, pipette 2.5 x 10^5 - 5 x 10^5 cells into a round bottom tube.

Add the calculated volumes of each of the three CytoTune™ 2.0 Sendai tubes to 1 mL of PBMC medium. Add the reprogramming virus mixture to the round bottom tube containing PBMCs. Centrifuge the cells and virus at 1000 x g for 30 minutes at room temperature. Once the centrifugation is complete, add an additional 1 mL of PBMC medium to the tube, resuspend the cells, and transfer them to 1 well of a 12-well plate. Incubate the plate overnight in a 37°C incubator with a humidified atmosphere of 5% CO_2.

At day 1, remove the cells and medium from the culture plate and transfer to a 15-mL centrifuge tube. Remove the CytoTune™ 2.0 Sendai viruses by centrifuging the cell suspension at 200 × g for 10 minutes, aspirating the supernatant, and resuspending the cells in 0.5 mL of complete PBMC medium per well of a 24-well plate. Culture the cells at 37°C in a humidified atmosphere of 5% CO_2 for 2 days.

At day 3, prepare matrigel-coated culture plates, count the cells and seed with 1 x 10^4 - 1 x 10^5 cells per well in 2 mL of complete StemPro™-34 medium without the cytokines. Incubate the cells at 37°C in a humidified atmosphere of 5% CO_2.

From day 4 to 6, remove 1 mL of the spent medium from the cells and replace it with 1 mL of fresh complete StemPro™-34 medium without cytokines.

At day 7, start transitioning cells to mTeSR1™ medium, by removing 1 mL of StemPro™-34 medium from the cells and replace it with 1 mL of mTeSR1™ medium.

From day 8 to 28, change the full volume of the medium to mTeSR1™ medium and replace the spent medium every day thereafter.

Starting on day 8, cell clumps, indicative of reprogrammed cells, begin to emerge.

By day 15 to 21, colonies should have grown to an appropriate size for transfer.

At this point, manually pick colonies and transfer them onto prepared matrigel-coated culture plates.

Human iPSCs were cultured on Matrigel-coated plates (BD Matrigel hESC qualified Matrix, BD Biosciences, San Jose, CA) and mTeSR™1 medium (StemCell Technologies, Vancouver, BC, Canada) supplemented with ROCK inhibitor (Y27632 10 µM, Tocris Bioscience).

3.5 Embryoid bodies generation and differentiation

Embryoid bodies (EBs) were generated from large colonies fragments of human iPSCs that were mechanically dissociated and placed in suspension culture in mTeSR™1 medium for 8 days. At this stage, EBs were then plated into adherent conditions in 0,1% gelatin-coated dishes (for RNA extraction) or coverslides (for immunostaining) and maintained in culture in a differentiation medium (DMEM/F12, 15% Knockout Serum Replacement (KSR), 2mM Glutamax, 2-mercaptoethanol, non-essential amino acids (NEAA)) for 15 days to induce spontaneous differentiation.

The cells were stained with specific markers for the three germ layers: PAX6 polyclonal antibody (Covance, NJ, USA), anti βIII-tubulin polyclonal antibody (Merck Millipore), anti α-smooth muscle actin (α-SMA) monoclonal antibody (Sigma-Aldrich), brachyury polyclonal antibody (R&D Systems), anti α-fetoprotein (AFP) polyclonal antibody (Dako, Denmark).

3.6 Karyotype analysis

Cytogenetic studies were performed on hiPSCs at passage 10^{th} or higher. Chromosome preparations were obtained according to standard techniques by incubating 10-20 iPSCs colonies in 10 µg/ml Colcemid (Irvine Scientific, Santa Ana, CA) diluted in Hank's balanced salt solution (Sigma-Aldrich) for 3 hours. At the end, iPSCs were dissociated with Trypsin / EDTA (Sigma-Aldrich), incubated in hypotonic solution and fixed in methanol and acetic acid (3:1). Metaphase suitable for analysis was sequentially Q-banded according to the routine methods.

These experiments were performed in collaboration with Dr. Giovanna Piovani from the Biology and Genetic Unit, Department of Molecular and Translational Medicine, University of Brescia.

3.7 Astrocyte culture

Primary cortical astrocytes were isolated from P1 mouse newborns. Cortices were dissected, collected in ice-cold HBSS (Sigma-Aldrich) and dissociated through a syringe connected to a 18G needle, followed by a 21G needle and a 25G needle. The cell suspension was diluted in DMEM 10% FBS, plated on 6 cm dishes and incubated at 37°C in 5% CO_2. Medium was replaced every 3 days.

3.8 Differentiation of human iPSCs into midbrain DA neuron phenotype

Human iPSCs clone F3 was used in the present study. This clone was previously generated, characterized and used in parallel experiments testing clone NAS2 (Collo G et al. 2018, Devine MJ et al. 2011). Human iPSCs were induced to differentiate into floorplate (FP)-derived midbrain DA neurons using dual-SMAD inhibition and FP induction (Kriks S et al. 2011, Fedele S et al. 2017) with minor modifications. Human iPSCs were dissociated with Accutase™ (StemCell Technologies, Vancouver, BC, Canada), seeded ($3x10^4$ cells/cm^2) on Matrigel-coated plates in Knockout Serum Replacement (KSR) medium containing Knockout™ DMEM, 15% KSR, GlutaMAX™ and 10 µM 2-mercaptoethanol, in the presence of LDN193189 (0.1 µM, Stemgent, Cambridge, MA), SB431542 (10 µM, Tocris Bioscience), Shh C25II (0.1 µg/ml, R&D Systems), Purmorphamine (2 µM, Stemgent), Fibroblast Growth Factor 8 (0.1 µg/ml, R&D Systems) and CHIR99021 (3 µM, Stemgent). From day 5, KSR medium was shifted to N2 medium (Knockout™ DMEM/F12, N2 supplement and GlutaMAX™, all from Gibco-Invitrogen). On day 11, the medium was changed to Neurobasal/B27/GlutaMAX™ supplemented with CHIR99021, BDNF (20 ng/ml, R&D Systems), ascorbic acid (AA; 0.2 mM, Sigma-Aldrich), dibutyryl cAMP (cAMP; 0.5 mM, Sigma-Aldrich), transforming growth factor type β3 (TGFβ3; 1 ng/ml, R&D Systems), glial cell line-derived neurotrophic factor (GDNF; 20 ng/ml, R&D Systems) and DAPT (10 nM, Tocris Bioscience). On day 21, cells were dissociated with accutase and seeded at a density of 5 x 10^4 cell/cm^2 on pre-coated plates with Polyornithine (15 µg/ml) / Fibronectin (2 µg/ml) / Laminin (1 µg/ml) (all from Sigma-Aldrich) and co-cultured with mouse primary cortical astrocytes (Collo G et al. 2018).

Pharmacological treatments were performed from day 70. Three days before pharmacological treatments, BDNF, AA, cAMP, TGFβ3, GDNF and DAPT were removed from the culture. Criteria to define DA neurons at day 70 were the co-expression of tyrosine hydroxylase (TH)/MAP2 and the co-

expression of TH/dopamine transporter (DAT) (Collo G et al. 2018). At this time $TH^+/MAP2^+$ DA neurons represented 30-40% of the total $MAP2^+$ neurons, in line with previous studies (Fedele S et al. 2017, Collo G et al. 2018). The other neuronal populations were GABAergic neurons (20-25%) and glutamatergic neurons (35-40%) (Collo G et al. 2018).

3.9 In vitro pharmacological experiments

All pharmacological treatments were performed at day 70 in culture. For morphological studies neuronal cultures were exposed to piribedil or pramipexole for 72 hours and cultures were fixed at 72 hours. For biochemical studies neuronal cultures were exposed to piribedil (10 µM) at different time points (2-60 minutes). Dopaminergic antagonists (SB277011-A (100 nM) or S33084 (10 nM)) and mTOR inhibitors (PD98059 (10 µM), LY294002 (10 µM) or rapamycin (20 nM)) were added to the cultures 20 minutes prior to treatment with piribedil or pramipexole. Each experiment was repeated at least twice. Each treatment group was assessed in duplicate coverslides. The optimal concentrations of dopaminergic antagonists and mTOR inhibitors were obtained in previous studies (Collo G et al. 2008).

3.10 Immunofluorescence and immunocytochemistry analysis

Cultures were either fixed with phosphate-buffered saline (PBS) containing 3% paraformaldehyde (Sigma-Aldrich) and 3% sucrose (Sigma-Aldrich) for 20 minutes at room temperature or with ice-cold methanol (Sigma-Aldrich) for 10 minutes. At the end of the incubation, they were permeabilized with PBS containing 0.2% Triton (Promega, Madison, WI, USA), 1% normal goat serum (NGS; Jackson ImmunoResearch, West Grove, PA, USA) and 5% bovine serum albumin (BSA; Sigma-Aldrich) for 30 minutes at room temperature, and incubated with the appropriate primary antibodies (Supplementary Table 2) overnight at 4°C. The following day, Alexa Fluor® 488- and Cy™3-conjugated secondary antibodies (Jackson ImmunoResearch, West Grove, PA) (Supplementary Table 3) were incubated 1 hour at room temperature, followed by DAPI (Molecular Probes-Invitrogen). The following primary antibodies were used: rabbit polyclonal antibody anti-TH (1:800; Santa Cruz Biotechnology, Santa Cruz, CA, USA), mouse monoclonal antibody p-p70S6K (1:500; Cell Signaling Technology, Danvers, MA). Coverslides were mounted with Vectashield Mounting Medium (Vector Laboratories). As negative control, cultured neurons were incubated with the secondary antibodies only. The samples were visualized using a Zeiss Axio Observer Z1

completed with ApoTome.2 or a Zeiss LSM510 completed with Zen Black (Carl Zeiss AG, Oberkochen, Germany). Each experiment was repeated two-three times.

For immunocytochemistry analysis, the cultures were incubated overnight with a rabbit polyclonal anti-tyrosine hydroxylase (TH) antibody (Santa Cruz Biotechnology) followed by 30 minutes incubation with a biotinylated goat anti-rabbit antibody (Jackson ImmunoResearch) and a final incubation with an ABComplex horseradish peroxidase detection system (Vector Laboratories, Burlingame, CA, USA). Color development was achieved by addition of 3,3'diaminobenzidine (DAB; Sigma-Aldrich) for 5 minutes. The samples were visualized with the Olympus IX51 microscope (Olympus Italia Srl, Milan, Italy). Each experiment was repeated two-three times.

3.11 Computer-assisted morphological analysis

Digital images were acquired with an Olympus IX51 microscope connected to an Olympus (Hamburg, Germany) digital camera and a PC. Morphometric measurements were performed by a blinded examiner on digitalized images using Image-Pro Plus software (Media Cybernetics, Bethesda, MD) or ImageJ (NIH, Bethesda, MD). Morphological indicators of structural plasticity of DA (TH^+) neurons were considered: (i) the maximal length of dendrites, (ii) the number of primary dendrites and (iii) the soma area (Collo G et al. 2018). Significant changes in these endpoints in a large number of neurons (>50 per group) were considered relevant indicators of structural plasticity changes (Schmidt U et al. 1996). Maximal length of dendrites was defined as the distance from the soma (hillock base) to the tip of the longest dendrite for each neuron; dendrites shorter than 20 µm were excluded from the morphometric analysis. Primary dendrites were defined as those directly stemming from the soma. Soma area was assessed by measuring the surface (μm^2) included by the external perimeter drawn on the cell membrane of neurons identified by TH^+ staining. Two coverslides per treatment groups were examined so to obtain more than 50 frames for each coverslide and at least 50 neuron measurements. Each experiment was repeated two-three times.

3.12 Western blotting

Western blotting was performed at different time points (0-60 minutes) following challenge with piribedil and/or after pretreatments with either dopaminergic antagonists (SB277011-A or S33084) and mTOR inhibitors (PD98059, LY294002 or rapamycin).

At each time point neuronal cultures were washed with ice-cold PBS and lysed in a buffer containing 50 mM Tris (pH 7.4), 150 mM NaCl, 0.5% sodium deoxycholate, 0.1% sodium dodecyl sulphate, 1%

Igepal, 1 mM polymethanesulphonyl fluoride and complete protease inhibitors (Roche Diagnostics, Mannhein, Germany) for 10 minutes in ice. Cells were homogenized with a probe-type sonicator on ice and centrifugated at 13.000 g for 10 minutes at 4°C. The protein concentration was measured with a DC-protein assay (Bio-Rad, Hercules, CA, USA). Ten micrograms of total proteins were resolved by NuPAGE™ 4 to 12%, Bis-Tris, Mini Protein Gel (Invitrogen™) and blotted onto a PVDF membrane (Immobilon-P; Millipore). Membranes were blocked in TBS/Tween-20 (25 mM Tris base, 137 mM NaCl, 2.7 mM KCl and 0.1% Tween-20, pH 7.6) 5% BSA, and incubated overnight with the primary antibodies dissolved in 5% BSA in TBS/Tween-20.

Primary antibodies used were the following: anti-p-p70S6K mouse monoclonal antibody (mAb) (1:4000), anti-p70S6K rabbit mAb (1:4000) (all from Cell Signaling Technology), anti-TH rabbit polyclonal antibody (pAb) (1:2000) (Merck Millipore) and anti-α-Tubulin mouse mAb (1:20000) (Sigma-Aldrich). In each experiment, the same membrane was processed in the following order: incubation with anti-p-p70S6K antibody, incubation with anti-p70S6K antibody, stripping with the Re-Blot Plus Strong Solution (Merck Millipore), incubation with anti-TH antibody, and final incubation with anti-α-Tubulin antibody. After the incubation with primary antibodies, blots were incubated with appropriate horseradish peroxidase-conjugated secondary antibodies for 1 hour (goat anti-rabbit or goat anti-mouse, Santa Cruz Biotechnology) and developed using a chemiluminescent substrate (ECL, LiteAblot Extend; EuroClone). Specific bands were analyzed by densitometric scanning of the exposed film using Gel-Pro analyzer software (Media Cybernetics, Bethesda, MD, USA). In each experiment, the specific signal of p-p70S6K protein was normalised to the corresponding p70S6K signal and then to the level of TH and α-Tubulin measured in the same preparation.

3.13 Measurement of dopamine release

The dopamine released in the culture medium was determined by the HPLC method coupled with electrochemical detection used for the assay of dopamine in rodent brain with minor modifications (Invernizzi RW 2013). Human iPSC-derived DA neurons cultured for 70 days were incubated with vehicle up to 24 hrs. Fractions of medium were collected at different time points, that is, at 0, 3, 6, 9, and 24 hrs after incubation. 2M $HClO_4$ containing 0.5% $Na_2S_2O_5$ and 1% Na_2EDTA (all from Sigma-Aldrich) was diluted at 1:20 in each fraction. Samples were kept at -80°C until HPLC assay. HPLC consisted of a constant flow LC20-AD pump (Shimadzu, Italy) and a Coulochem II electrochemical detector equipped with a dual electrode 5011 analytical cell (ESA, Chelmsford, MA). Potential

settings were E1-175mV and E2-300 mV. 25 µl of sample were injected into the HPLC with a refrigerated (5°C) autosampler (Midas, Spark Holland, The Netherlands). Dopamine was separated through an Accucore XL C18 column, 150 × 3 mm, particle size 4 µm (Thermo Fisher Scientific) protected with a guard column (NewGuard RP-18, 7 µm, 15 × 3.2 mm; Perkin Elmer, Italy). The column was maintained at 40°C. Mobile phase consisted of 5 g/l anhydrous CH_3COONa, 3.57 g/l citric acid, 112 mg/l Na_2EDTA, 200 mg/l sodium octane sulfate, and 70 ml/l CH_3OH. Flow rate was 0.5 ml/min. Assay was calibrated daily by injecting 2.5, 25, and 250 fmol/25 µl DA made up in $HClO_4$ 0.2M plus 0.05% $Na_2S_2O_5$ and 0.1% Na_2EDTA. The detection limit was 2 fmol on the column (signal-to noise ratio 2).

These experiments were performed in collaboration with Dr. Roberto William Invernizzi from the Laboratory of Neurochemistry and Behavior, Istituto di Ricerche Farmacologiche "Mario Negri", Milan.

3.14 RNA extraction and RT-PCR analysis

Total RNA was extracted using Quick-RNA MiniPrep (Zymo Research) according to the manufacturer's instructions. RNA quantification and quality controls were performed using spectrophotometric analysis (NanoDrop Technologies). Reverse transcription was carried out using Moloney Murine Leukemia Virus-Reverse Transcriptase (MMLV-RT). Briefly, 1 µg of total RNA were mixed with 1 µl of 0.3 ng/ml random hexamer, 1 µl of 10 mM dNTP Mix, 4 µl of 5X First-Strand Buffer, 2 µl of 0.1 M DTT, 1 µl of 40 U/µl RNaseOUT and 1 µl MMLV-RT (200 units) in a final volume of 20 µl (Life Technologies). The reaction mixture was incubated at 37°C for 2 min, 25°C for 10 min, 37°C for 50 min and then the enzyme was inactivated at 70°C for 15 min. To analyze the RNA expression pattern of target genes, the Eppendorf Master Cycler PCR system (Eppendorf) with Thermo Scientific DreamTAQ Green PCR Master Mix (2X) were used following the manufacturer's instructions. 25 ng of sample were used in each amplification in PCR. PCR products were visualized by agarose/ethidium bromide gel electrophoresis. Sequences of individual primer pairs and melting temperature (Tm) are detailed in Supplementary Table 4.

3.15 RNA isolation, retrotranscription and quantitative PCR analysis

Total cellular RNA was isolated using RNeasy Plus Mini Kit (Qiagen) according to the manufacturer's instructions. The concentration and purity of the RNA samples were assessed using a NanoDrop® 1000 spectrophotometer (Thermo Fisher, Waltham, MA, USA). Here, 1 µg of RNA was reverse

transcribed into cDNA using High-Capacity cDNA Reverse Transcription Kit (Applied Biosystems, Foster City, CA, USA). qPCR was performed on three independent biological replicates, in technical duplicate for each biological replicate using the SensiFAST™ SYBR®Lo-ROX Kit (Applied Biosystems) method and an Applied Biosystems 7500 System. The reaction mixture contained 50 ng of cDNA template and 400 nM of each forward and reverse primer in a final volume of 15 µl. The PCR conditions included a denaturation step (95°C for 10 min) followed by 40 cycles of amplification and quantification (95°C for 35 s, 60°C for 1 min). The relative gene expression levels were normalized to the reference gene Glyceraldehyde-3-phosphate dehydrogenase (GAPDH), the expression of which is not affected under the experimental conditions and calculated by the 2-ΔΔCt method. The sequences of the primers used are listed in Supplementary Table 4.

3.16 Electrophysiology

Recordings on human hiPSC-derived DA neurons were performed at room temperature applying the patch-clamp technique in the whole-cell configuration. The set-up was equipped with a Multiclamp 700B patch-clamp amplifier, a Digidata 1440A (both from Axon Instruments, Molecular Device, Sunnyvale, CA, USA), and pClamp 10.3 software (Molecular Devices LLC, Sunnyvale, CA, USA). The resting membrane potential and the spontaneous activity were measured immediately after obtaining the whole-cell configuration in current-clamp mode applying a gap-free protocol. The extracellular solution was composed as follows: 129 mM NaCl, 1.25 mM NaH_2PO_4, 1.8 mM $MgSO_4$, 1.6 mM $CaCl_2$, 3 mM KCl, 10 mM Na-HEPES, and 5 mM glucose, pH 7.4 with NaOH; while the internal pipette solution contained: 120 mM K-gluconate, 15 mM KCl, 2 mM $MgCl_2$, 0.2 mM EGTA, 20 mM phosphocreatine-Tris, 2 mM ATP-Na_2, 0.2 mM GTP-Na_2 , 0.1 mM leupeptin, and 10 mM K-HEPES, pH 7.2 with KOH.

These experiments were performed in collaboration with Dr. Ilaria Rivolta from the School of Medicine and Surgery, University of Milano-Bicocca, Monza.

3.17 Electrical field treatments

The stimulation system consists of several parts:

1) a patented C-Dish™. The lid is suitable for a 6-well culture dish and it is equipped with 12 carbon electrode elements. The electrodes are placed in order to have two electrodes for each well. The carbon electrodes have been demonstrated to be suitable for biomedical applications and they have

been used in several works to stimulate the cells *in vitro*. A ribbon cable connector provides access to the field stimulating electrodes;

2) a custom circuit board, properly designed for this specific application. The circuit board is connected to the C-Dish^{TM} and it injects a controlled current through the electrodes of two wells at the same time. The current profile is defined via software by the user. The board generates both positive and negative supply voltage (+/- 15 V), generates the proper current which passes through the electrodes and the culture medium of two wells, and measures the voltage across the two coupled electrodes referred to one well and monitor the stimulation current. The board allows the impedance measurements of the well confined by the two coupled electrodes;

3) a commercial data acquisition system (DAQ) connected to a laptop. It provides the power supply, reads the voltage output, and defines the current value for the electrical stimulation;

4) a user interface programmed in Labview environment to communicate with the DAQ and the custom circuit board. Furthermore, the interface allows the user to display and store the measurements acquired by the DAQ.

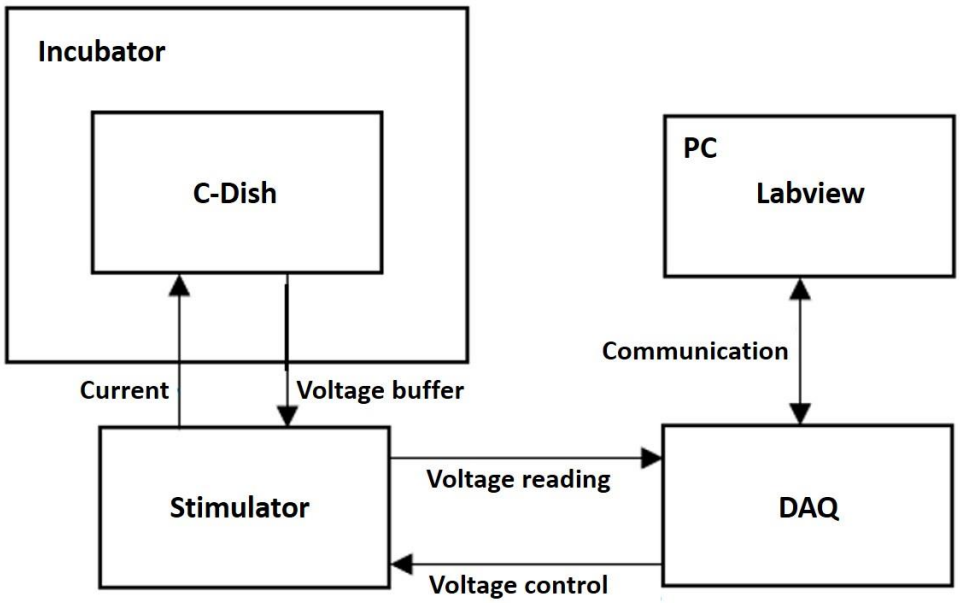

Figure 7. *Representative schema of the stimulation system.*

3.18 Statistical analysis

Each experiment was repeated at least two-three times. Data were expressed as mean ± standard error of the mean (S.E.M.) if not stated otherwise. Significant differences from control conditions were determined using either one-way or two-way analysis of variance (ANOVA) followed by a posteriori Bonferroni's test for multiple comparisons provided by GraphPad Prism, version 6.0 software package (GraphPad Software, San Diego, CA, USA). Two way ANOVA was generally performed between the factor "piribedil/vehicle" or "pramipexole/vehicle" and the factor "antagonist" which includes the various pharmacological antagonists used.

4. Results

4.1 First subproject

4.1.1 Differentiation of human iPSCs into midbrain floor plate progenitors

Several protocols have been developed to differentiate human DA neurons from ESCs and iPSCs (Engel M et al. 2016, Kirkeby A et al. 2012, Kriks S et al. 2011). Here was selected and optimized a recent protocol who represents a modification of the method from Kriks and colleagues (2011) offering the advantage of generating a large number of homogeneous midbrain floor plate progenitors (mFPPs) for cryobanking. When needed, mFPPs can be differentiated into mature DA neurons *in vitro* and *in vivo* (Fedele S et al. 2017). Therefore, this protocol is useful for studies that require large number of mFPPs or DA neurons for understanding cellular and molecular mechanisms of human diseases, for drug screening, and for transplantation. For the optimization of this protocol, one hiPSC clones generated from a healthy donor and named F3 (Collo G et al. 2018), was cultured on matrigel-coated plates in mTeSR1 medium for 24 hours. Once reached 80-90% confluency, the medium was changed to KSR medium and cells were cultured for 2 days. At day 3, after starting the floor plate induction with FGF8, SHH and Purmorphamin, WNT signaling was activated by addition of the GSK3-β inhibitor CHIR99021. On day 5, the medium was gradually switched to N2 medium and SB431542 was omitted from the culture. By day 11, the cells were growing in a KSR/N2 medium (ratio of 1:3). At this point, cells were passaged and replated onto fresh matrigel-coated plates in N2 medium at a density of 75×10^3 cells/cm^2. Cells were maintained in N2 medium until 90% confluency (which usually required 4 days), changing the medium every other day. Once the mFPPs had reached 90% confluency, they were passaged and replated onto fresh matrigel-coated plates at a density of 75×10^3 cells/cm^2 and cultured further in N2 medium. mFPPs were passaged and replated every 4-5 days for at least 4 passages and cells were counted and stored in liquid nitrogen at each passage (Figure 8).

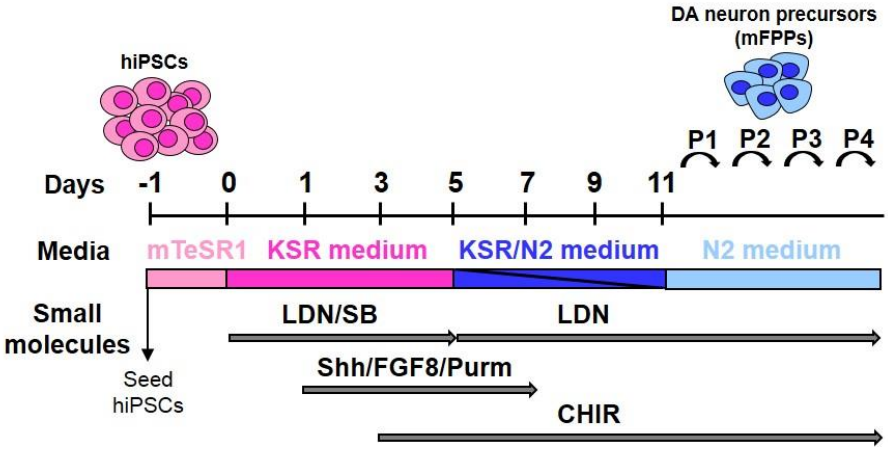

Figure 8. *Differentiation of human iPSCs into midbrain floor plate progenitors (mFPPs).* Schematic diagram of the time and conditions used for the generation of mFPPs from human iPSCs. KSR, knockout serum replacement; LDN, LDN193189; SB, SB431542; Shh, Shh C25II; FGF8, fibroblast growth factor 8; Purm, purmorphamine; CHIR, CHIR99021.

4.1.2 Differentiation of midbrain floor plate progenitors into mature DA neurons

At day 11, F3 mFPPs showed the distinctive co-expression of the floor plate marker FOXA2 and the roof plate marker LMX1α as confirmed by immunofluorescence analysis (Figure 10).

DA neuron differentiation was induced when the expanded mesencephalic DA neuron precursors reached 90% confluency by switching the cultures to Neurobasal/B27 medium containing BDNF, ascorbic acid, cAMP, TGFβ3, GDNF and DAPT.

At day 21, mFPPs were transferred on plates pre-coated with Poly-DL-ornithine / Fibronectin / Laminin and pre-seeded with a feeder layer of mouse primary cortical astrocytes.

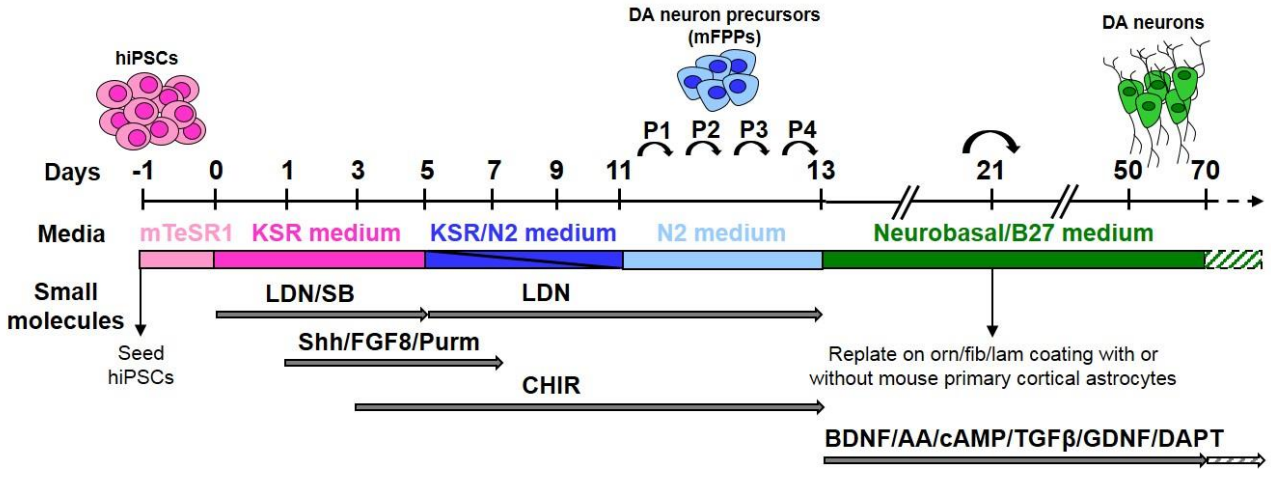

Figure 9. *Differentiation of mFPPs into mature DA neurons.* Schematic diagram of the time and conditions used for the differentiation of mature DA neurons from human iPSCs. KSR, knockout serum replacement; LDN, LDN193189; SB, SB431542; Shh, Shh C25II; FGF8, fibroblast growth factor 8; Purm, purmorphamine; CHIR, CHIR99021; BDNF, brain-derived neurotrophic factor; AA, ascorbic acid; cAMP, dibutyryl cAMP; TGFβ, transforming growth factor type β3; GDNF, glial cell line-derived neurotrophic factor.

At day 30, $MAP2^+/TH^+$ neurons were visualized in the cultures. At day 70, most TH^+ neurons consistently co-expressed the dopamine transporter (DAT), indicating a mature DA neuronal phenotype.

GABAergic and glutamatergic neurons identified by expression of GAD67 and VGLUT2, respectively, were also present. Cell count indicated 30% ± 5% of TH^+ neurons, 23% ± 4% of $GAD67^+$ neurons, and 28% ± 6% of $VGLUT2^+$ neurons co-stained with anti-MAP2 antibody. 5-HT neurons were also present (Figure 10).

Semiquantitative RT-PCR analysis confirmed the expression of LMX1α, LMX1β, FOXA2, NURR1, ENGRAILED 1 (EN1), TH and Dopa decarboxylase (DDC) from day 11. The mRNAs for Oct3/4 and Nanog, markers of pluripotency, progressively decreased during differentiation (Figure 10).

The neurochemical evidence of a functional DAT uptake of DA neurons cultured for 70 days was obtained by measuring the level of dopamine in the culture supernatant by HPLC over a time course up to 24 hrs. One-way ANOVA showed a highly significant treatment effect at 9 hrs ($*P < 0.05$) and at 24 hrs ($***P < 0.001$), post-hoc Bonferroni's test (Figure 10). These results indicate spontaneous release of dopamine, as shown by the progressive increase of dopamine levels after vehicle over time, as expected by mature DA neurons.

The ability of the DA neurons to activate spontaneous action potentials at 60 days was shown by electrophysiological analysis using patch-clamp technique (Figure 10). These results confirm the functionality and the maturity of the DA neurons differentiated from mFPPs.

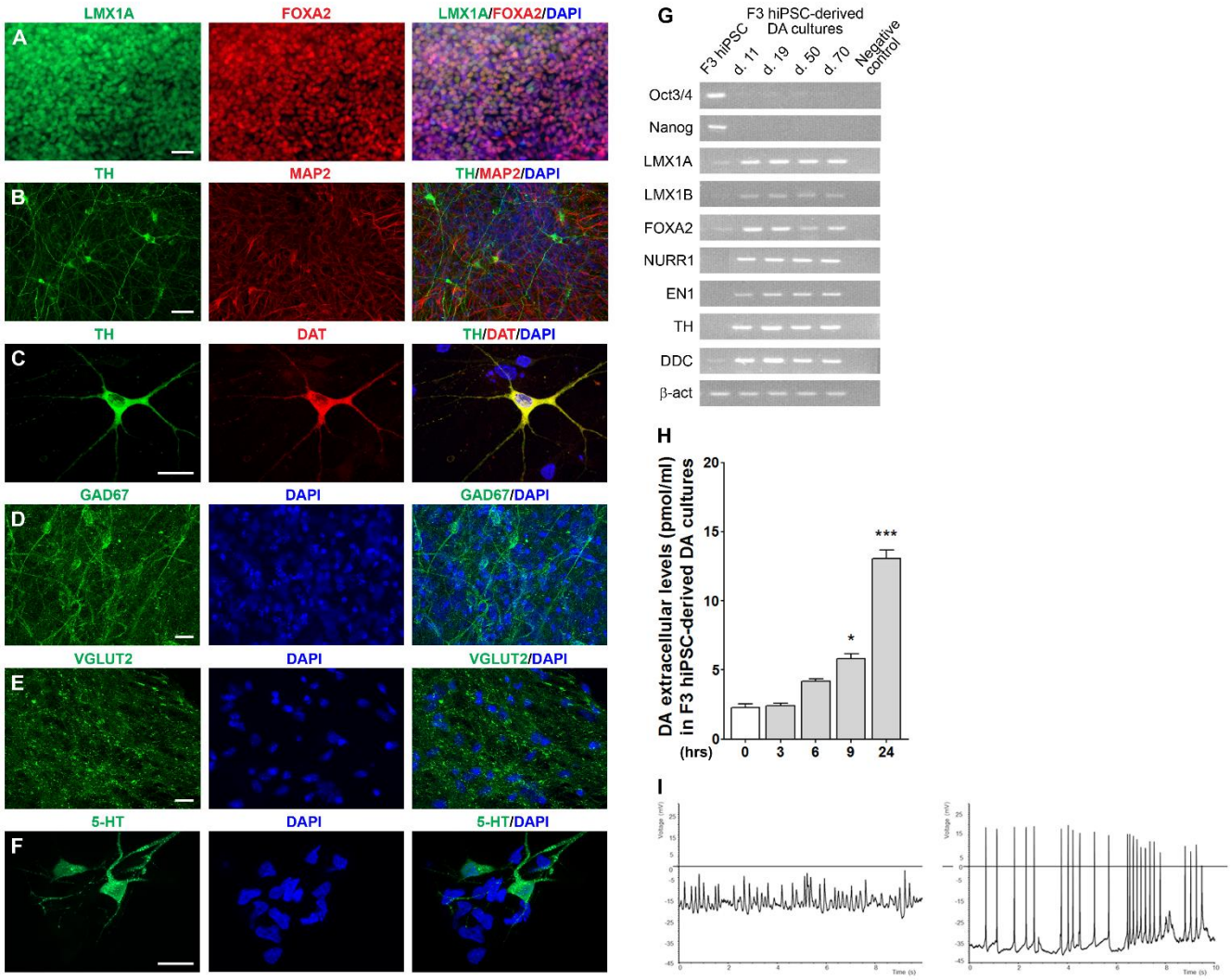

Figure 10. *Representative images of dual immunofluorescence indicating co-expression of:* LMX1α (green) and FOXA2 (red) in dopaminergic progenitors at day 11, TH (green) and MAP2 (red) in neurons at day 30; TH (green) and DAT (red) in DA neurons at day 70. Immunofluorescence of GAD67 (green), VGLUT2 (green) and 5-HT (green) in neuronal cultures at day 70. Cell nuclei were stained with DAPI (blue). Scale bar: (A, B, D and E) = 40 μm; (C and F) = 20 μm.

(G) Semiquantitative RT-PCR analysis of gene expression at the iPSC stage and at day 11, 19, 50, and 70 of dopaminergic differentiation (negative controls contain PCR Master Mix and primers, but no cDNA).

(H) Dopamine level measured by HPLC in the supernatant of F3 DA cultures (day 70) over a time course (0, 3, 6, 9, and 24 hrs after administration).

(I) Electrophysiology test using patch-clamp technique. Oscillation of the resting membrane potential at day 40 and spontaneous action potentials at day 60.

Data are expressed as mean ± SEM (***P < 0.001 versus vehicle at 24 hrs, *P < 0.05 versus vehicle at 9 hrs; post-hoc Bonferroni's test).

4.2 Second subproject

4.2.1 Effects of piribedil and pramipexole on structural plasticity of hiPSC-derived DA neurons

Recent data have demonstrated a neurotrophic effect produced by the anti-parkinsonian DA D2/D3 receptor (D2R/D3R) agonist, ropinirole (Collo G et al. 2018). Based on these findings, the cellular and molecular effects of piribedil and pramipexole on human DA neurons were evaluated by studying morphological changes linked to structural plasticity and the activation of the associated intracellular pathways.

DA neurons derived from F3 hiPSCs were exposed to piribedil for 72 hours (hrs). DA neurons were visualized using an anti-TH antibody (Figure 12A). Piribedil (0.01-20 µM) produced a dose-dependent effect on structural plasticity 72 hrs after the beginning of treatment when measured as maximal length of dendrites, number of primary dendrites and soma area. One-way ANOVA indicated a significant dose-dependent effect for the maximal length of dendrites, number of primary dendrites and soma area (Bonferroni's test) (Figure 12B-D). Post-hoc multiple comparisons indicated that the treatment effect versus vehicle for the three parameters started at the dose of 10 µM ($P < 0.001$, Bonferroni's test) (Figure 12B-D). The statistical analysis is indicated in Table 1.

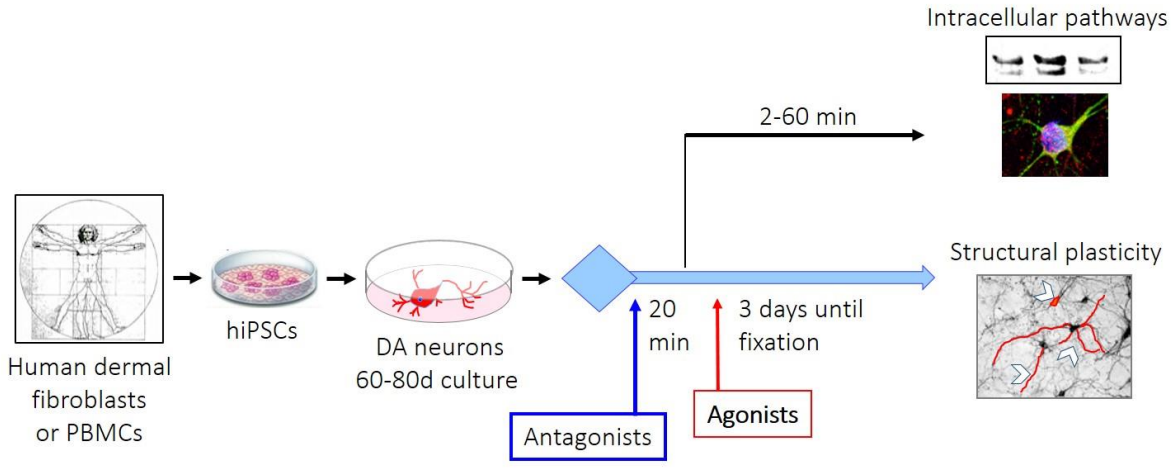

Figure 11. *Experimental paradigm used to investigate the effects of pharmacological agents in human hiPSC-derived DA neurons.* DA neurons derived from F3 hiPSCs were exposed to dopaminergic agonists piribedil and pramipexole and the cellular and molecular effects were studied by immunohistochemistry, morphological analysis, and biochemistry. Agonists: Piribedil, Pramipexole. Antagonists: a) D3R preferential antagonists SB277011-A, S33084; b) MEK inhibitor PD98059; c) PI3K inhibitor LY294002; d) mTOR inhibitor rapamycin.

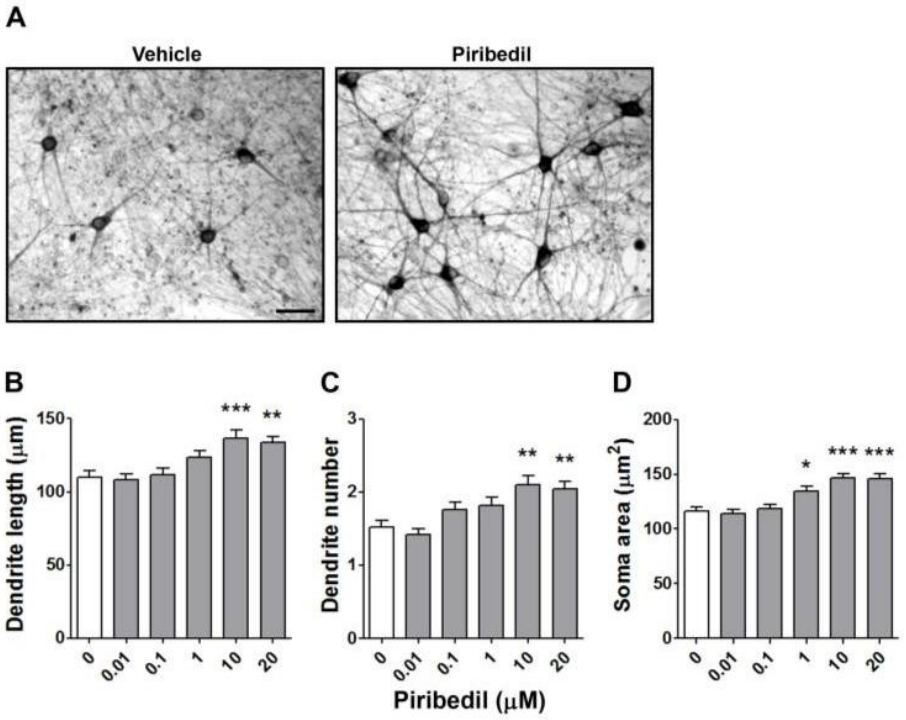

Figure 12. *Piribedil promotes structural plasticity of human iPSC-derived DA neurons.* **(A)** Representative photomicrographs of human F3 DA neurons (70 days in culture) 72 hrs after exposure to vehicle or to 10 μM piribedil. Scale bar: 30 μm. **(B-D)** Concentration response curves of the effect of piribedil on maximal length of dendrites, number of primary dendrites and soma area of human F3 DA neurons. In all panels, values are represented as mean ± S.E.M. (***P<0.001; **P<0.01; *P<0.05 vs. vehicle (0); post-hoc Bonferroni's test).

Table 1. *Statistical analysis.*

Experiment	One-way ANOVA	Dendrite length	Dendrite number	Soma area
Dose curve	Treatment	F(5,174) = 7.58 *** P<0.001	F(5,294) = 6.89 *** P<0.001	F(5,234) = 13.81 *** P<0.001

4.2.2 Effects of pramipexole on structural plasticity of hiPSC-derived DA neurons

DA neurons derived from F3 hiPSCs were exposed to pramipexole for 72 hrs. Pramipexole (0.01-20 μM) produced a dose-dependent effect on structural plasticity 72 hrs after the beginning of treatment when measured as maximal length of dendrites, number of primary dendrites and soma area. One-way ANOVA indicated a significant dose-dependent effect for the maximal length of dendrites, number of primary dendrites and soma area (Bonferroni's test) (Figure 13B-D). Post-hoc multiple comparisons indicated that the treatment effect versus vehicle for the three parameters started at the dose of 1 μM ($P < 0.01$, Bonferroni's test) (Figure 13B-D). The statistical analysis is indicated in Table 2.

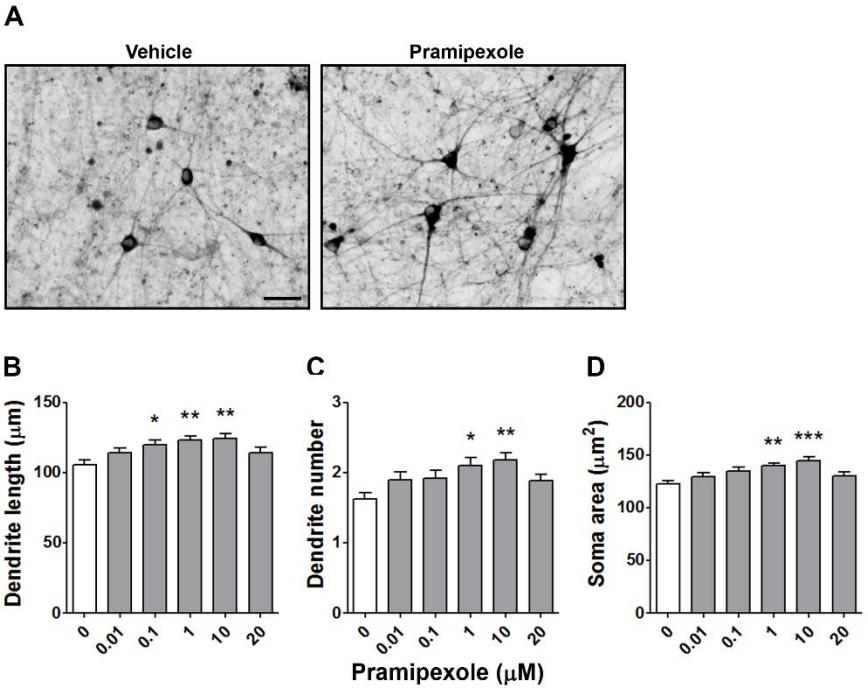

Figure 13. *Pramipexole promotes structural plasticity of human iPSC-derived DA neurons.* **(A)** Representative photomicrographs of human F3 DA neurons (70 days in culture) 72 hrs after exposure to vehicle or to 10 µM pramipexole. Scale bar: 30 µm. **(B-D)** Concentration response curves of the effect of pramipexole on maximal length of dendrites, number of primary dendrites and soma area of human F3 DA neurons. In all panels, values are represented as mean ± S.E.M. (***P<0.001; **P<0.01; *P<0.05 vs. vehicle (0); post-hoc Bonferroni's test).

Table 2. *Statistical analysis.*

Experiment	One-way ANOVA	Dendrite length	Dendrite number	Soma area
Dose curve	Treatment	F(5,174) = 4.32 *** P<0.001	F(5,294) = 3.53 ** P<0.01	F(5,234) = 5.01 *** P<0.001

4.2.3 Piribidil-induced structural plasticity is mediated via mTOR pathway activation

The effect of piribedil (10 µM) on the phosphorylation of p70S6K, one of the main substrates of the activated mammalian target of rapamycin complex 1 (mTORC1), was investigated in F3 hiPSC-derived DA neurons by western blot and immunofluorescence analysis. In acute experiments, using western blot quantification, piribedil significantly increased phosphorylated p70S6K (p-p70S6K) after 2 min (Figure 14A). The potential involvement of MEK-ERK and PI3K-Akt pathways in mediating the effects of piribedil on p-p70S6K was studied using the MEK inhibitor PD98059 (10 µM) and the PI3-K inhibitor LY294002 (10 µM). The mTORC1 involvement was studied using its inhibitor rapamycin (20 nM). Pretreatments (20 minutes) with each inhibitor separately blocked the effects

of piribedil measured in F3 hiPSC-derived DA cultures. Two-way ANOVA indicated a significant treatment effect, a significant inhibition effect of PD98059, LY294002 and rapamycin and a significant interaction. No effects on p-p70S6K were observed when PD98059, LY294002 or rapamycin were incubated with vehicle (Figure 14B and Table 3).

Parallel immunofluorescence experiments showed that piribedil significantly increased the basal levels of p-p70S6K in TH^+ neurons (Figure 14C-D) while pretreatments with PD98059, LY294002 or rapamycin followed by piribedil prevented the increase of p-p70S6K (Figure 14E-G). No effects on p-p70S6K were observed when PD98059, LY294002 or rapamycin were incubated with vehicle (Figure 14H-J).

The role of intracellular signaling leading to mTOR pathway activation in structural plasticity of DA neurons induced by piribedil was investigated using the same kinase inhibitors of the intracellular pathways. Pretreatments with PD98059 (10 µM), LY294002 (10 µM) and rapamycin (20 nM) significantly ($P < 0.01$, Bonferroni's test) counteracted the effects of piribedil on all three structural plasticity parameters as supported by the significant two-way ANOVA interaction obtained on the maximal length of dendrites, number of primary dendrites and soma area. No changes were seen when the D3R antagonists were dosed in the presence of vehicle (Figure 14K-M). The statistical analysis is indicated in Table 3.

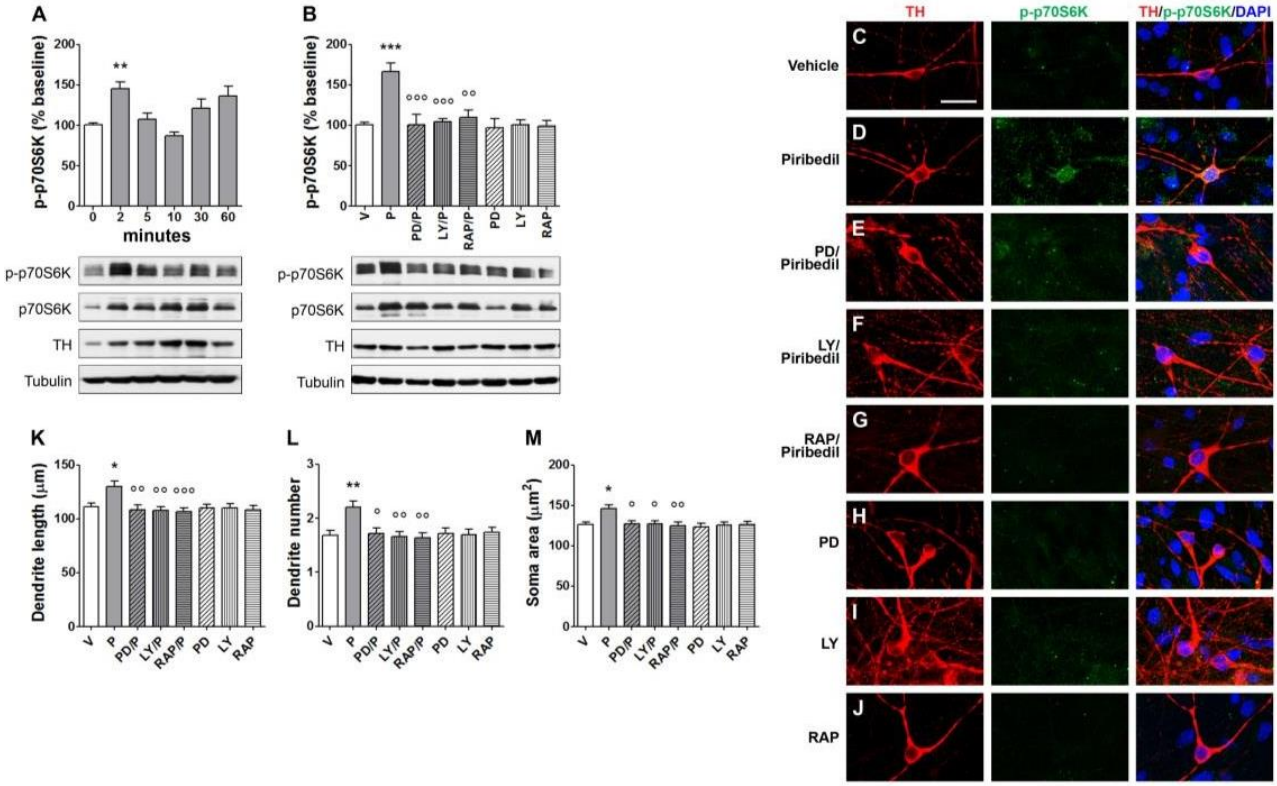

Figure 14. *Piribedil increases phosphorylation of p70S6K in human iPSC-derived DA neurons.* **(A)** Time course of phosphorylated p70S6K (p-p70S6K) induced by piribedil (10 µM) respectively, at 0, 2, 5, 10, 30 and 60 min, analysed by densitometry of western blots (n=6) (top panels); the specific levels of p-p70S6K were normalised to the corresponding p70S6K, TH and tubulin levels. The densitometric values are represented as percentage of vehicle values. Lower panels: representative western blots. (**B**) Blockade of p-p70S6K induced by piribedil (10 µM) after pretreatment (20 min) with the MEK inhibitor PD98059 (10 µM), the PI3-K inhibitor LY294002 (10 µM) or the mTORC1 inhibitor rapamycin (20 nM) assessed after 2 min and analyzed by densitometry of western blots (n=3) (top panels). Lower panels: representative western blots. **(C-J)** Representative photomicrographs of F3 DA neurons showing p-p70S6K increase in the soma and dendrites of TH^+ neurons 2 min after piribedil (10 µM) following pretreatment with vehicle **(D)**. **(E)** Blockade of p-p70S6K by pretreatment (20 min) with PD98059 (10 µM), **(F)** LY294002 (10 µM) or **(G)** the mTORC1 inhibitor rapamycin (20 nM) followed by piribedil (2 min). **(C)** Vehicle; **(H)** PD98059 alone; **(I)** LY294002 alone; **(J)** rapamycin alone. TH (green), p-p70S6K (red). Cell nuclei were stained with DAPI (blue). Scale bar: 20 µm. **(K-M)** Inhibition of the effects of piribedil (10 µM) on structural plasticity of F3 DA neurons following pretreatment (20 min) with the MEK inhibitor PD98059 (10 µM), the PI3-K inhibitor LY294002 (10 µM) or the mTORC1 inhibitor rapamycin (20 nM) assessed as **(K)** maximal length of dendrites, **(L)** number of primary dendrites and **(M)** soma area after 72 hrs. When inhibitors were tested with the vehicle, no changes of structural plasticity were visualized. In all panels, values are represented as mean ± S.E.M. (***P<0.001; **P<0.01; *P<0.05 vs. vehicle; °°°P<0.001; °°P<0.01; °P<0.05 vs. piribedil; post-hoc Bonferroni's test). V = vehicle; P = piribedil; PD = PD98059; LY = LY294002; RAP = rapamycin.

Table 3. *Statistical analysis.*

Experiment	One-way ANOVA	p-p70S6K
Time course	Treatment	F(5,54) = 6.67 *** P<0.001

Experiment	Two-way ANOVA	p-p70S6K
(mTOR inh.)	Interaction	F(3,40) = 6.95 *** P<0.001
X	Piribedil Factor	F(1,40) = 9.12 ** P<0.01
(Pir/Veh)	Inhibitor Factor	F(3,40) = 7.89 ** P<0.01

Experiment	Two-way ANOVA	Dendrite length	Dendrite number	Soma area
(PD98059)	Interaction	F(1,116) = 6.18 * P<0.05	F(1,196) = 6.56 * P<0.05	F(1,156) = 3.59 * P<0.05
X	Piribedil Factor	F(1,116) = 4.72 * P<0.05	F(1,196) = 6.56 * P<0.05	F(1,156) = 8.40 ** P<0.01
(Pir/Veh)	Inhibitor Factor	F(1,116) = 7.57 ** P<0.01	F(1,196) = 4.69 * P<0.05	F(1,156) = 6.67 * P<0.05

Experiment	Two-way ANOVA	Dendrite length	Dendrite number	Soma area
(LY294002)	Interaction	F(1,116) = 7.26 ** P<0.01	F(1,196) = 7.95 ** P<0.01	F(1,156) = 5.29 * P<0.05
X	Piribedil Factor	F(1,116) = 4.56 * P<0.05	F(1,196) = 5.84 * P<0.05	F(1,156) = 6.44 * P<0.05
(Pir/Veh)	Inhibitor Factor	F(1,116) = 8.58 ** P<0.01	F(1,196) = 6.86 ** P<0.01	F(1,156) = 5.54 * P<0.05

Experiment	Two-way ANOVA	Dendrite length	Dendrite number	Soma area
(Rapamycin)	Interaction	F(1,116) = 6.73 * P<0.05	F(1,196) = 9.61 ** P<0.01	F(1,156) = 6.04 * P<0.05
X	Piribedil Factor	F(1,116) = 4.92 * P<0.05	F(1,196) = 4.41 * P<0.05	F(1,156) = 4.62 * P<0.05
(Pir/Veh)	Inhibitor Factor	F(1,116) = 10.70 ** P<0.01	F(1,196) = 6.25 * P<0.05	F(1,156) = 5.91 * P<0.05

4.2.4 Pramipexole-induced structural plasticity is mediated via mTOR pathway activation

The role of intracellular signaling leading to mTOR pathway activation in structural plasticity of DA neurons induced by pramipexole was investigated using kinase inhibitors of the intracellular pathways PD98059, LY294002 and rapamycin. Pretreatments with PD98059 (10 µM), LY294002 (10 µM) and rapamycin (20 nM) significantly ($P < 0.01$, Bonferroni's test) counteracted the effects of pramipexole on all three structural plasticity parameters as supported by the significant two-way ANOVA interaction obtained on the maximal length of dendrites, number of primary dendrites and soma area. No changes were seen when the kinase inhibitors were dosed in the presence of vehicle (Figure 15A-C). The statistical analysis is indicated in Table 4.

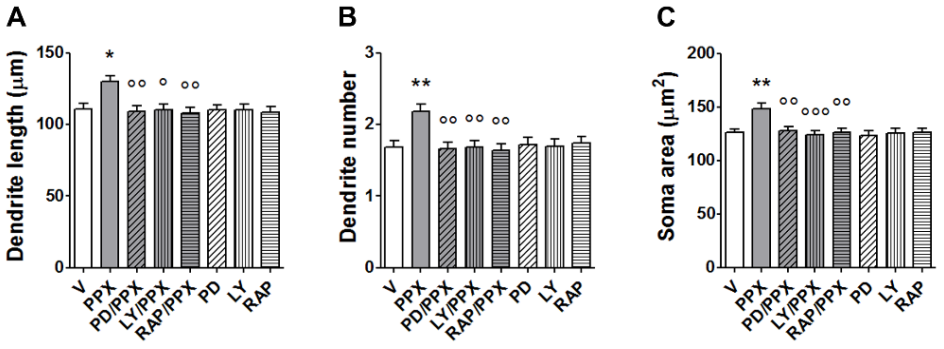

Figure 15. *Pramipexole activates mTOR pathway in human iPSC-derived DA neurons.* **(A-C)** Inhibition of the effects of pramipexole (10 µM) on structural plasticity of F3 DA neurons following pretreatment (20 min) with the MEK inhibitor PD98059 (10 µM), the PI3-K inhibitor LY294002 (10 µM), and the mTORC1 inhibitor rapamycin (20 nM) assessed as **(A)** maximal length of dendrites, **(B)** number of primary dendrites and **(C)** soma area after 72 hrs. When inhibitors were tested with the vehicle, no changes of structural plasticity were visualized. In all panels, values are represented as mean ± S.E.M. (**P<0.01; *P<0.05 vs. vehicle; °°°P<0.001; °°P<0.01; °P<0.05 vs. pramipexole; post-hoc Bonferroni's test). V = vehicle; PPX = pramipexole; PD = PD98059; LY = LY294002; RAP = rapamycin.

Table 4. *Statistical analysis.*

Experiment	Two-way ANOVA	Dendrite length	Dendrite number	Soma area
(PD98059)	Interaction	F(1,116) = 4.81 * P<0.05	F(1,196) = 3.74 ** P<0.01	F(1,156) = 2.65 * P<0.05
X	Pramipexole Factor	F(1,116) = 3.96 * P<0.05	F(1,196) = 2.31 * P<0.05	F(1,156) = 5.90 ** P<0.01
(PPX/Veh)	Inhibitor Factor	F(1,116) = 5.91 ** P<0.01	F(1,196) = 2.75 * P<0.05	F(1,156) = 4.59 ** P<0.01

Experiment	Two-way ANOVA	Dendrite length	Dendrite number	Soma area
(LY294002)	Interaction	F(1,116) = 4.17 * P<0.05	F(1,196) = 3.35 ** P<0.01	F(1,156) = 4.84 ** P<0.01
X	Pramipexole Factor	F(1,116) = 4.29 * P<0.05	F(1,196) = 2.86 * P<0.05	F(1,156) = 3.45 * P<0.05
(PPX/Veh)	Inhibitor Factor	F(1,116) = 5.02 * P<0.05	F(1,196) = 2.86 * P<0.05	F(1,156) = 5.02 ** P<0.01

Experiment	Two-way ANOVA	Dendrite length	Dendrite number	Soma area
(Rapamycin)	Interaction	F(1,116) = 4.40 * P<0.05	F(1,196) = 4.38 ** P<0.01	F(1,156) = 4.39 ** P<0.01
X	Pramipexole Factor	F(1,116) = 4.29 * P<0.05	F(1,196) = 1.95 * P<0.05	F(1,156) = 4.46 ** P<0.01
(PPX/Veh)	Inhibitor Factor	F(1,116) = 7.20 ** P<0.01	F(1,196) = 2.80 * P<0.05	F(1,156) = 4.30 ** P<0.01

4.2.5 Activation of mTOR pathway and structural plasticity induced by piribedil depend on D3R signaling

The role of D3 receptor in mediating p70S6K phosphorylation and structural plasticity of DA neurons induced by piribedil was investigated by pretreatments with two selective D3R antagonists SB277011-A (100 nM) and S33084 (10 nM). Both antagonists significantly attenuated the increase of p-p70S6K produced by piribedil as measured by western blot in F3 DA neuronal cultures 2 min after exposure. Two-way ANOVA indicated a significant treatment effect, a significant inhibition effect of PD98059, LY294002 and rapamycin and a significant interaction. No effects on p-p70S6K were observed when SB277011-A or S33084 was incubated with vehicle (Figure 16A and Table 5). Parallel immunofluorescence experiments showed that piribedil significantly increased the basal levels of p-p70S6K in TH^+ neurons (Figure 16B-C) while pretreatments with SB27701-A or S33084 followed by piribedil prevented the increase of p-p70S6K (Figure 16D-E). No effects on p-p70S6K were observed when SB277011-A or S33084 were incubated with vehicle (Figure 16F-G).

The role of D3R-dependent signaling in structural plasticity produced by piribedil was assessed 72 hrs after the pharmacological blockade of D3R. Pretreatments with SB277011-A (50 nM) and S33084 (10 nM) significantly (P<0.0001, Bonferroni's test) counteracted the effects of piribedil on all three structural plasticity parameters as supported by the significant two-way ANOVA interaction obtained on the maximal length of dendrites, number of primary dendrites and soma area. No changes were seen when the kinase inhibitors were dosed in the presence of vehicle (Figure 16H-J). The statistical analysis is indicated in Table 5.

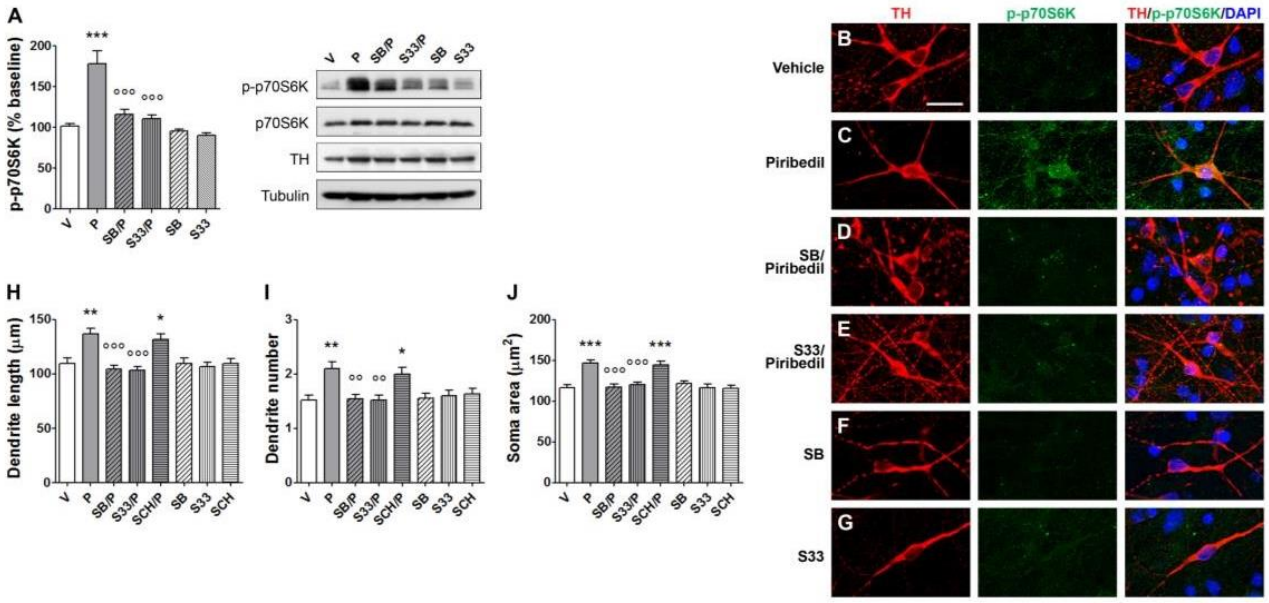

Figure 16. *Piribedil increases phosphorylation of p70S6K in human iPSC-derived DA neurons via activation of D3 receptor.* **(A)** Blockade of p-p70S6K induced by piribedil (10 µM) in F3 DA neurons after pretreatment (20 min) with the D3R antagonists SB277011-A (50 nM) or S33084 (10 nM) assessed after 2 min and analyzed bydensitometry of western blots (n=3) (top panels). Lower panels: representative western blots. **(B-G)** Representative photomicrographs of F3 DA neurons showing p-p70S6K increase in the soma and dendrites of TH^+ neurons 2 min after piribedil (10 µM) following pretreatment with vehicle **(C)**. **(D)** Blockade of p-p70S6K by pretreatment (20 min) with SB277011-A (50 nM) or **(E)** S33084 (10 nM) followed by piribedil (2 min). **(B)** Vehicle; **(F)** SB277011-A alone; **(G)** S33084 alone. TH (green), p-p70S6K (red). Cell nuclei were stained with DAPI (blue). Scale bar: 20 µm. **(H-J)** Inhibition of the effects of piribedil (10 µM) on structural plasticity of F3 DA neurons following pretreatment (20 min) with the D3R antagonists SB277011-A (50 nM) or S33084 (10 nM) assessed as **(H)** maximal length of dendrites, **(I)** number of primary dendrites and **(J)** soma area after 72 hrs. Pretreatment (20 min) with the D1R antagonist SCH23390 (1 µM) was ineffective. When antagonists were tested with the vehicle, no changes of structural plasticity were visualized. In all panels, values are represented as mean ± S.E.M. (***P<0.001; **P<0.01; *P<0.05 vs. vehicle; ^{ooo}P<0.001; ^{oo}P<0.01 vs. piribedil; post-hoc Bonferroni's test). V = vehicle; P = piribedil; SB = SB277011-A; S33 = S33084; SCH = SCH23390.

Table 5. *Statistical analysis.*

Experiment	Two-way ANOVA	p-p70S6K
(DA antag.)	Interaction	F(2,44) = 6.15 ** P<0.01
X	Piribedil Factor	F(1,44) = 21.88 *** P<0.001
(Pir/Veh)	Inhibitor Factor	F(2,44) = 10.62 *** P<0.001

Experiment	Two-way ANOVA	Dendrite length	Dendrite number	Soma area
(SB277011-A)	Interaction	F(1,116) = 11.34 ** P<0.01	F(1,196) = 9.62 ** P<0.01	F(1,156) = 11.61 *** P<0.001
X	Piribedil Factor	F(1,116) = 5.03 * P<0.05	F(1,196) = 8.38 ** P<0.01	F(1,156) = 6.36 *** P<0.001
(Pir/Veh)	Inhibitor Factor	F(1,116) = 11.52 *** P<0.001	F(1,196) = 7.22 ** P<0.01	F(1,156) = 5.67 *** P<0.001

Experiment	Two-way ANOVA	Dendrite length	Dendrite number	Soma area
(S33084)	Interaction	F(1,116) = 11.71 *** P<0.001	F(1,196) = 10.52 ** P<0.01	F(1,156) = 6.50 *** P<0.001
X	Piribedil Factor	F(1,116) = 6.47 * P<0.05	F(1,196) = 6.04 * P<0.05	F(1,156) = 10.02 *** P<0.001
(Pir/Veh)	Inhibitor Factor	F(1,116) = 16.56 *** P<0.001	F(1,196) = 6.04 * P<0.05	F(1,156) = 6.08 *** P<0.001

Experiment	Two-way ANOVA	Dendrite length	Dendrite number	Soma area
(SCH23390)	Interaction	F(1,116) = 0.21 NS	F(1,196) = 0.98 NS	F(1,156) = 0.04 NS
X	Piribedil Factor	F(1,116) = 23.87 *** P<0.001	F(1,196) = 17.97 *** P<0.001	F(1,156) = 26.64 *** P<0.001
(Pir/Veh)	Inhibitor Factor	F(1,116) = 0.25 NS	F(1,196) = 0.01 NS	F(1,156) = 0.07 NS

4.2.6 Activation of mTOR pathway and structural plasticity induced by pramipexole depend on D3R signaling

The role of D3 receptor in mediating p70S6K phosphorylation and structural plasticity of DA neurons induced by pramipexole was investigated by pretreatments with two selective D3R antagonists SB277011-A (100 nM) and S33084 (10 nM). Pretreatments with the selective D3R antagonists SB277011-A (50 nM) and S33084 (10 nM) significantly (P<0.001, Bonferroni's test) counteracted the effects of pramipexole on all three structural plasticity parameters as supported by the significant two-way ANOVA interaction obtained on the maximal length of dendrites, number of primary dendrites and soma area. No blocking effects on three structural plasticity parameters were obtained when DA neurons were pretreated with the D1R antagonist SCH23390 (1 µM). Finally, no changes were seen when the D3R antagonists were dosed in the presence of vehicle (Figure 17A-C). The statistical analysis is indicated in Table 6.

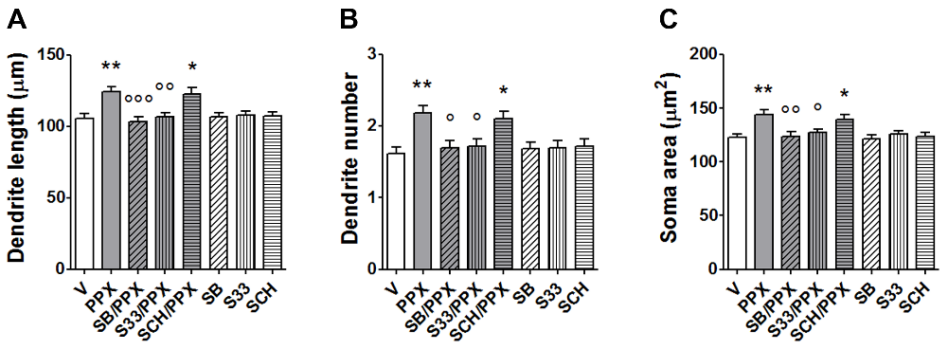

Figure 17. *Pramipexole activates mTOR pathway in human iPSC-derived DA neurons via activation of D3 receptor.* **(A-C)** Inhibition of the effects of pramipexole (10 µM) on structural plasticity of F3 DA neurons following pretreatment (20 min) with the D3R antagonists SB277011-A (50 nM) or S33084 (10 nM) assessed

as **(A)** maximal length of dendrites, **(B)** number of primary dendrites and **(C)** soma area after 72 hrs. Pretreatment (20 min) with the D1R antagonist SCH23390 (1 μM) was ineffective. When antagonists were tested with the vehicle, no changes of structural plasticity were visualized. In all panels, values are represented as mean ± S.E.M. (**P<0.01; *P<0.05 vs. vehicle; ^{ooo}P<0.001; ^{oo}P<0.01; ^{o}P<0.05 vs. pramipexole; post-hoc Bonferroni's test). V = vehicle; PPX = pramipexole; SB = SB277011-A; S33 = S33084; SCH = SCH23390.

Table 6. *Statistical analysis.*

Experiment	Two-way ANOVA	Dendrite length	Dendrite number	Soma area
(SB277011-A)	Interaction	F(1,116) = 7.81 ** P<0.01	F(1,196) = 3.62 ** P<0.01	F(1,156) = 3.74 * P<0.05
X	Pramipexole Factor	F(1,116) = 3.92 * P<0.05	F(1,196) = 4.18 ** P<0.01	F(1,156) = 5.52 ** P<0.01
(PPX/Veh)	Inhibitor Factor	F(1,116) = 6.71 ** P<0.01	F(1,196) = 2.19 * P<0.05	F(1,156) = 4.68 ** P<0.01

Experiment	Two-way ANOVA	Dendrite length	Dendrite number	Soma area
(S33084)	Interaction	F(1,116) = 6.37 ** P<0.01	F(1,196) = 3.53 ** P<0.01	F(1,156) = 4.66 ** P<0.01
X	Pramipexole Factor	F(1,116) = 5.19 ** P<0.01	F(1,196) = 4.07 ** P<0.01	F(1,156) = 6.48 *** P<0.001
(PPX/Veh)	Inhibitor Factor	F(1,116) = 4.22 * P<0.05	F(1,196) = 1.75 NS	F(1,156) = 2.38 * P<0.05

Experiment	Two-way ANOVA	Dendrite length	Dendrite number	Soma area
(SCH23390)	Interaction	F(1,116) = 0.12 NS	F(1,196) = 0.36 NS	F(1,156) = 0.25 NS
X	Pramipexole Factor	F(1,116) = 15.67 *** P<0.001	F(1,196) = 9.76 *** P<0.001	F(1,156) = 13.74 *** P<0.001
(PPX/Veh)	Inhibitor Factor	F(1,116) = 0.00 NS	F(1,196) = 0.00 NS	F(1,156) = 0.15 NS

4.2.7 Structural plasticity induced by piribedil and pramipexole requires active BDNF-TrkB signaling

The blocking of BDNF-TrkB signaling in human iPSC-derived DA neurons prevented structural plasticity induced by D3R preferential agonist ropinirole (Collo G et al. 2018). Here the same BDNF-TrkB signaling inhibitors were used: an anti-BDNF blocking antibody (α-BDNF) (10 μg/ml) (Lepack AE et al. 2014), a TrkB-Fc Chimera (5 μg/ml) (Jourdi H et al. 2009), a TrkB receptor blocker K252a (200 nM) (Jourdi H et al. 2009), and a Src phosphorylation inhibitor PP2 (10 μM) (Sanna PP et al. 2000).
F3 DA neuronal cultures were pretreated with the BDNF-TrkB signaling inhibitors (20 min) before exposing to piribedil or pramipexole. All the inhibitors antagonized the effects of piribedil and pramipexole on all three structural plasticity parameters as supported by the significant two-way ANOVA interaction obtained on the maximal length of dendrites, number of primary dendrites and soma area (Figure 18A-D and Table 7). No changes were seen when BDNF-TrkB signaling blockers were dosed in the presence of vehicle (Figure 18A-D). The statistical analysis is indicated in Table 7.

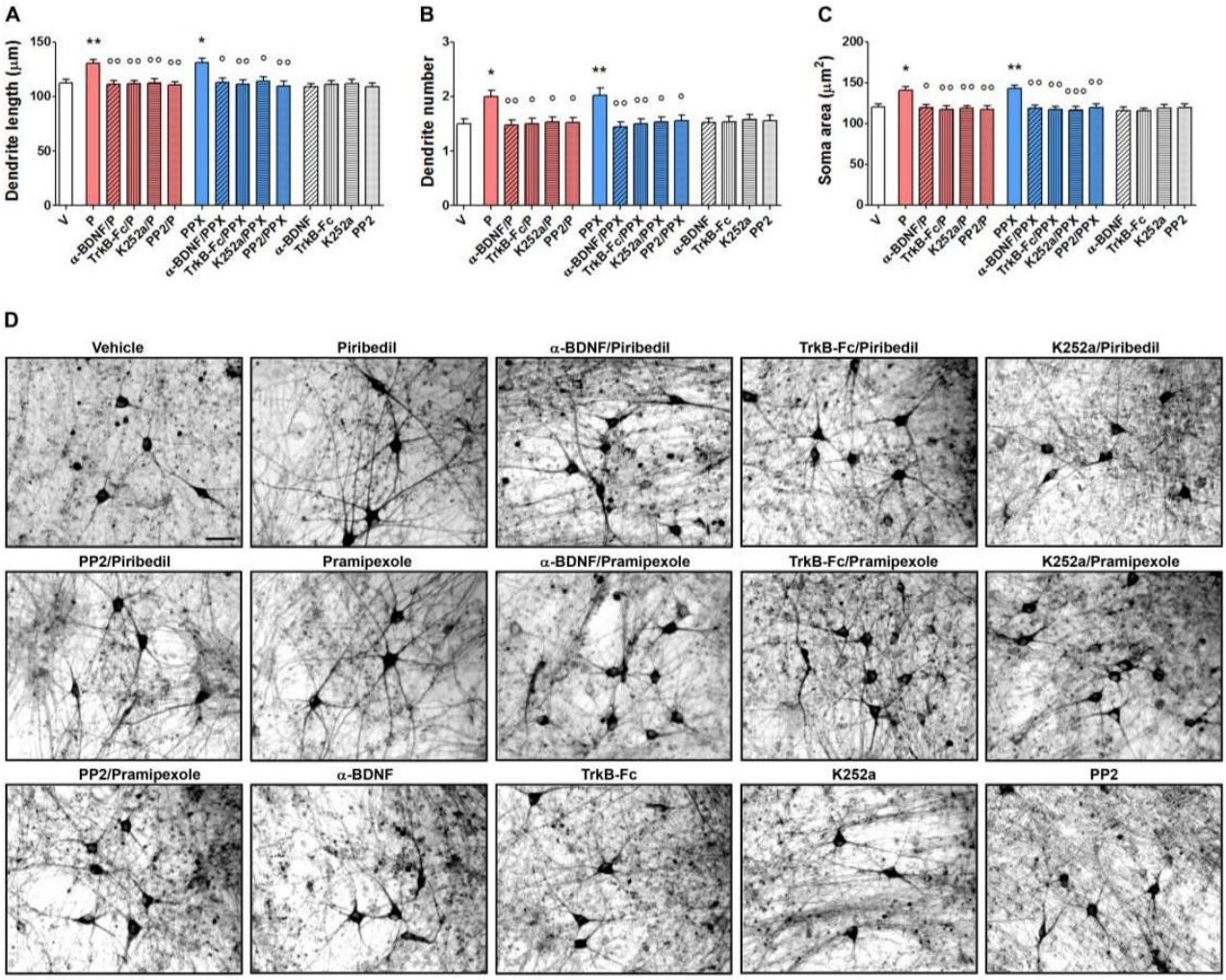

Figure 18. *Structural plasticity induced by piribedil and pramipexole in human iPSC-derived DA neurons is prevented by BDNF-TrkB signaling inhibitors.* **(A-C)** Inhibition of the effects of piribedil (10 µM) and pramipexole (10 µM) on structural plasticity of F3 DA neurons following pretreatment (20 min) with an anti-BDNF blocking antibody (α-BDNF) (10 µg/ml), a TrkB-Fc Chimera (5 µg/ml), the TrkB-phosphorylation inhibitor K252a (200 nM) and the TrkB-Src phosphorylation inhibitor PP2 (10 µM), assessed as **(A)** maximal length of dendrites, **(B)** number of primary dendrites and **(C)** soma area after 72 hrs. When inhibitors were tested with the vehicle, no changes of structural plasticity were visualized. In all panels, values are represented as mean ± S.E.M. (**P<0.01; *P<0.05 vs. vehicle; °°°P<0.001; °°P<0.01; °P<0.05 vs. piribedil or pramipexole; post-hoc Bonferroni's test). **(D)** Representative photomicrographs of human F3 DA neurons 72 hrs after exposure to vehicle, 10 µM piribedil, 10 µM pramipexole, 10 µg/ml α-BDNF, 5 µg/ml TrkB-Fc Chimera, 200 nM K252a or 10 µM PP2 together with piribedil, pramipexole or vehicle. Scale bar: 30 µm. Abbreviations: V = vehicle; P = piribedil; PPX = pramipexole; α-BDNF = anti-BDNF blocking antibody; TrkB-Fc = TrkB-Fc Chimera.

Table 7. *Statistical analysis.*

Experiment	Two-way ANOVA	Dendrite length	Dendrite number	Soma area
(α-BDNF)	Interaction	F(1,116) = 5.17 * P<0.05	F(1,196) = 7.99 ** P<0.01	F(1,156) = 4.39 * P<0.05
X	Piribedil Factor	F(1,116) = 9.32 * P<0.05	F(1,196) = 5.80 * P<0.05	F(1,156) = 8.81 ** P<0.01
(Pir/Veh)	Inhibitor Factor	F(1,116) = 10.71 ** P<0.01	F(1,196) = 6.85 ** P<0.01	F(1,156) = 9.37 ** P<0.01

Experiment	Two-way ANOVA	Dendrite length	Dendrite number	Soma area
(TrkB-Fc)	Interaction	F(1,116) = 7.20 ** P<0.01	F(1,196) = 7.33 ** P<0.01	F(1,156) = 5.53 * P<0.05
X	Piribedil Factor	F(1,116) = 7.33 ** P<0.01	F(1,196) = 5.32 * P<0.05	F(1,156) = 7.48 ** P<0.01
(Pir/Veh)	Inhibitor Factor	F(1,116) = 8.44 ** P<0.01	F(1,196) = 5.32 * P<0.05	F(1,156) = 12.00 *** P<0.001

Experiment	Two-way ANOVA	Dendrite length	Dendrite number	Soma area
(K252)	Interaction	F(1,116) = 5.73 * P<0.05	F(1,196) = 8.02 ** P<0.01	F(1,156) = 6.93 ** P<0.01
X	Piribedil Factor	F(1,116) = 5.82 * P<0.05	F(1,196) = 5.82 * P<0.05	F(1,156) = 6.53 * P<0.05
(Pir/Veh)	Inhibitor Factor	F(1,116) = 5.95 * P<0.05	F(1,196) = 3.97 * P<0.05	F(1,156) = 8.81 ** P<0.01

Experiment	Two-way ANOVA	Dendrite length	Dendrite number	Soma area
(PP2)	Interaction	F(1,116) = 6.44 * P<0.05	F(1,196) = 7.34 ** P<0.01	F(1,156) = 7.23 ** P<0.01
X	Piribedil Factor	F(1,116) = 8.87 ** P<0.01	F(1,196) = 5.33 * P<0.05	F(1,156) = 4.87 * P<0.05
(Pir/Veh)	Inhibitor Factor	F(1,116) = 12.02 *** P<0.001	F(1,196) = 4.44 * P<0.05	F(1,156) = 8.03 ** P<0.01

Experiment	Two-way ANOVA	Dendrite length	Dendrite number	Soma area
(α-BDNF)	Interaction	F(1,116) = 4.19 * P<0.05	F(1,196) = 8.62 ** P<0.01	F(1,156) = 6.23 * P<0.05
X	Pramipexole Factor	F(1,116) = 10.28 ** P<0.01	F(1,196) = 4.64 * P<0.05	F(1,156) = 9.41 ** P<0.01
(PPX/Veh)	Inhibitor Factor	F(1,116) = 8.88 ** P<0.01	F(1,196) = 7.51 ** P<0.01	F(1,156) = 12.05 *** P<0.001

Experiment	Two-way ANOVA	Dendrite length	Dendrite number	Soma area
(TrkB-Fc)	Interaction	F(1,116) = 7.55 ** P<0.01	F(1,196) = 7.22 ** P<0.01	F(1,156) = 7.29 ** P<0.01
X	Pramipexole Factor	F(1,116) = 7.15 ** P<0.01	F(1,196) = 5.31 * P<0.05	F(1,156) = 9.79 ** P<0.01
(PPX/Veh)	Inhibitor Factor	F(1,116) = 8.75 ** P<0.01	F(1,196) = 5.31 * P<0.05	F(1,156) = 14.99 *** P<0.001

Experiment	Two-way ANOVA	Dendrite length	Dendrite number	Soma area
(K252)	Interaction	F(1,116) = 5.24 * P<0.05	F(1,196) = 7.81 ** P<0.01	F(1,156) = 8.99 ** P<0.01
X	Pramipexole Factor	F(1,116) = 8.15 ** P<0.01	F(1,196) = 5.74 * P<0.05	F(1,156) = 5.74 * P<0.05
(PPX/Veh)	Inhibitor Factor	F(1,116) = 5.46 * P<0.05	F(1,196) = 5.74 * P<0.05	F(1,156) = 11.02 ** P<0.01

Experiment	Two-way ANOVA	Dendrite length	Dendrite number	Soma area
(PP2)	Interaction	F(1,116) = 6.51 * P<0.05	F(1,196) = 6.34 * P<0.05	F(1,156) = 6.96 ** P<0.01
X	Pramipexole Factor	F(1,116) = 7.33 * P<0.05	F(1,196) = 6.34 * P<0.05	F(1,156) = 6.88 ** P<0.01
(PPX/Veh)	Inhibitor Factor	F(1,116) = 11.49 ** P<0.01	F(1,196) = 5.41 * P<0.05	F(1,156) = 7.73 ** P<0.01

4.2.8 Neuroprotective and neuroregenerative effects of piribedil and pramipexole on structural plasticity of hiPSC-derived DA neurons

A preliminary test was performed exposing human iPSC-derived DA neurons to various doses of 6-hydroxydopamine (6-OHDA, 0.5-20 µM) for 24 hrs and assessing the changes of structural plasticity after 72 hrs. 6-OHDA produced a neurotoxic dose-dependent effect that was significant at the doses of 10 and 20 µM (Figure 19). In the following tests, the higher dose of 20 µM was used. The statistical analysis is indicated in Table 8.

In a first set of experiments, human DA neurons were pretreated with piribedil (10 µM) or pramipexole (10 µM) for 48 hrs before exposing to 6-OHDA for 24 hrs. Both piribedil and pramipexole significantly counteracted the effects of 6-OHDA on all three structural plasticity parameters as supported by the significant two-way ANOVA interaction obtained on the maximal length of dendrites, number of primary dendrites and soma area at 72 hrs (Figure 20). The statistical analysis is indicated in Table 9. When 6-OHDA was tested with the vehicle, a significant reduction of structural plasticity was visualized. When piribedil or pramipexole were tested with vehicle, significant increases of structural plasticity were visualized.

In a second set of experiments, human DA neurons were pretreated with 6-OHDA (20 µM) for 24 hrs before exposing to piribedil (10 µM) or pramipexole (10 µM) for 48 hrs. Both piribedil and pramipexole significantly counteracted the effects of 6-OHDA on all three structural plasticity parameters as supported by the significant two-way ANOVA interaction obtained on the maximal length of dendrites, number of primary dendrites and soma area at 72 hrs (Figure 21). The statistical analysis is indicated in Table 10.

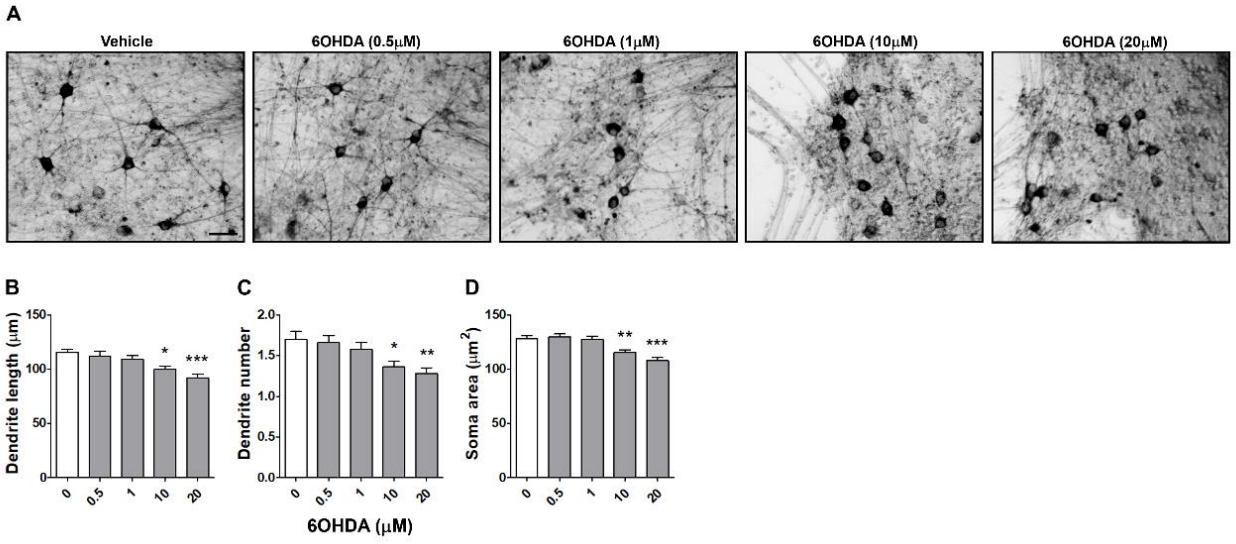

Figure 19. *Effects of 6-OHDA on structural plasticity of human iPSC-derived DA neurons.* **(A)** Representative photomicrographs of human F3 DA neurons (70 days in culture) 24 hrs after exposure to vehicle or to 6-OHDA (0.5 μM, 1 μM, 10 μM or 20 μM). Scale bar: 30 μm. **(B-D)** Concentration response curves of the effect of 6-OHDA on maximal length of dendrites, number of primary dendrites and soma area of human F3 DA neurons. In all panels, values are represented as mean ± S.E.M. (***P<0.001; **P<0.01; *P<0.05 vs. vehicle (0); post-hoc Bonferroni's test).

Table 8. *Statistical analysis.*

Experiment	One-way ANOVA	Dendrite length	Dendrite number	Soma area
Dose curve	Treatment	F(4,149) = 7.58 *** P<0.001	F(4,249) = 5.09 *** P<0.001	F(4,199) = 13.41 *** P<0.001

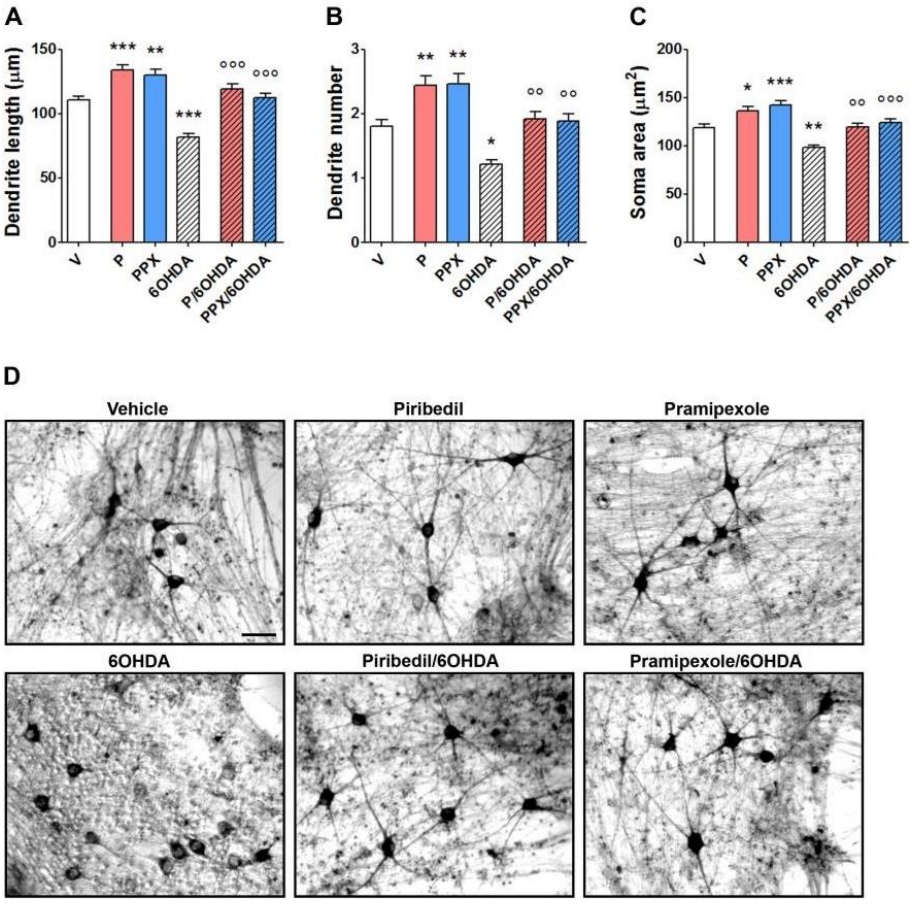

Figure 20. *Piribedil and pramipexole promote neuroprotective effects in human iPSC-derived DA neurons exposed to 6-OHDA.* **(A-C)** Effects on structural plasticity produced by pretreatment (48 hrs) with piribedil (10 μM) or pramipexole (10 μM) followed by exposure (24 hrs) to 6-OHDA (20 μM), assessed as **(A)** maximal length of dendrites, **(B)** number of primary dendrites and **(C)** soma area at 72 hrs. When piribedil or pramipexole were tested with vehicle, significant increases of structural plasticity were visualized. When 6-OHDA was tested with the vehicle, a significant reduction of structural plasticity was visualized. In all panels, values are represented as mean ± S.E.M. (***P<0.001; **P<0.01; *P<0.05 vs. vehicle; °°°P<0.001; °°P<0.01;

vs. 6-OHDA; post-hoc Bonferroni's test). **(D)** Representative photomicrographs of human F3 DA neurons 72 hrs after exposure to vehicle, piribedil (10 µM), pramipexole (10 µM), 6-OHDA (20 µM), piribedil followed by 6-OHDA, pramipexole followed by 6-OHDA. Scale bar: 30 µm. Abbreviations: V = vehicle; P = piribedil; PPX = pramipexole; 6OH = 6-hydroxydopamine.

Table 9. *Statistical analysis.*

Experiment	Two-way ANOVA	Dendrite length	Dendrite number	Soma area
(6OH)	Interaction	F(1,116) = 6.89 ** P<0.01	F(1,196) = 0.07 NS	F(1,156) = 0.29 NS
X	Piribedil Factor	F(1,116) = 67.17 *** P<0.001	F(1,196) = 35.31 *** P<0.001	F(1,156) = 30.70 *** P<0.001
(P/Veh)	Inhibitor Factor	F(1,116) = 32.21 *** P<0.001	F(1,196) = 23.80 *** P<0.001	F(1,156) = 27.61 *** P<0.001

Experiment	Two-way ANOVA	Dendrite length	Dendrite number	Soma area
(6OH)	Interaction	F(1,116) = 1.45 NS	F(1,196) = 0.00 NS	F(1,156) = 0.09 NS
X	Pramipexole Factor	F(1,116) = 71.83 *** P<0.001	F(1,196) = 31.32 *** P<0.001	F(1,156) = 47.63 *** P<0.001
(PPX/Veh)	Inhibitor Factor	F(1,116) = 61.88 *** P<0.001	F(1,196) = 24.19 *** P<0.001	F(1,156) = 29.24 *** P<0.001

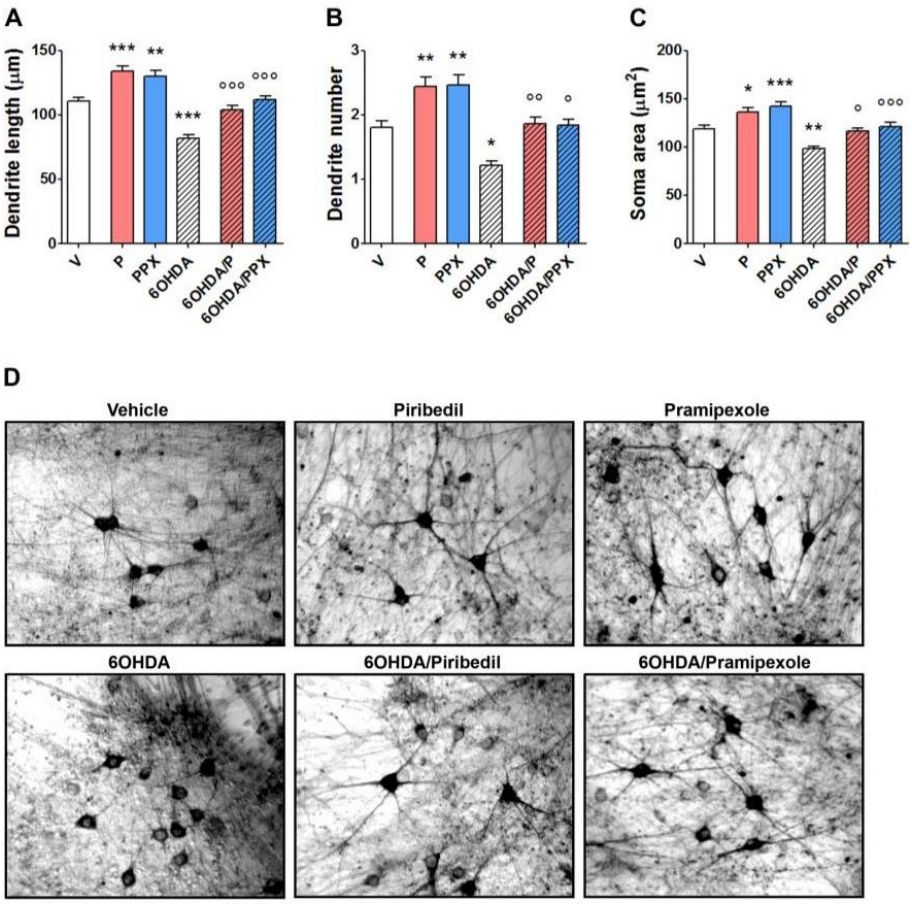

Figure 21. *Piribedil and pramipexole promote neuroregenerative effects in human iPSC-derived DA neurons exposed to 6-OHDA.* **(A-C)** Effects on structural plasticity produced by treatment (48 hrs) with piribedil (10 µM) or pramipexole (10 µM) after exposure (24 hrs) to 6-OHDA (20 µM), assessed as **(A)** maximal length of dendrites, **(B)** number of primary dendrites and **(C)** soma area at 72 hrs. When piribedil or pramipexole

were tested with vehicle, significant increases of structural plasticity were visualized. When 6-OHDA was tested with the vehicle, a significant reduction of structural plasticity was visualized. In all panels, values are represented as mean ± S.E.M. (***P<0.001; **P<0.01; *P<0.05 vs. vehicle; °°°P<0.001; °°P<0.01; °P<0.05 vs. 6-OHDA; post-hoc Bonferroni's test). **(D)** Representative photomicrographs of human F3 DA neurons 72 hrs after exposure to vehicle, piribedil (10 µM), pramipexole (10 µM), 6-OHDA (20 µM), 6-OHDA followed by piribedil, 6-OHDA followed by pramipexole. Scale bar: 30 µm. Abbreviations: V = vehicle; P = piribedil; PPX = pramipexole; 6OH = 6-hydroxydopamine.

Table 10. *Statistical analysis.*

Experiment	Two-way ANOVA	Dendrite length	Dendrite number	Soma area
(6OH)	Interaction	F(1,116) = 0.03 NS	F(1,196) = 0.00 NS	F(1,156) = 0.01 NS
X	Piribedil Factor	F(1,116) = 47.85 *** P<0.001	F(1,196) = 33.20 *** P<0.001	F(1,156) = 27.76 *** P<0.001
(P/Veh)	Inhibitor Factor	F(1,116) = 81.66 *** P<0.001	F(1,196) = 27.26 *** P<0.001	F(1,156) = 35.04 *** P<0.001

Experiment	Two-way ANOVA	Dendrite length	Dendrite number	Soma area
(6OH)	Interaction	F(1,116) = 2.52 NS	F(1,196) = 0.03 NS	F(1,156) = 0.00 NS
X	Pramipexole Factor	F(1,116) = 55.13 *** P<0.001	F(1,196) = 31.43 *** P<0.001	F(1,156) = 42.98 *** P<0.001
(PPX/Veh)	Inhibitor Factor	F(1,116) = 50.55 *** P<0.001	F(1,196) = 27.62 *** P<0.001	F(1,156) = 33.68 *** P<0.001

4.3 Third subproject

4.3.1 Electrical field treatments

Some recent reports have shown that electrical stimulation can promote neuronal differentiation and neurite growth of various neuronal cell types *in vitro*, including rat pheochromocytoma cells PC12 (Jing W et al. 2019) murine neuroblastoma cells N2 (Pelletier SJ et al. 2014) and human neural stem cells (Stewart E et al. 2015).

The structural plasticity effects of electrical stimulation were studied on DA neurons differentiated from F3 iPSCs at day 30 of *in vitro* differentiation (Figure 22). A customized chamber was designed and developed in collaboration with Professor Emilio Sardini and Dr. Michela Borghetti from the Department of Information Engineering, University of Brescia. The chamber consisted of six wells, each one equipped with electrodes to stimulate human DA neurons with an external electrical field. The stimuli were generated by a customized stimulator able to produce a square waveform with arbitrary parameters (frequency, pulse duration and peak value) in order to verify the behavior of the cells under different types of electrical stimulation and thus to find the optimal stimulus for cells growth and maturation. As shown in Figure 23, human DA neurons were exposed to a current with amplitude of respectively 0 mA, 1 mA, 2 mA or 4 mA, 2 hours/day for 3 days. Before starting the

stimulation, the electrical impedance was measured by PalmSense3. On day 4, human DA neurons were fixed, stained by immunocytochemistry and studied for morphological changes (i.e., changes in the maximal length of dendrites, number of primary dendrites and soma area).

Parallel wells were used as controls (no electrical stimulation) and exposed to vehicle or ropinirole, the dopamine D3 receptor agonist with a known positive effect on structural plasticity of DA neurons. A repeated electric stimulation (2 hours/day for 3 days) produced a dose-dependent structural plasticity effect on human iPSC-derived DA neurons. This effect was similar to the one produced by ropinirole and characterized by a significant increase of the maximal length of dendrites, number of primary dendrites and soma area (Figure 23). The statistical analysis is indicated in Table 11.

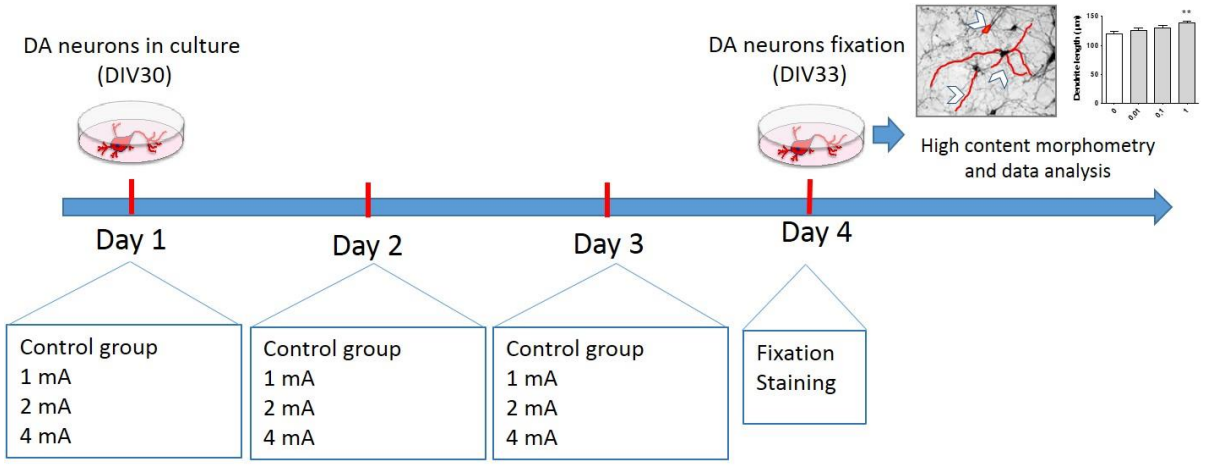

Figure 22. *Experimental protocol to study the effect of the repeated electric stimulation in hiPSC-derived DA neurons.*

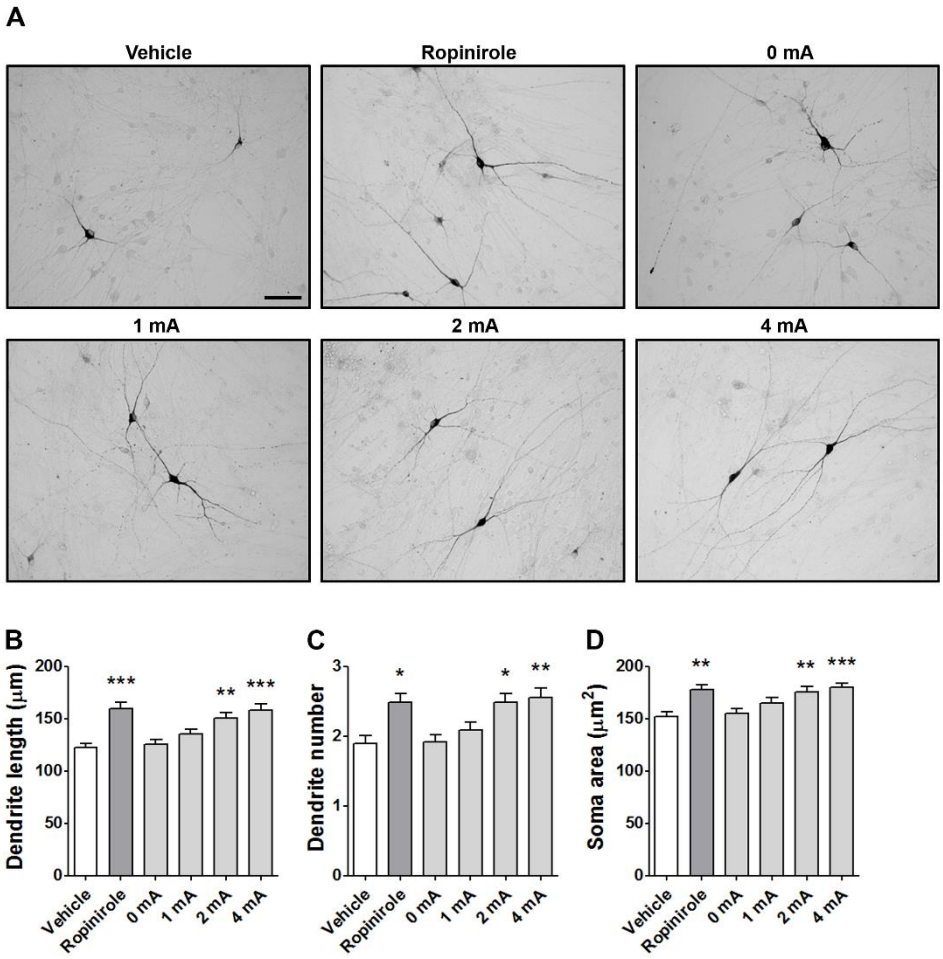

Figure 23. *Repeated electric stimulation promotes structural plasticity of human iPSC-derived DA neurons.* **(A)** Representative photomicrographs of human F3 DA neurons (30 days *in vitro*) 72 hrs after exposure to vehicle, 10 µM ropinirole or electric stimulation 2 hours/day for 3 days at amplitude currents of 0 mA, 1 mA, 2 mA or 4 mA. Scale bar: 50 µm. **(B-D)** Effect of amplitude currents (0-4 mA) on maximal length of dendrites, number of primary dendrites and soma area of human F3 DA neurons. In all panels, values are represented as mean ± S.E.M. (***P<0.001; **P<0.01; *P<0.05 vs. vehicle (0); post-hoc Bonferroni's test).

Table 11. *Statistical analysis.*

Experiment	One-way ANOVA	Dendrite length	Dendrite number	Soma area
Repeated electric stimulation	Treatment	F(5,242) = 9.39 *** P<0.001	F(5,359) = 6.22 *** P<0.001	F(5,299) = 6.47 *** P<0.001

4.4 Fourth subproject

4.4.1 Generation of hiPSCs from patients affected by multiple system atrophy

Human iPSCs were generated from peripheral blood mononuclear cells (PBMCs) donated from a novel set of healthy controls and patients affected by a Parkinsonism, i.e., the multiple system atrophy (MSA). The iPSC clones obtained from the control and the patient underwent a phenotypic characterization to examine the presence of pluripotency markers by immunofluorescence and quantitative PCR analysis, karyotype analysis, pluripotency and trilineage differentiation potential. The iPSCs were subsequently differentiated into mesencephalic DA neurons and assessed for their pharmacological response to dopaminergic agonists.

PBMCs from healthy subjects and MSA patients were isolated from peripheral blood by density gradient centrifugation on Ficoll (Merck Millipore) and were reprogrammed using the Cytotune reprogramming kit (Thermo Fisher Scientific) as described in Materials and Methods (Figure 24). Control PBMCs were called MSAC1, while the patients PBMCs were called respectively MSA1 and MSA2. After the reprogramming period, several emerging colonies were identified, picked, mechanically dissociated, transferred on matrigel-coated culture plates and expanded. After several passages, four clones for MSA1, two clones from MSA2 and four clones for MSAC1 were selected, further expanded and cryobanked. Here, one representative clone for MSAC1 (MSAC1-12) and one representative clone for MSA1 (MSA1-8) are described (Figure 25 and Figure 26).

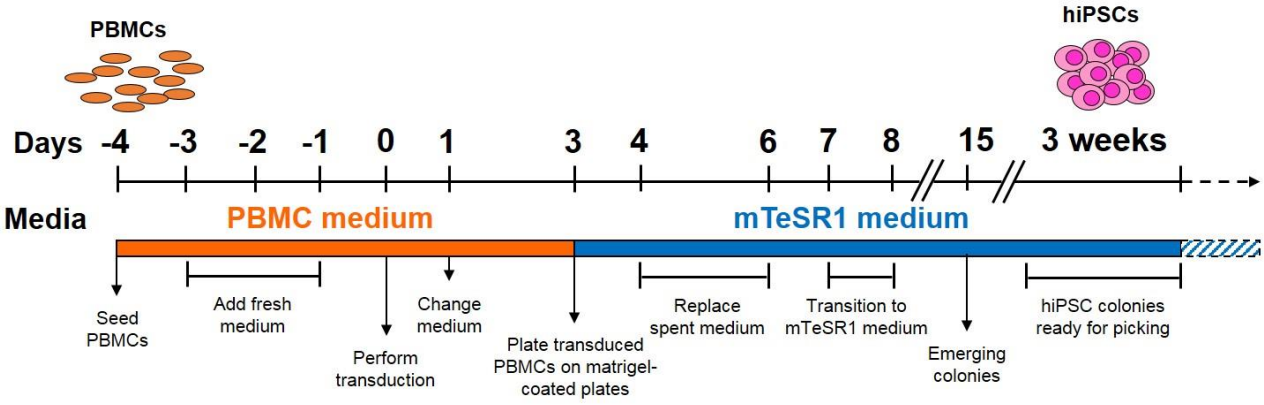

Figure 24. *Diagram of the time line and culture conditions required for reprogramming PBMCs into hiPSCs.*

4.4.2 Phenotypic characterization and karyotype analysis of MSAC1-12 and MSA1-8 hiPSCs

MSAC1-12 and MSA1-8 hiPSC clones exhibit a hESC-like morphology, characterized by high cell density, high ratio nucleus-citoplasm and bright and well-defined borders (Figure 25A and Figure 26A). Both hiPSC clones strongly expressed the pluripotency markers Oct3/4, Sox2 and Nanog by immunocytochemistry (Figure 25B-C and Figure 26B-C). Real-time PCR confirmed the expression of the pluripotency genes Oct4, Sox2 and Nanog (Figure 25G and Figure 26G). Analysis of the karyotype of the two hiPSC clones over several passages showed a normal karyotype with no chromosomal aberrations (Figure 25F and Figure 26F). These results all together indicated that the hiPSCs from the two clones strongly resembled hESCs and fulfilled all criteria of pluripotency.

4.4.3 Embryoid body-mediated differentiation of MSAC1-12 and MSA1-8 hiPSCs

The pluripotency potential of the two hiPSC clones was examined *in vitro* by embryoid body (EBs) formation and differentiation. After 8 days in suspension culture both hiPSC clones formed ball-shaped structures that were transferred to adherent conditions and cultured for 8 more days giving rise to cells of the three germ layers. Adherent cells showed various types of morphologies (Figure 25D and Figure 26D). Immunofluorescence analysis showed endodermal cells expressing α-fetoprotein (AFP), mesodermal cells expressing smooth muscle actin (SMA) and brachyury, and ectodermal cells expressing PAX6 and βIII Tubulin (Figure 25E and Figure 26E). Real-time PCR confirmed the expression of endodermal markers (AFP and SOX17), mesodermal markers (NCAM and α-SMA) and ectodermal markers (PAX6 and TUB3β) (Figure 25G and Figure 26G). These results indicate that MSAC1-12 and MSA1-8 hiPSC clones are able to differentiate into three germ layers *in vitro* as expected for hiPSCs.

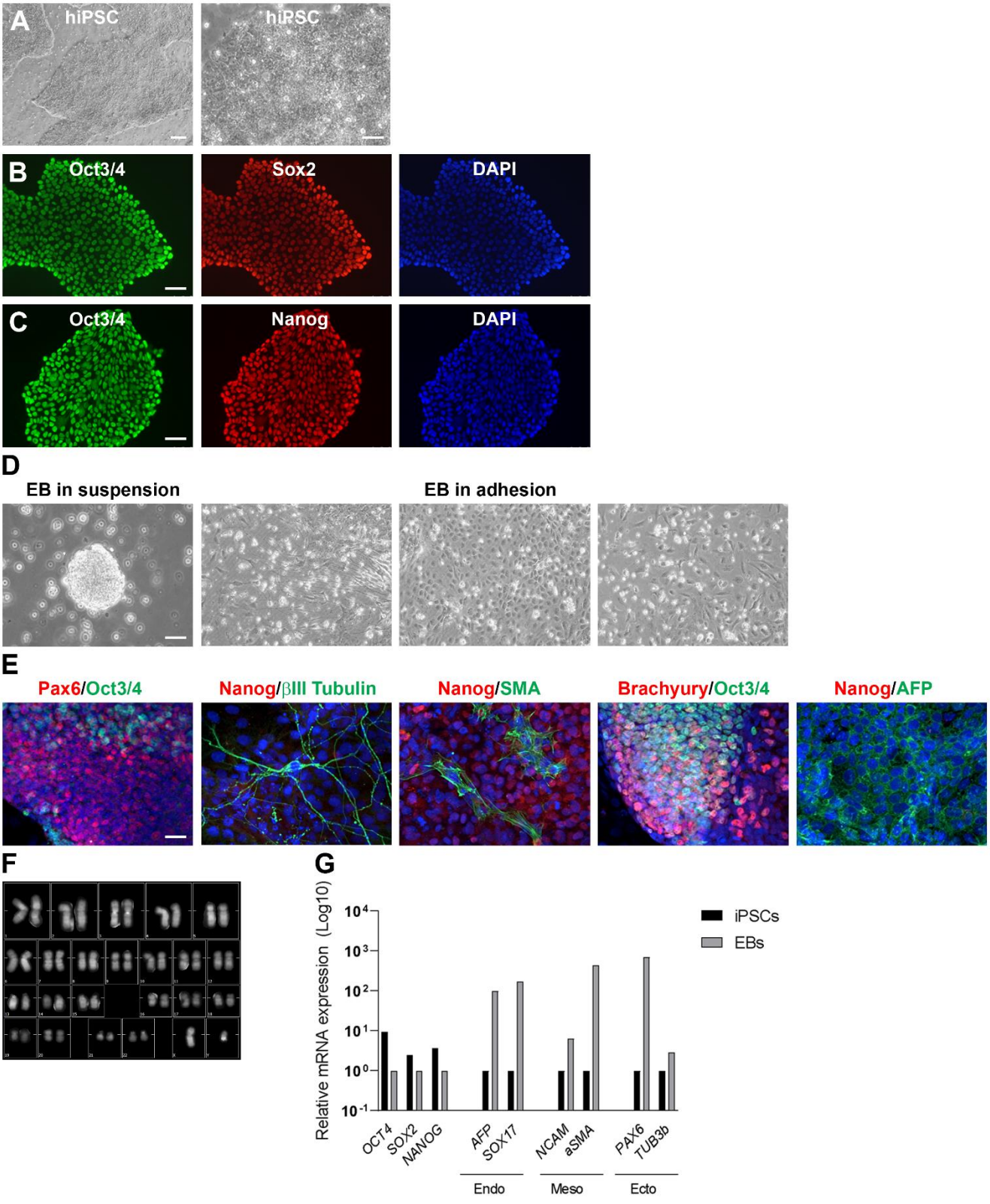

Figure 25. *Generation and characterization of MSAC1-12 hiPSCs.* **(A)** Representative phase contrast images showing the morphology of established hiPSC colonies 30 days after reprogramming, cultured on matrigel in feeder-free conditions. **(B-C)** Representative photomicrographs of hiPSC immunostaining showing the expression of pluripotent markers, **(B)** Oct3/4 and Sox2, **(C)** Oct3/4 and Nanog. **(D)** Representative image of embryoid bodies (EBs) after 8 days culture in suspension followed by 8 days culture in adhesion. **(E)** Immunofluorescence analysis of the three germ layer cells differentiated from EBs cultured 8 days in

adherent condition: PAX6/Oct3/4, Nanog/βIII Tubulin, Nanog/smooth muscle actin (SMA), Brachyury/Oct3/4, Nanog/α-fetoprotein (AFP). Cell nuclei were stained with DAPI (blue). Scale bar: 40 µm. **(F)** Karyotype analysis of MSAC1-12 hiPSCs after 13 passages. **(G)** Quantitative PCR analysis for pluripotency markers and the three germ layer markers.

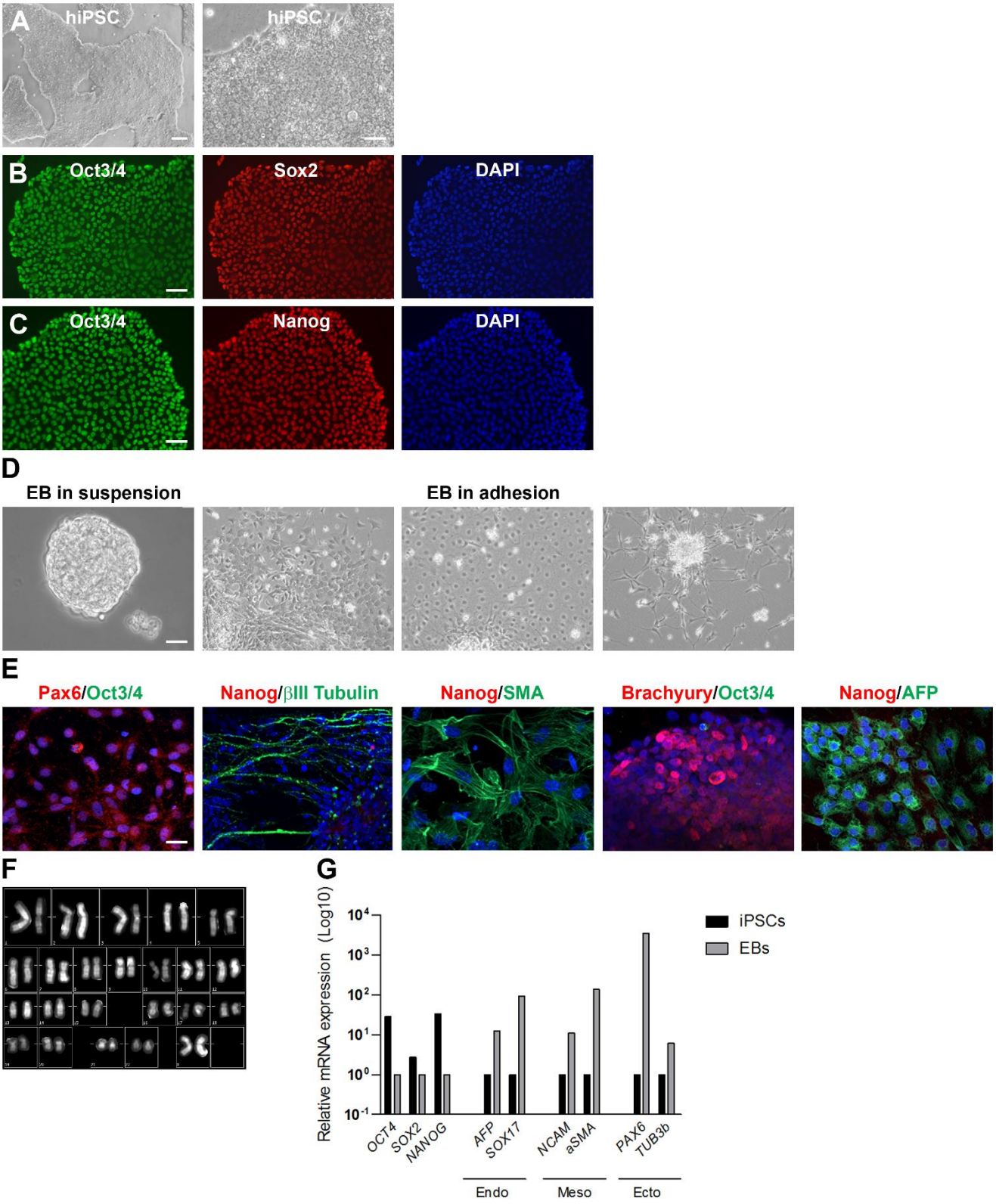

Figure 26. *Generation and characterization of MSA1-8 hiPSCs.* **(A)** Representative phase contrast images showing the morphology of established hiPSC colonies 30 days after reprogramming cultured on matrigel in feeder-free conditions. **(B-C)** Representative photomicrographs of hiPSC immunostaining showing the expression of pluripotent markers, **(B)** Oct3/4 and Sox2, **(C)** Oct3/4 and Nanog. **(D)** Representative image of embryoid bodies (EBs) after 8 days culture in suspension followed by 8 days culture in adhesion. **(E)** Immunofluorescence analysis of the three germ layer cells differentiated from EBs cultured 8 days in adherent condition: PAX6/Oct3/4, Nanog/βIII Tubulin, Nanog/smooth muscle actin (SMA), Brachyury/Oct3/4, Nanog/α-fetoprotein (AFP). Cell nuclei were stained with DAPI (blue). Scale bar: 40 µm. **(F)** Karyotype analysis of MSA1-8 hiPSCs after 15 passages. **(G)** Quantitative PCR analysis for pluripotency markers and the three germ layer markers.

4.4.4 Differentiation of MSAC1-12 and MSA1-8 hiPSCs into mFPPs and DA neurons

MSAC1-12 and MSA1-8 were cultured on matrigel-coated plates in mTeSR1 medium. For the generation of mFPPs the protocol from Fedele S et al. (2017), optimized in chapter 4.1.1 was used. mFPPs at day 11 were passaged every 4–5 days for at least 4 passages and stored in liquid nitrogen at each passage.

At day 11, MSAC1-12 and MSA1-8 mFPPs showed the distinctive co-expression of the floor plate marker FOXA2 and the roof plate marker LMX1α, as confirmed by immunofluorescence analysis (Figure 27 and Figure 28).

DA neuron differentiation was induced when mFPPs reached 90% confluency by switching the medium to Neurobasal/B27 containing BDNF, ascorbic acid, cAMP, TGFβ3, GDNF and DAPT.

At day 21, mFPPs were transferred on plates pre-coated with Poly-DL-ornithine / Fibronectin / Laminin and pre-seeded with a feeder layer of mouse primary cortical astrocytes.

At day 30, βIII Tubulin^{+}/TH^{+} neurons were visualized by immunofluorescence (Figure 27 and Figure 28).

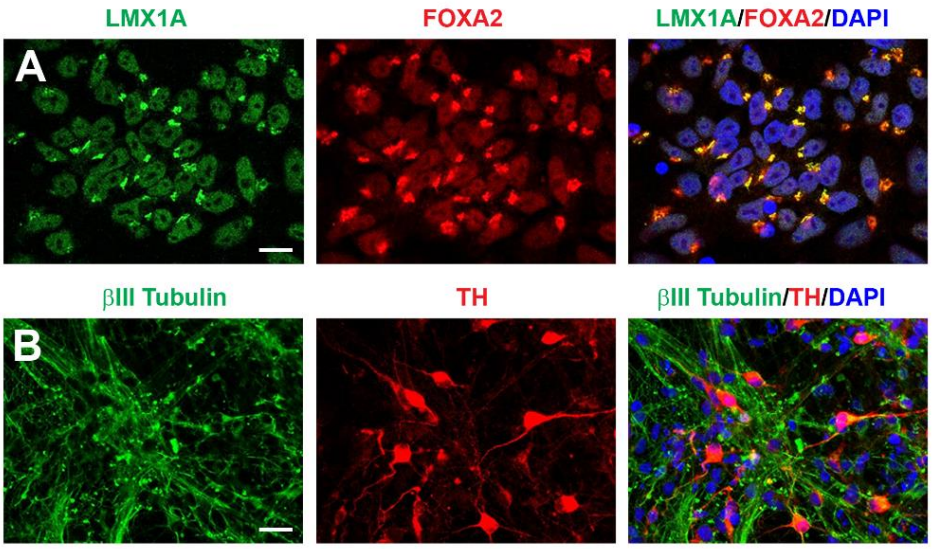

Figure 27. *MSAC1-12 hiPSC differentiation into DA neurons.* Representative images of dual immunofluorescence indicating co-expression of: LMX1α (green) and FOXA2 (red) in mFPPs at day 11 **(A)**, co-expression of TH (red) and βIII Tubulin (green) in DA neurons at day 30 **(B)**. Cell nuclei were stained with DAPI (blue). Scale bar: 20 µm.

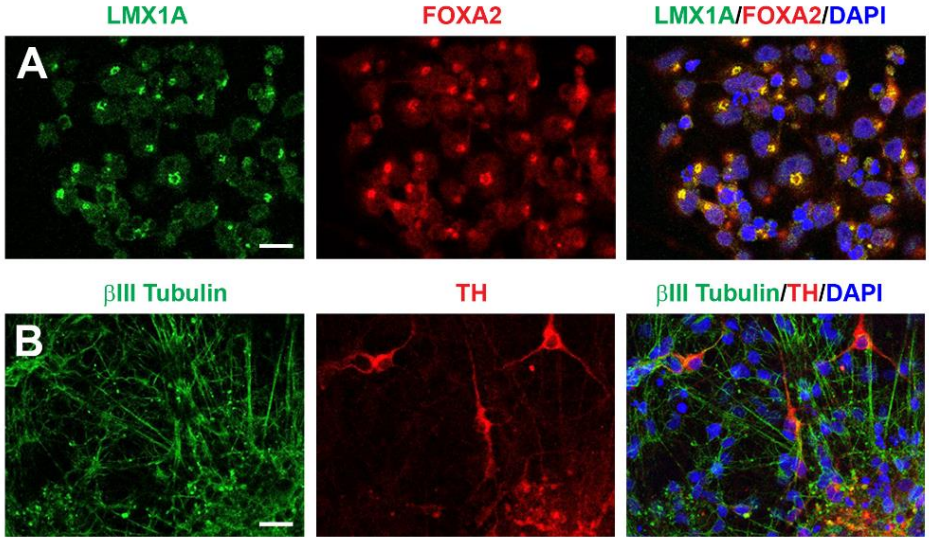

Figure 28. *MSA1-8 hiPSC differentiation into DA neurons.* Representative images of dual immunofluorescence indicating co-expression of: LMX1α (green) and FOXA2 (red) in mFPPs at day 11 **(A)**, co-expression of TH (red) and βIII Tubulin (green) in DA neurons at day 30 **(B)**. Cell nuclei were stained with DAPI (blue). Scale bar: 20 µm.

4.4.5 Structural plasticity effects of ropinirole and pramipexole on DA neurons differentiated from MSAC1-12 and MSA1-8 hiPSCs

In a preliminary experiment, the structural plasticity effects produced by D2R/D3R agonists ropinirole and pramipexole in human DA neurons differentiated from MSAC1-12 and MSA1-8 hiPSCs were evaluated by studying morphological changes (i.e., maximal length of dendrites, number of primary dendrites and soma area).

MSAC1-12 DA neurons at day 40 *in vitro* were exposed to ropinirole and pramipexole for 72 hrs, fixed and stained with an anti-TH antibody (Figure 29). Ropinirole (10 µM) and pramipexole (10 µM) produced a significant effect on structural plasticity when measured as maximal length of dendrites, number of primary dendrites and soma area (Figure 29 and Table 12).

In a parallel experiment, MSA1-8 DA neurons at day 40 *in vitro* were exposed to ropinirole and pramipexole for 72 hrs, fixed and stained with an anti-TH antibody (Figure 30). Ropinirole (10 µM) and pramipexole (10 µM) produced a significant effect on structural plasticity when measured as maximal length of dendrites, number of primary dendrites and soma area (Figure 30 and Table 13).

Overall the structural plasticity effects produced by ropinirole and pramipexole on DA neurons differentiated from the hiPSCs of the MSA patient and the control are similar to the effects produced by the same D2R/D3R agonists on DA neurons differentiated from other hiPSC lines confirming the good quality of the new clones.

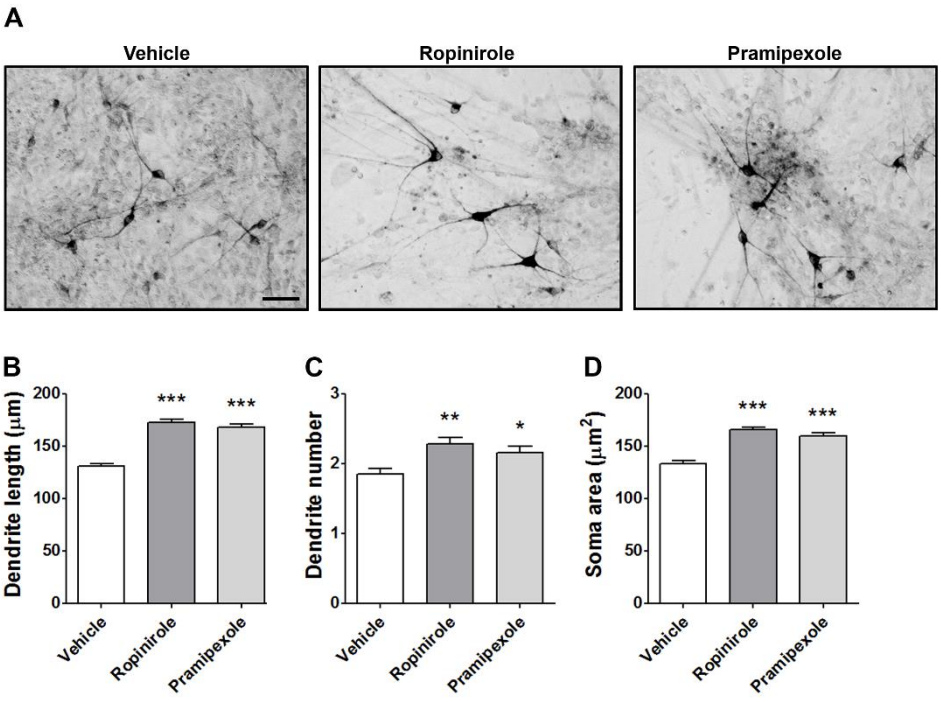

Figure 29. *Structural plasticity effects of dopaminergic agonists on MSAC1-12 hiPSC-derived DA neurons.* **(A)** Representative photomicrographs of human MSAC1-12 DA neurons (40 days *in vitro*) 72 hrs after exposure to vehicle, 10 µM ropinirole or 10 µM pramipexole. Scale bar: 50 µm. **(B-D)** Effect of ropinirole and pramipexole on maximal length of dendrites, number of primary dendrites and soma area of human MSAC1-12 DA neurons. In all panels, values are represented as mean ± S.E.M. (***P<0.001; **P<0.01; *P<0.05 vs. vehicle (0); post-hoc Bonferroni's test).

Table 12. *Statistical analysis.*

Experiment	One-way ANOVA	Dendrite length	Dendrite number	Soma area
Dopaminergic agonists	Treatment	F(2,299) = 66.44 *** P<0.001	F(2,299) = 6.82 ** P<0.01	F(2,299) = 38.11 *** P<0.001

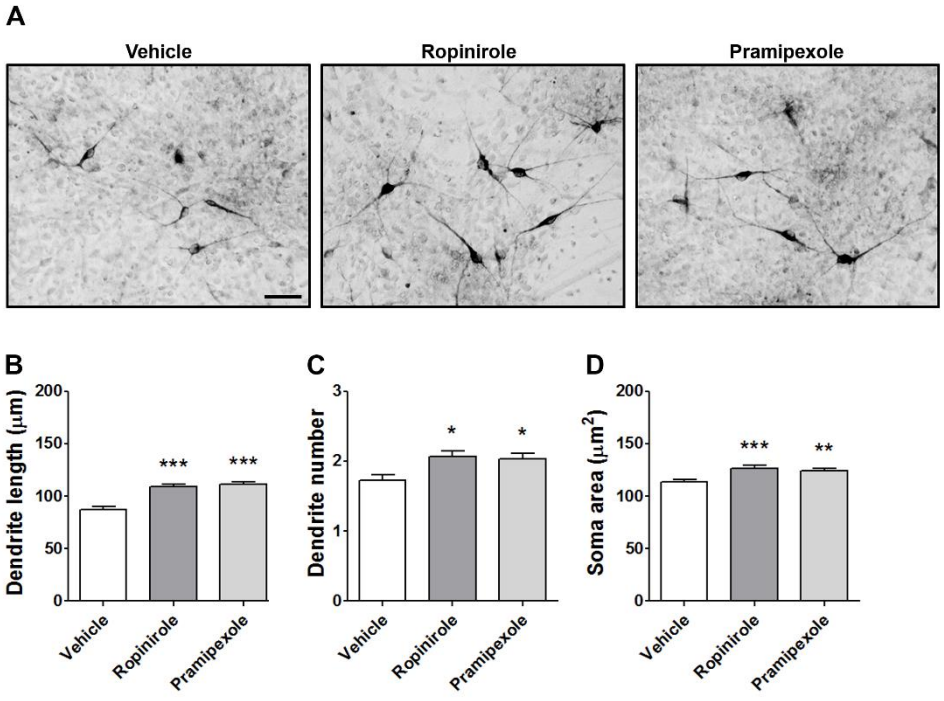

Figure 30. *Structural plasticity effects of dopaminergic agonists on MSA1-8 hiPSC-derived DA neurons.* **(A)** Representative photomicrographs of human MSA1-8 DA neurons (40 days *in vitro*) 72 hrs after exposure to vehicle, 10 µM ropinirole or 10 µM pramipexole. Scale bar: 50 µm. **(B-D)** Effect of ropinirole and pramipexole on maximal length of dendrites, number of primary dendrites and soma area of human MSA1-8 DA neurons. In all panels, values are represented as mean ± S.E.M. (***P<0.001; **P<0.01; *P<0.05 vs. vehicle (0); post-hoc Bonferroni's test).

Table 13. *Statistical analysis.*

Experiment	One-way ANOVA	Dendrite length	Dendrite number	Soma area
Dopaminergic agonists	Treatment	F(2,299) = 29.63 *** P<0.001	F(2,299) = 5.60 ** P<0.01	F(2,299) = 8.47 *** P<0.001

5. Discussion

Pluripotent stem cells are stem cells derived from the inner cell mass of the blastocyst. These cells retain the ability to differentiate into cells of the three germ layers.

The introduction of the iPSCs technology (Takahashi K et al. 2007, Yu J et al. 2007), a novel approach to induce the pluripotent status into adult somatic cells, has enabled the derivation of patient-specific pluripotent cells, providing a valid support to model human disease (Park IH et al. 2008, Soldner F et al. 2009) and opening the possibility of implementing patient-specific cell therapy applications. iPSCs have been used for several purposes including disease modeling, regenerative medicine, drug discovery and drug cytotoxicity studies.

In particular, the introduction of iPSCs allowed overcoming the limitations connected with the study of brain diseases associated with dopaminergic neurons, such as Parkinson's disease and Parkinson's-related disorders. Thanks to iPSCs differentiation into mesencephalic dopaminergic neurons, it is possible to obtain patients' specific cells that can be used to study these diseases and to identify possible therapeutic approaches.

The iPSCs differentiation into dopaminergic neurons is based on the knowledge of how these cells originate *in vivo*: the coordinated action of FGF8 (produced by isthmus organizer), SHH (produced by floor plate), WNT signaling and retinoic acid allow to designate the region in which mesodiencephalic dopaminergic neurons are born. The isthmus organizer and the floor plate are also crucial for the induction of ventral mesencephalon dopaminergic phenotype; the coordinated action of FGF8 and SHH activates a cascade of events that conduct to the formation of Nurr1-positive post-mitotic neurons, which differentiate into tyrosine hydroxylase (TH)-positive mesencephalic DA neurons. The main protocols of differentiation allowed to establish an efficient differentiation method based on dual-SMAD inhibition, which induces neuroectodermal differentiation. This is followed by the activation of WNT canonical pathway, which increases the transcriptional activity of Nurr1, and the activation of SHH signaling that induces dopaminergic differentiation.

The first subproject of this thesis was aimed to the optimization of the methods of differentiation of human iPSCs into mesencephalic DA neuron precursors using a previously published protocol (Fedele S et al. 2017). These DA neuron precursors can be expanded for several passages and stored in liquid nitrogen for any future use.

Human iPSCs generated from a healthy subject were differentiated into mesencephalic dopaminergic precursors. At day 11 of differentiation, cells were expanded for at least 4 passages and then frozen.

This expansion procedure presents several advantages compared to the protocol of direct differentiation. In particular, mesencephalic dopaminergic precursors can be obtained from different hiPSC lines, they can be passaged several times and they can be cryopreserved at each passage to generate a storage bank of identical cells that can be thawed as a starting material.

The second subproject was dedicated to the differentiation of mesencephalic DA precursors into mature DA neurons. These neurons were characterized by immunofluorescence, quantitative PCR, HPLC and electrophysiological analyses. The DA phenotype of the neurons was investigated by testing their response to two pharmacological D3R-preferential DA D2/D3 agonist agents, pramipexole and piribedil, two marketed drugs indicated for the treatment of Parkinson's disease. Recent data have demonstrated a neurotrophic effect produced by another anti-parkinsonian D3R-preferential DA D2/D3 receptor agonist, ropinirole (Collo G et al. 2018). Based on these findings, the cellular and molecular effects of pramipexole and piribedil on human DA neurons were evaluated by studying morphological changes related to structural plasticity and the activation of intracellular pathways. Pramipexole and piribedil produced a dose-dependent increase of dendrite outgrowth and soma area in DA neurons derived from human iPSCs. The effects were mediated through mTOR-signaling, a well-known intracellular pathway activated also by BDNF and involved in cell growth and plasticity (Kumar V et al. 2005, Hoeffer CA and Klann E 2010, Mendoza MC et al. 2011).

In particular, piribedil produced a D3R-dependent rapid activation of mTOR pathway measured by western blot and immunofluorescence co-localization of phosphorylated p70S6K, in soma and dendrites of DA neurons at 2 min. Transient increases of Akt-mTOR signaling in mouse DA neurons were previously observed with cocaine and nicotine, two agents that increase the extracellular levels of dopamine (Collo G et al. 2012, 2013). This effect was also expected based on the knowledge of the D3R signaling previously characterized in cell lines (Cussac D et al. 1999, Beom SR et al. 2004) and on the knowledge of the cross-activation between MEK-ERK and Akt-mTOR pathways (Mendoza MC et al. 2011). Accordingly, the mTOR pathway has been implicated in structural remodeling and plasticity of neurons exposed to various conditions, including learning, adaptive response to damage or to response to drugs (Hoeffer CA and Klann E 2010). This evidence suggests a possible role of the mTOR pathway in determining piribedil-induced structural plasticity reported in the present study. In line with this hypothesis we showed that intracellular kinase inhibitors known to block the mTOR

signaling, such as LY294002 or rapamycin, were able to block both p70S6K transient phosphorylation and long term structural plasticity in human DA neurons. The critical role of D3R is also supported by data previously obtained in D3KO mice, in which DA agonists did not increase the phosphorylation of p70S6K and did not produce structural plasticity (Collo G et al. 2012, 2013). Similar morphological effects were also observed with pramipexole.

The involvement of D3R in pramipexole and piribedil mechanism of action in human DA neurons was supported by the evidence of complete blockade of structural plasticity following pre-incubation with the selective D3R DA antagonists SB277011-A and S33084, but not by the selective D1R antagonist SCH23390. This response profile is compatible with the primary role of D3R autoreceptors, since only D3R and the short form of the D2R are expressed in DA neurons in both rodents and humans (Diaz J et al. 2000, Searle G et al. 2010), while D1R are not (Meador-Woodruff JH et al. 1991). Published findings, mostly in rodents, indicated that the activation of D3R engages neurotrophic-like mechanisms, resulting in structural remodeling of the DA systems (Van Kampen JM and Eckman CB 2006, Collo G et al. 2008, 2012, 2013).

Pramipexole and piribedil effects on structural plasticity were dependent upon viable and active BDNF-TrkB signaling pathways by the neutralization of the extracellular BDNF using an anti-BDNF antibody and a TrkB-Fc scavenger, as successfully described by Jourdi H et al. (2009), and by blocking the phosphorylation of the BDNF receptor (TrkB) with K252a and its intracellular pathway with the Src inhibitor PP2, as previously described by Kumar V et al. (2005). Pretreatments with all these agents blocked the structural changes produced by pramipexole and piribedil, suggesting a necessary active BDNF-TrkB signaling to support pramipexole and piribedil enhanced neurotrophic-like response.

Accordingly, a conservative interpretation suggests that the molecular pathways of D3R-signaling and BDNF-TrkB-signaling are partially overlapping (Collo G et al. 2014, Mendoza MC et al. 2011).

Intriguingly, the use of pramipexole and ropinirole was associated to the occurrence of pathologic compulsive behavior (Weiss HD and Marsh L 2012) in some patients with Parkinson's disease, possibly those with relatively high BDNF levels. On the other hand, pramipexole and ropinirole were also found to produce beneficial antidepressant effects in some patients with Parkinson's disease (Howells DW et al. 2000, Barone P et al. 2010) possibly in those with moderate BDNF levels. In preclinical studies in rodents, low levels of BDNF were associated to anhedonia (Der-Avakian A et al. 2014) and antidepressant-like effects were produced by DA D3R preferential agonists (Leggio GM et al. 2013), the latter results also supported by human studies (Cassano P et al. 2005). Overall, these

findings suggest that the levels of BDNF intracellular signaling are possible moderators of D3R activation in midbrain DA neurons.

In Parkinson's patients, chronic treatment with ropinirole or pramipexole showed a significantly less compromised DA terminal system (Whone AL et al. 2003, Parkinson Study Group, JAMA, 2002). Based on the present results, it is tempting to suggest that the activation of D3R by piribedil could drive structural restorative process in the DA system in Parkinson's patients. The information generated in this study could help in better describing the mechanism of action of piribedil. Accordingly, piribedil would not only act at post-synaptic striatal D2R/D3R activator that acutely improves motor symptoms, but also as presynaptic midbrain D3R activator, chronically driving the intracellular mTOR pathway towards structural remodeling of DA neurons (Joyce JN and Millan MJ 2007). Finally, the role of D3 receptor in the neuroprotective and neuroregenerative properties of pramipexole and piribedil were also studied in animal models. For example, Van Kampen and Eckman (2006) showed neurorestorative response of the nigrostriatal DA system to the D3R preferential DA agonist 7-OH-DPAT in rats previously damaged with the neurotoxin 6-OHDA. The results on DA neurons derived from hiPSCs showed that the pre- and the post-treatment with either pramipexole and piribedil produced a neurorestorative effect associated with 6-OHDA.

In conclusion of this second subproject, piribedil and pramipexole increased structural plasticity in human iPSC-derived DA neurons via a D3R-driven mTOR signaling activation, suggesting the possibility that their mechanism of action may include a direct neurorestorative effect on DA neurons of patients with Parkinson's disease. This study performed on DA neurons differentiated from the hiPSC clone of a human donor possibly reduced the translational risk associated to the use of rodents. hiPSC-derived DA neurons can be used reliably for pharmacologic studies *in vitro* with human translational relevance, supporting their use for the identification of novel treatments.

The third subproject was dedicated to the study of the effects of the electrical stimulation on the structural plasticity of human DA neurons. Several reports have shown that electrical stimulation can promote neuronal differentiation and neurite growth of various neuronal cell types *in vitro*, including PC12 (Jing W et al. 2019) and human neural stem cells (Stewart E et al. 2015).

In the experiments performed on dopaminergic neurons derived from hiPSCs, a repeated electric stimulation produced structural plasticity by increase of the maximal length of dendrites, number of primary dendrites and soma area of dopaminergic neurons. These effects were similar to the effect observed using neurotrophic factors, such as BDNF, or the D3R-preferential DA D2R/D3R agonists pramipexole, piribedil or ropinerole, as shown in the present work. These results are in line

with some of the positive effects observed by deep brain stimulation obtained using electrical stimuli of various intensities in patients with Parkinson's disease (Jakobs M et al. 2019). It is important to state that these data are still preliminary and need to be confirmed with other experiments, but still provide an initial evidence for a plasticity-driven role of adaptive cellular mechanisms in response to local electrical field modulation as a possible therapeutic restorative approach to neurodegeneration.

The fourth subproject was dedicated to the generation of human iPSCs from peripheral blood mononuclear cells (PBMCs) donated from a novel set of healthy controls and patients affected by a Parkinsonism, i.e., the multiple system atrophy (MSA). hiPSCs were generated using the CytoTune™-iPS 2.0 Reprogramming System based on the use of the Sendai virus to drive the four Yamanaka's factors. The hiPSC clones obtained from the control and the patient underwent a phenotypic characterization. hiPSCs showed a hESC-like morphology and the presence of pluripotency markers, as stated by immunofluorescence and quantitative PCR analysis, displays a normal karyotype and exhibit the pluripotency and trilineage differentiation potential. The hiPSCs were subsequently differentiated into mesencephalic DA neurons and evaluated for their pharmacological response to ropinirole and pramipexole. The results obtained indicated that the two dopaminergic D3R-preferential D2R/D3R agonists produced structural plasticity effects either on the clone derived from the healthy control and on the clone derived from the MSA patient. This preliminary observation constitutes the first report of structural plasticity produced in hiPSC-derived dopaminergic neurons from donors affected by a parkinsonism disorders such as MSA, suggesting the preservation of the D3 receptor intracellular pathways engaging the neurotrophic effects. This observation needs further confirmation in hiPSC-derived neurons from other MSA donors, but it can be seen as an encouraging finding that would suggest a possible rationale for the therapeutic use of D3R-preferential DA D2R/D3R agonists in certain MSA patients.

In conclusion, this work robustly argued for a relevant role of D3R-preferential DA D2R/D3R agonists in driving increase in dendritic length and number as well as increasing the soma area of human dopaminergic neurons derived from hiPSCs of healthy donors. These data were obtained also thanks to a technical improvement of the methodology that lead from hiPSC generation to expansion of neural precursors into neurons with the A9 dopaminergic phenotype. In addition, two sets of preliminary observation were reported. The first one regards the use of electrical stimulation, that was able to trigger dendritic outhgrowth and soma size increase in hiPSC-derived dopaminergic

neurons, not really different from the effect observed using neurotrophic factors such as BDNF or D3R-preferential DA D2R/D3R agonists. The second one regards evidence of structural neuroplasticity also induced in dopaminergic neurons differentiated from hiPSCs donated by one patient affected by the parkinsonian disorder MSA. This result indicated the presence of a spared D3 receptor-dependent mechanism driving structural neuroplasticity. This result, still awaiting to be confirmed with further studies, is opening the possibility to partially explain one of the mechanisms of action behind the therapeutic role of D3R-preferential DA D2R/D3R agonists and electrical stimulation in Parkinson's disease and other parkinsonisms.

6. Acknowledgements

I thank Dr. Luigia Rinalda Collo, Section of Pharmacology, Department of Translational Medicine, University of Brescia, for her mentorship and intellectual support during the development of the laboratory work, as well as in the preparation of this thesis.

I thank Professor Emilio Sardini and Dr. Michela Borghetti, Department of Information Engineering, University of Brescia, for the generation of a customized stimulator for electrical stimulation; Professor Ilaria Rivolta, School of Medicine and Surgery, University of Milano-Bicocca, for the electrophysiology analysis; and Dr. Giovanna Piovani, Biology and Genetic Unit, Department of Molecular and Translational Medicine, University of Brescia, for karyotype analysis.

7. Supplementary

Supplementary Table 1. *Pharmacological agents used in this study.*

Name	Supplier	Catalog number	Solvent	Final concentration
6-hydroxydopamine	Tocris Bioscience	2547	Water	10-20 µM
α-BDNF	Merck Millipore	AB1513P	Water	10 µg/ml
K252a	Tocris Bioscience	1683	DMSO	0.2 µM
LY294002	Tocris Bioscience	1130	DMSO	10 µM
PD98059	Tocris Bioscience	1213	DMSO	10 µM
Piribedil	Tocris Bioscience	1031	Water	0.01-10 µM
PP2	Tocris Bioscience	1407	DMSO	10 µM
Pramipexole	Tocris Bioscience	4174	DMSO	0.01-10 µM
Rapamycin	Tocris Bioscience	1292	DMSO	0.02 µM
Ropinirole	Tocris Bioscience	3680	Water	0.1-20 µM
RX821002	Tocris Bioscience	**1324**	DMSO	10 µM
S33084	Institut de Recherches Servier	/	DMSO	0.01 µM
SB277011-A	Tocris Bioscience	4207	DMSO	0.05 µM
SCH23390	Tocris Bioscience	0925	Water	1 µM
TrkB-Fc Chimera	R&D Systems	688-TK	PBS	5 µg/ml

Supplementary Table 2. *Primary antibodies used in this study.*

Name	Supplier	Catalog number	Species	Final dilution	Detection method
α-Tubulin	Sigma-Aldrich	T5168	Mouse mAb	1:20000	WB
βIII Tubulin	Sigma-Aldrich	T8660	Mouse mAb	1:600	IF
AFP	R&D Systems	MAB1368	Mouse mAb	1:100	IF
Brachyury	R&D Systems	AF2085	Goat pAb	1:100	IF
DAT	Santa Cruz Biotechnology	sc-32258	Rat mAb	1:400	IF
HNF-3β (FoxA2)	Santa Cruz Biotechnology	sc-9187	Goat pAb	1:500	IF
GAD67	Merck Millipore	MAB5406	Mouse mAb	1:700	IF
LMX1A	Sigma-Aldrich	HPA030088	Rabbit pAb	1:1000	IF
MAP2	Merck Millipore	AB5622	Rabbit pAb	1:1000	IF
Nanog	Merck Millipore	MABD24	Mouse mAb	1:200	IF
Oct3/4	Merck Millipore	MAB4419	Mouse mAb	1:200	IF
p70S6K	Cell Signaling Technology	2708	Rabbit mAb	1:4000	WB
p-p70S6K$^{(Thr389)}$	Cell Signaling Technology	9206	Mouse mAb	1:500	IF
				1:4000	WB
SMA	Dako	M0851	Mouse mAb	1:200	IF
Sox2	Merck Millipore	MAB4423	Mouse mAb	1:200	IF
TH	Merck Millipore	MAB318	Mouse mAb	1:500	IF
TH	Merck Millipore	AB152	Rabbit pAb	1:4000	WB
TH	Santa Cruz Biotechnology	sc-14007	Rabbit pAb	1:500	IF, IHC
VGLUT2	Merck Millipore	MAB5504	Mouse mAb	1:500	IF

Supplementary Table 3. *Secondary antibodies used in this study.*

Name	Supplier	Catalog number	Final dilution	Detection method
Biotinylated goat anti-rabbit IgG	Vector Laboratories	BA-1000	1:350	ICC
Cy™3-conjugated goat anti-mouse IgG	Jackson ImmunoResearch	115-166-062	1:800	IF
Cy™3-conjugated goat anti-rabbit IgG	Jackson ImmunoResearch	111-166-045	1:1000	IF
Cy™3-conjugated goat anti-rat IgG	Jackson ImmunoResearch	112-165-167	1:1000	IF
Alexa Fluor® 488-conjugated goat anti-mouse IgG	Jackson ImmunoResearch	115-546-071	1:500	IF
Alexa Fluor® 488-conjugated goat anti-rabbit IgG	Jackson ImmunoResearch	111-485-144	1:500	IF
HRP-conjugated goat anti-mouse IgG	Santa Cruz Biotechnology	sc-2005	1:5000	WB
HRP-conjugated goat anti-rabbit IgG	Santa Cruz Biotechnology	sc-2030	1:5000	WB

Supplementary Table 4. *Primers used in this study.*

Primers	Primers sequence	Primers length	Tm
β-actin F	GAAGAGCTACGAGCTGCCTGA	21	60°C
β-actin R	TGATCTTCATTGTGCTGGGTG	21	
AFP F	CCAACAGGAGGCCATGCTT	19	57°C
AFP R	GAATGCAGGAGGGACATATGTTT	23	
DDC F	CGCCAGGATCCCCGCTTTGAAATCTG	26	68°C
DDC R	TCGGCCGCCAGCTCTTTGATGTGTTC	26	
EN1 F	GCAACCCGGCTATCCTACTTATG	23	60°C
EN1 R	ATGTAGCGGTTTGCCTGGAAC	21	
FOXA2 F	CTGGGAGCGGTGAAGATGGA	20	62°C
FOXA2 R	ACGTACGACGACATGTTCATGGAG	24	
GAPDH F	GCTCAGACACCATGGGGAAGGT	22	68°C
GAPDH R	GTGGTGCAGGAGGCATTGCTGA	22	
LMX1A F	CAGCCTCAGACTCAGGTAAAAGTG	24	60°C
LMX1A R	TGAATGCTCGCCTCTGTTGA	20	
LMX1B F	ACGAGGAGTGTTTGCAGTGCG	21	62°C
LMX1B R	CCCTCCTTGAGCACGAATTCG	21	
Nanog F	CAGCCCTGATTCTTCCACCAGTCCC	25	68°C
Nanog R	TGGAAGGTTCCCAGTCGGGTTCACC	25	
NCAM F	ATGGAAACTCTATTAAAGTGAACCTG	26	55°C
NCAM R	TAGACCTCATACTCAGCATTCCAGT	25	
NURR1 F	CTATTCCAGGTTCCAGGCGAA	21	60°C

NURR1 R	CTGGGTTGGACCTGTATGCTAA	22	
Oct3/4 F	GACAGGGGGAGGGGAGGAGCTAGG	24	68°C
Oct3/4 R	CTTCCCTCCAACCAGTTGCCCCAAAC	26	
PAX6 F	CATATTCGAGCCCCGTGGAA	20	57°C
PAX6 R	TCACTCCGCTGTGACTGTTC	20	
SMA F	ACTGAGCGTGGCTATTCCTCCGTT	24	59°C
SMA R	GCAGTGGCCATCTCATTTTCA	21	
Sox2 F	GGGAAATGGGAGGGGTGCAAAAGAGG	26	68°C
Sox2 R	TTGCGTGAGTGTGGATGGGATTGGTG	26	
SOX17 F	CTCTGCCTCCTCCACGAA	18	56°C
SOX17 R	CAGAATCCAGACCTGCACAA	20	
TH F	GTCCCCTGGTTCCCAAGAAAAGT	23	62°C
TH R	TCCAGCTGGGGGATATTGTCTTC	23	
TUB3β F	CTCAGGGGCCTTTGGACATC	20	57°C
TUB3β R	CAGGCAGTCGCAGTTTTCAC	20	

Supplementary Table 5. *Media and reagents.*

Name	Supplier	Catalog number
2-mercaptoethanol	Gibco	21985023
ABComplex	Vector Laboratories	PK-6100
Accumax	Sigma-Aldrich	**A7089**
Accutase	StemCell Technologies	07920
Ascorbic acid	Sigma-Aldrich	A4403
B27 supplement	Gibco	17504044
BDNF	R&D Systems	248-BD
BSA	Sigma-Aldrich	A2153
CHIR99021	Stemgent	04-0004
DAB	Sigma-Aldrich	D5637
DAPI	Molecular Probes	D1306
DAPT	Tocris Bioscience	2634
Dibutyryl cAMP	Sigma-Aldrich	D0627
ECL, LiteAblot Extend	EuroClone	EMP013001
FGF8	R&D Systems	423-F8
Fibronectin	Sigma-Aldrich	F4759
GDNF	R&D Systems	212-GD
GlutaMAX™	Gibco	35050061
Knockout Serum Replacement	Gibco	10828028
Knockout™ DMEM	Gibco	10829018
Knockout™ DMEM/F12	Gibco	11330032

Laminin	Sigma-Aldrich	**L2020**
LDN193189	Stemgent	04-0074
L-Glutamine	EuroClone	ECB3000D
Matrigel	Corning	354234
N2 supplement	Gibco	17502048
Neurobasal medium	Gibco	21103049
Normal goat serum	EuroClone	BK5425S
Paraformaldehyde	Sigma-Aldrich	P6148
PBS	EuroClone	ECB4053L
Poly-DL-Ornithine	Sigma-Aldrich	P0671
Poly-D-Lysine	Sigma-Aldrich	P7405
Purmorphamine	Stemgent	04-0009
Re-Blot Plus Strong Solution	Merck Millipore	2504
SB431542	Tocris Bioscience	1614
Shh C25II	R&D Systems	464-SH
Sucrose	Sigma-Aldrich	S7903
TGFβ3	R&D Systems	243-B3
Triton	Sigma-Aldrich	T8787

8. Bibliography

Abati E, Di Fonzo A, Corti S. (2018). In vitro models of multiple system atrophy from primary cells to induced pluripotent stem cells. J Cell Mol Med. 22:2536-2546.

Acampora D, Avantaggiato V, Tuorto F, Simeone A. (1997). Genetic control of brain morphogenesis through Otx gene dosage requirement. Development. 124:3639-3650.

Ahmed Z, Asi YT, Sailer A, Lees AJ, Houlden H, Revesz T, Holton JL. (2012). The neuropathology, pathophysiology and genetics of multiple system atrophy. Neuropathol Appl Neurobiol. 38:4-24.

Al Abbar A, Ngai SC, Nograles N, Alhaji SY, Abdullah S. (2020). Induced Pluripotent Stem Cells: Reprogramming Platforms and Applications in Cell Replacement Therapy. Biores Open Access. 9:121-136.

Alonso M, Medina JH, Pozzo-Miller L. (2004). ERK 1/2 activation is necessary for BDNF to increase dendritic spine density in hippocampal CA1 pyramidal neurons, Learning and Memory. 11:172-178.

Alves dos Santos MTM, Smidt MP. (2011). En1 and Wnt signaling in midbrain dopaminergic neuronal development. Neural Development. 6:23.

Andersson E, Tryggvason U, Deng Q, Friling S, Alekseenko Z, Robert B, Perlmann T, Ericson J. (2006). Identification of intrinsic determinants of midbrain dopamine neurons. Cell. 124:393-405.

Ang SL. (2006). Transcriptional control of midbrain dopaminergic neuron development. Development. 133:3499-3506.

Aubert I, Ghorayeb I, Normand E, Bloch B. (2000). Phenotypical characterization of the neurons expressing the D1 and D2 dopamine receptors in the monkey striatum. Journal of Comparative Neurology. 418:22-32.

Avantaggiato V, Acampora D, Tuorto F, Simeone A. (1996). Retinoic acid induces stage-specific repatterning of the rostral central nervous system. Dev Biol. 175:347-357.

Avilion AA, Nicolis SK, Pevny LH, Perez L, Vivian N, Lovell-Badge R. (2003). Multipotent cell lineages in early mouse development depend on SOX2 function. Genes Dev. 17:126-140.

Avior Y, Sagi I, Benvenisty N. (2016). Pluripotent stem cells in disease modelling and drug discovery. Nat Rev Mol Cell Biol. 17:170-182.

Balestrino R, Schapira AHV. (2020). Parkinson disease. European Journal of Neurology. 27:27-42.

Ballou LM, Lin RZ. (2008). Rapamycin and mTOR kinase inhibitors. J Chem Biol. 1:27-36.

Barone P, Poewe W, Albrecht S, Debieuvre C, Massey D, Rascol O, Tolosa E, Weintraub D. (2010). Pramipexole for the treatment of depressive symptoms in patients with Parkinson's disease: a randomised, double-blind, placebo-controlled trial. Lancet Neurol. 9:573-580.

Barzilai A, Melamed E. (2003). Molecular mechanisms of selective dopaminergic neuronal death in Parkinson’s disease. Trends Mol Med. 9:126-132.

Ben-Shlomo Y, Wenning GK, Tison F, Quinn NP. (1997). Survival of patients with pathologically proven multiple system atrophy: a meta-analysis. Neurology. 48:384-393.

Bensimon G, Ludolph A, Agid Y, Vidailhet M, Payan C, Leigh PN. (2009). Riluzole treatment, survival and diagnostic criteria in Parkinson plus disorders: the NNIPPS study. Brain. 132:156-171.

Beom SR, Cheong D, Torres G, Caron MG, Kim KM. (2004). Comparative studies of molecular mechanisms of dopamine D2 and D3 receptors for the activation of extracellular signal-regulated kinase. Journal of Biological Chemistry. 279:28304-28314.

Bezard E, Ferry S, Mach U, Stark H, Leriche L, Boraud T, Gross C, Sokoloff P. (2003). Attenuation of levodopa-induced dyskinesia by normalizing dopamine D3 receptor function. Nature Medicine. 9:762-767.

Bjorklund A, Lindvall O. (1984). Dopamine-containing system in the CNS. Handbook of Chemical Neuroanatomy. 2:55-111.

Bolin MH, Svennersten K, Nilsson D, Sawatdee A, Jager EW, Richter-Dahlfors A, Berggren M. (2009). Active control of epithelial cell-density gradients grown along the channel of an organic electrochemical transistor. Adv Mater. 21:4379-4382.

Bordet R, Ridray S, Schwartz JC, Sokoloff P. (2000). Involvement of the direct striatonigral pathway in levodopa-induced sensitization in 6-hydroxydopamine lesioned rats. European Journal of Neuroscience. 12:2117-2123.

Bower JH, Maraganore DM, McDonnell SK, Rocca WA. (1997). Incidence of progressive supranuclear palsy and multiple system atrophy in Olmsted County, Minnesota, 1976 to 1990. Neurology. 49:1284-1288.

Brault V, Moore R, Kutsch S, Ishibashi M, Rowitch DH, McMahon AP, Sommer L, Boussadia O, Kemler R. (2001). Inactivation of the beta-catenin gene by Wnt1-Cre-mediated deletion results in dramatic brain malformation and failure of craniofacial development. Development. 128:1253-1264.

Brodski C, Blaess S, Partanen J, Prakash N. (2019). Crosstalk of Intercellular Signaling Pathways in the Generation of Midbrain Dopaminergic Neurons In Vivo and from Stem Cells. J Dev Biol. 7:3.

Calatayud C, Carola G, Fernandez-Carasa I, Valtorta M, Jimenez-Delgado S, Diaz M, Soriano- Fradera J, Cappelletti G, Garcia-Sancho J, Raya A, Consiglio A. (2019). CRISPR/Cas9-mediated generation of a tyrosine hydroxylase reporter iPSC line for live imaging and isolation of dopaminergic neurons. Sci Rep. 9:6811.

Carlsson A, Falck B, Hillarp NA. (1962). Cellular localization of brain monoamines, Acta Physiologica Scandinavica Supplementum 56:1-28.

Cartwright P, McLean C, Sheppard A, Rivett D, Jones K, Dalton S. (2005). LIF/STAT3 controls ES cell self-renewal and pluripotency by a Myc-dependent mechanism. Development. 132:885-896.

Cassano P, Lattanzi L, Fava M, Navari S, Battistini G, Abelli M, Cassano GB. (2005). Ropinirole in treatment-resistant depression: a 16-week pilot study. Can J Psychiatry. 50:357-360.

Cassano P, Lattanzi L, Soldani F, Navari S, Battistini G, Gemignani A, Cassano GB. (2004). Pramipexole in treatment-resistant depression: an extended follow-up. Depression and Anxiety. 20:131-138.

Castelo-Branco G, Rawal N, Arenas E. (2004). GSK-3beta inhibition/beta-catenin stabilization in ventral midbrain precursors increases differentiation into dopamine neurons. J Cell Sci. 117:5731-5737.

Catalano SM, Shatz CJ. (1998). Activity-dependent cortical target selection by thalamic axons. Science. 281:559-562.

Chen S, Zhang X, Yang D, Du Y, Li L, Li X, Ming M, Le W. (2008). D2/D3 receptor agonist ropinirole protects dopaminergic cell line against rotenone-induced apoptosis through inhibition of caspase- and JNK-dependent pathways. FEBS Lett. 582:603-610.

Chilov D, Sinjushina N, Saarimaki-Vire J, Taketo MM, Partanen J. (2010). Beta- Catenin regulates intercellular signaling networks and cell-type specific transcription in the developing mouse midbrain-rhombomere 1 region. PLoS One. 5:e10881.

Civelli O, Bunzow JR, Grandy DK. (1993). Molecular diversity of the dopamine receptors. Annual Review of Pharmacology and Toxicology. 33:281-307.

Clementi F, Fumagalli G. (1999). Farmacologia generale e molecolare. Seconda edizione UTET.

Clotman F, Maele-Fabry GV, Picard JJ. (1997). Retinoic acid induces a tissue-specific deletion in the expression domain of Otx2. Neurotoxicol. Teratol. 19:163-169.

Collo G, Bono F, Cavalleri L, Plebani L, Merlo Pich E, Millan MJ, Spano PF, Missale C. (2012). Presynaptic dopamine D3 receptor mediates cocaine-induced structural plasticity in mesencephalic dopaminergic neurons via ERK and Akt pathways. J Neurochem. 120:765-778.

Collo G, Bono F, Cavalleri L, Plebani L, Mitola S, Zoli M, Maskos U, Millan MJ, Merlo Pich E, Spano PF, Missale C. (2013). Nicotine-induced structural plasticity in mesencephalic dopaminergic neurons is mediated by dopamine D3 receptors and Akt-mTORC1 signalling. Mol Pharmacol. 83:1176-1189.

Collo G, Cavalleri L, Bono F, Mora C, Fedele S, Invernizzi RW, Gennarelli M, Piovani G, Kunath T, Millan MJ, Merlo Pich E, Spano P. (2018). Ropinirole and Pramipexole Promote Structural Plasticity in Human iPSC-Derived Dopaminergic Neurons via BDNF and mTOR Signaling. Neural Plast. 2018:4196961.

Collo G, Cavalleri L, Spano PF. (2014). Structural plasticity in mesencephalic dopaminergic neurons produced by drugs of abuse: critical role of BDNF and dopamine. Front Pharmacol 5:259.

Collo G, Gregorini A, Missale C, Spano PF. (2008a). D3 receptor involvement in neurotrophic effects of amphetamine and cocaine on mesencephalic dopaminergic neurons. European Neuropsychopharmacology. 18:S243-S244.

Collo G, Zanetti S, Missale C, Spano PF. (2008b). Dopamine D3 receptor-preferring agonists increase dendrite arborization of mesencephalic dopaminergic neurons via extracellular signal-regulated kinase phosphorylation. European Journal of Neuroscience. 28:1231-1240.

Cramer T, Chelli B, Murgia M, Barbalinardo M, Bystrenova E, de Leeuw D, Biscarini F. (2013). Organic ultra-thin film transistors with a liquid gate for extracellular stimulation and recording of electric activity of stem cell-derived neuronal networks. Phys Chem Chem Phys. 15:3897-3905.

Croll SD, Chesnutt CR, Rudge JS, Acheson A, Ryan TE, Siuciak JA, DiStefano PS, Wiegand SJ, Lindsay RM. (1998). Co-infusion with a TrkB-Fc receptor body carrier enhances BDNF distribution in the adult rat brain. Exp Neurol. 152:20-33.

Curran EJ, Watson SJ Jr. (1995). Dopamine receptor mRNA expression patterns by opioid peptide cells in the nucleus accumbens of the rat: a double in situ hybridization study. Journal of Comparative Neuroscience. 361:57-76.

Cussac D, Newman-Tancredi A, Pasteau V, Millan MJ. (1999). Human dopamine D3 receptors mediate mitogen-activated protein kinase activation via a phosphatidylinositol 3-kinase and an atypical protein kinase C-dependent mechanism. Molecular Pharmacology. 56:1025-1030.

Dahlström A, Fuxe K. (1964). Evidence for the existence of monoamine containing neurons in the central nervous system: demonstration of monoamines in the cell bodies of brain stem neurons. Acta Physiologica Scandinavica Supplementum. 232:1-55.

Dailly E, Chenu F, Renard CE, Bourin M. (2004). Dopamine, depression and antidepressants. Fundam. Clin. Pharmacol. 18: 601-607.

Dantzker JL, Callaway EM. (1998). The development of local, layer-specific visual cortical axons in the absence of extrinsic influences and intrinsic activity. J Neurosci. 18:4145-4154.

Daubner SC, Le T, Wang S. (2011). Tyrosine Hydroxylase and Regulation of Dopamine Synthesis. Arch Biochem Biophys. 508: 1-12.

de Rijk MC, Rocca WA, Anderson DW, Melcon MO, Breteler MM, Maraganore DM. (1997). A population perspective on diagnostic criteria for Parkinson's disease. Neurology. 48:1277-1281.

Deleu D, Northway MG, Hanssens Y. (2002). Clinical pharmacokinetic and pharmacodynamic properties of drugs used in the treatment of Parkinson’s disease. Clin Pharmacokinet. 41:261-309.

Der-Avakian A, Mazei-Robison MS, Kesby JP, Nestler EJ, Markou A. (2014). Enduring deficits in brain reward function after chronic social defeat in rats: susceptibility, resilience, and antidepressant response. Biol Psychiatry. 76:542-549.

Desbief S, di Lauro M, Casalini S, Guerin D, Tortorella S, Barbalinardo M, Kyndiah A, Murgia M, Cramer T, Biscarini F, Vuillaume D. (2016). Electrolyte-gated organic synapse transistor interfaced with neurons. Org Electron. 38:21-28.

Devine MJ, Ryten M, Vodicka P, Thomson AJ, Burdon T, Houlden H, Cavaleri F, Nagano M, Drummond NJ, Taanman JW, Schapira AH, Gwinn K, Hardy J, Lewis PA, Kunath T. (2011). Parkinson's disease induced pluripotent stem cells with triplication of the α-synuclein locus. Nature Communications. 2:440.

Di Ciano P, Underwood RJ, Hagan JJ, Everitt BJ. (2003). Attenuation of cue-controlled cocaine-seeking by a selective D3 dopamine receptor antagonist SB-277011-A. Neuropsychopharmacology. 28:329-338.

Diaz J, Pilon C, Le Foll B, Gros C, Triller A, Schwartz JC, Sokoloff P. (2000). Dopamine D3 receptors expressed by all mesencephalic dopamine neurons. J Neurosci. 20:8677-8684.

Dietz DM, Dietz EJ, Nestler EJ, Russo SJ. (2009). Molecular mechanisms of psycostimulant-induced structural plasticity. Pharmacopsychiatry. 42:S69-S78.

Du F, Li R, Huang Y, Xuping L, Le W. (2005). Dopamine D3 receptor-preferring agonists induce neurotrophic effects on mesencephalic dopamine neurons. European Journal of Neuroscience. 22:2422-2430.

Duty S, Jenner P. (2011). Animal models of Parkinson's disease: a source of novel treatments and clues to the cause of the disease. Br J Pharmacol. 164:1357-1391.

Eden RJ, Costall B, Domeney AM, Gerrard PA, Harvey CA, Kelly ME, Naylor RJ, Owen DA, Wright A. (1991). Preclinical pharmacology of ropinirole (SKF 101468-A) a novel Dopamine D2 agonist. Pharmacol. Biochem. Behav. 38:147-154.

Engel M, Do-Ha D, Muñoz SS, Ooi L. (2016). Common pitfalls of stem cell differentiation: a guide to improving protocols for neurodegenerative disease models and research. Cell Mol Life Sci. 73:3693-3709.

Evans MJ, Kaufman MH. (1981). Establishment in culture of pluripotential cells from mouse embryos. Nature. 292:154-156.

Fedele S, Collo G, Behr K, Bischofberger J, Müller S, Kunath T, Christensen K, Gündner AL, Graf M, Jagasia R, Taylor V. (2017). Expansion of human midbrain floor plate progenitors from induced pluripotent stem cells increases dopaminergic neuron differentiation potential. Sci Rep. 7:6036.

Ferri AL, Lin W, Mavromatakis YE, Wang JC, Sasaki H, Whitsett JA, Ang SL. (2007). Foxa1 and Foxa2 regulate multiple phases of midbrain dopaminergic neuron development in a dosage-dependent manner. Development. 134:2761-2769.

Fibiger HC, Phillips AG. (1986). Reward, motivation and cognition: psychobiology of mesotelencephalic dopamine systems. Handbook of Physiology The Nervous System. 4:647-675.

Fusaki N, Ban H, Nishiyama A, Saeki K, Hasegawa M. (2009). Efficient induction of transgenefree human pluripotent stem cells using a vector based on Sendai virus, an RNA virus that does not integrate into the host genome. Proc Jpn Acad, Ser B, Phys Biol Sci. 85:348-362.

Garrington TP, Johnson GL. (1999). Organization and regulation of mitogen-activated protein kinase signaling pathways, Current Opinion in Cell Biology. 2:211-218.

Gerfen CR, Keefe KA, Gauda EB. (1995). D1 and D2 dopamine receptor function in the striatum: coactivation of D1- and D2-dopamine receptors on separate populations of neurons results in potentiated immediate early gene response in D1-containing neurons. Journal of Neuroscience. 15:8167-8176.

Gerfen CR, Wilson CJ. (1996). The basal ganglia. Handbook of Chemical Neuroanatomy, Integrated Systems of the CNS Part III. 12:371-468.

Gingrich JA, Caron MG. (1993). Recent advances in the molecular biology of dopamine receptors. Annual Review of Neuroscience. 16:299-321.

Graybiel AM. (1990). Neurotransmitters and neuromodulators in the basal ganglia. Trends in Neurosciences. 13:244-254.

Hanke JH, Gardner JP, Dow RL, Changelian PS, Brissette WH, Weringer EJ, Pollok BA, Connelly PA. (1996). Discovery of a novel, potent, and Src family-selective tyrosine kinase inhibitor. Study of Lck- and FynT-dependent T cell activation. J Biol Chem. 271:695-701.

Hanna J, Markoulaki S, Schorderet P, Carey BW, Beard C, Wernig M, Creyghton MP, Steine EJ, Cassady JP, Foreman R, Lengner CJ, Dausman JA, Jaenisch R. (2008). Direct reprogramming of terminally differentiated mature B lymphocytes to pluripotency. Cell. 133:250-264.

Harland R. (2000). Neural induction. Curr. Opin. Genet. Dev. 10:357-362.

Hay N, Sonenberg N. (2004). Upstream and downstream of mTOR. Genes & Development. 18:1926-1945.

Hegarty SV, Sullivan AM, O'Keeffe GW. (2013). Midbrain dopaminergic neurons: A review of the molecular circuitry that regulates their development. Developmental Biology. 379:123-138.

Heimer L, Zahm DS, Alheid GF. (1995). Basal ganglia. The Rat Nervous System. 2:579-628.

Hemmati-Brivanlou A, Melton D. (1997). Vertebrate neural induction. Annu. Rev. Neurosci. 20:43-60.

Hillefors M, von Euler G. (2001). Pharmacology of [3H]R(+)-7-OH-DPAT binding in the rat caudate-putamen. Neurochemistry International. 38:31-42.

Hirsch E, Graybiel AM, Agid YA. (1988). Melanized dopaminergic neurons are differentially susceptible to degeneration in Parkinson's disease. Nature. 334:345-348.

Hoeffer CA, Klann E. (2010). mTOR signaling: at the crossroads of plasticity, memory, and disease. Trends Neurosci. 33:67.

Hökfelt T. (1984). Distributional of tyrosine hydroxylase immunoreactive neurons in the rat brain. Handbook of Chemical Neuroanatomy 2:277-379.

Holder N, Hill J. (1991). Retinoic acid modifies development of the midbrain–hindbrain border and affects cranial ganglion formation in zebrafish embryos. Development. 113:1159-1170.

Howells DW, Porritt MJ, Wong JY, Batchelor PE, Kalnins R, Hughes AJ, Donnan GA. (2000). Reduced BDNF mRNA expression in the Parkinson's disease substantia nigra. Exp Neurol. 166:127-135.

Huang S, Bjornsti MA, Houghton PJ. (2003). Rapamycins: mechanism of action and cellular resistance. Cancer Biology & Therapy. 2:222-232.

Hynes M, Porter JA, Chiang C, Chang D, Tessier-Lavigne M, Beachy PA, Rosenthal A. (1995). Induction of midbrain dopaminergic neurons by Sonic hedgehog. Neuron. 15:35-44.

Hynes M, Stone DM, Dowd M, Pitts-Meek S, Goddard A, Gurney A, Rosenthal A. (1997). Control of cell pattern in the neural tube by the zinc finger transcription factor and oncogene Gli-1. Neuron. 19:15-26.

Hynes M, Ye W, Wang K, Stone D, Murone M, Sauvage Fd, Rosenthal A. (2000). The seven-transmembrane receptor smoothened cell-autonomously induces multiple ventral cell types. Nat Neurosci. 3:41-46.

Hynes M, Rosenthal A. (1999). Specification of dopaminergic and serotonergic neurons in the vertebrate CNS. Curr. Opin. Neurobiol. 9:26-36.

Ikemoto S. (2007). Dopamine reward circuitry: two projection systems from the ventral midbrain to the nucleus accumbens-olfactory tubercle complex. Brain Research Reviews. 56:27-78.

Invernizzi RW. (2013). Monitoring extracellular monoamines with in vivo microdialysis in awake rats: a practical approach. Microdialysis Techniques in Neuroscience, G. Giovanni and V. Matteo, Eds. 75:175-208.

Ishizawa K, Komori T, Sasaki S, Arai N, Mizutani T, Hirose T. (2004). Microglial activation parallels system degeneration in multiple system atrophy. J Neuropathol Exp Neurol. 63:43-52.

Jackson DM, Westlind-Danielsson A. (1994). Dopamine receptors: molecular biology, biochemistry and behavioral aspects. Pharmacology Therapy. 64:291-369.

Jakobs M, Fomenko A, Lozano AM, Kiening KL. (2019). Cellular, molecular, and clinical mechanisms of action of deep brain stimulation - a systematic review on established indications and outlook on future developments. EMBO Mol Med. 11:e9575.

Jaworski J, Splanger DP, Hoogenraad CC, Sheng M. (2005). Control of dendritic arborisation by the phosphoinositide-3'-kinase-Akt-mammalian target of rapamycin pathway. Journal of Neuroscience. 25:11300-11312.

Jecmenica-Lukic M, Poewe W, Tolosa E, Wenning GK. (2012). Premotor signs and symptoms of multiple system atrophy. Lancet Neurol. 11:361-368.

Jefferies HB, Fumagalli S, Dennis PB, Reinhard C, Pearson RB, Thomas G. (1997). Rapamycin suppresses 5'TOP mRNA translation through inhibition of p70s6k. EMBO J. 16:3693-3704.

Jing W, Zhang Y, Cai Q, Chen G, Wang L, Yang X, Zhong W. (2019). Study of Electrical Stimulation with Different Electric-Field Intensities in the Regulation of the Differentiation of PC12 Cells. ACS Chem Neurosci. 10:348-357.

Joksimovic M, Yun BA, Kittappa R, Anderegg AM, Chang WW, Taketo MM, McKay RD, Awatramani RB. (2009). Wnt antagonism of Shh facilitates midbrain floor plate neurogenesis. Nat Neurosci. 12:125-131.

Jourdi H, Hsu YT, Zhou M, Qin Q, Bi X, Baudry M. (2009). Positive AMPA receptor modulation rapidly stimulates BDNF release and increases dendritic mRNA translation. J Neurosci. 29:8688-8697.

Joyce JN. (2001). Dopamine D3 receptor as a therapeutic target for antipsychotic and antiparkinsonian drugs. Pharmacol. Ther. 90:231-259.

Joyce JN, Millan MJ. (2007). Dopamine D3 receptor agonists for protection and repair in Parkinson's disease. Curr. Opin. in Pharmacol. 7:100-105.

Karagiannis P, Takahashi K, Saito M, Yoshida Y, Okita K, Watanabe A, Inoue H, Yamashita JK, Todani M, Nakagawa M, Osawa M, Yashiro Y, Yamanaka S, Osafune K. (2019). Induced pluripotent stem cells and their use in human models of disease and development. Physiol Rev. 99:79-114.

Kase H, Iwahashi K, Matsuda Y. (1986). K-252a, a potent inhibitor of protein kinase C from microbial origin. J Antibiot (Tokyo). 39:1059-1065.

Katzeff JS, Phan K, Purushothuman S, Halliday GM, Kim WS. (2019). Cross-examining candidate genes implicated in multiple system atrophy. Acta neuropathol commun. 7:117.

Kele J, Simplicio N, Ferri AL, Mira H, Guillemot F, Arenas E, Ang SL. (2006). Neurogenin 2 is required for the development of ventral midbrain dopaminergic neurons. Development. 133:495-505.

Khan ZU, Gutierrez A, Martin R, Penafiel A, Rivera A, de la Calle A. (2000). Dopamine D5 receptors of rat and human brain. Neuroscience. 100:689-699.

Khodagholy D, Gelinas JN, Thesen T, Doyle W, Devinsky O, Malliaras GG, Buzsáki G. (2014). NeuroGrid: recording action potentials from the surface of the brain. Nat Neurosci. 18:310-316.

Kikuchi A, Takeda A, Okamura N, Tashiro M, Hasegawa T, Furumoto S, Kobayashi M, Sugeno N, Baba T, Miki Y, Mori F, Wakabayashi K, Funaki Y, Iwata R, Takahashi S, Fukuda H, Arai H, Kudo Y, Yanai K, Itoyama Y. (2010). In vivo visualization

of alpha-synuclein deposition by carbon-11-labelled 2-[2-(2- dimethylaminothiazol-5-yl)ethenyl]-6- [2-(fluoro)ethoxy]benzoxazole positron emission tomography in multiple system atrophy. Brain. 133:1772-1778.

Kim DH, Sarbassov DD, Ali SM, King JE, Latek RR, Erdjument-Bromage H, Tempst P, Sabatini DM. (2002). mTOR interacts with raptor to form a nutrient-sensitive complex that signals to the cell growth machinery. Cell. 110:163-75.

Kim HJ. (2011). Stem cell potential in Parkinson's disease and molecular factors for the generation of dopamine neurons. Biochim. Biophys. Acta. 1812:1-11.

Kirkeby A, Grealish S, Wolf DA, Nelander J, Wood J, Lundblad M, Lindvall O, Parmar M. (2012). Generation of Regionally Specified Neural Progenitors and Functional Neurons from Human Embryonic Stem Cells under Defined Conditions. Cell Reports, 1:703-714.

Klein R, Conway D, Parada LF, Barbacid M. (1990). The trkB tyrosine protein kinase gene codes for a second neurogenic receptor that lacks the catalytic kinase domain. Cell. 61:647-656.

Klockegether T. (2004). Parkinson's disease: clinical aspects. Cell Tissue Res. 318:115-120.

Kolb B, Gorny G, Li Y, Samaha AN, Robinson TE. (2003). Amphetamine or cocaine limits the ability of later experience to promote structural plasticity in the neocortex and nucleus accumbens. Proceedings of the National Academy of Sciences of the USA. 100:10523-10528.

Köllensperger M, Geser F, Ndayisaba JP, Boesch S, Seppi K, Ostergaard K, Dupont E, Cardozo A, Tolosa E, Abele M, Klockgether T, Yekhlef F, Tison F, Daniels C, Deuschl G, Coelho M, Sampaio C, Bozi M, Quinn N, Schrag A, Mathias CJ, Fowler C, Nilsson CF, Widner H, Schimke N, Oertel W, Del Sorbo F, Albanese A, Pellecchia MT, Barone P, Djaldetti R, Colosimo C, Meco G, Gonzalez-Mandly A, Berciano J, Gurevich T, Giladi N, Galitzky M, Rascol O, Kamm C, Gasser T, Siebert U, Poewe W, Wenning GK; EMSA-SG. (2010). Presentation, diagnosis, and management of multiple system atrophy in Europe: final analysis of the European multiple system atrophy registry. Mov Disord. 25:2604-2612.

Kostrzewa RM. (2014). Handbook of neurotoxicity. In Handbook of Neurotoxicity. 1-3.

Kriks S, Shim JW, Piao J, Ganat YM, Wakeman DR, Xie Z, Carrillo-Reid L, Auyeung G, Antonacci C, Buch A, Yang L, Beal MF, Surmeier DJ, Kordower JH, Tabar V, Studer L. (2011). Dopamine neurons derived from human ES cells efficiently engraft in animal models of Parkinson's disease. Nature. 480:547-551.

Kumar V, Zhang M-X, Swank MW, Kunz J, Wu G-Y. (2005). Regulation of dendritic morphogenesis by Ras-PI3-K-Akt-mTOR and Ras-MAPK signaling pathways. J Neurosci. 25:11288-11299.

Lahti L, Peltopuro P, Piepponen TP, Partanen J. (2012). Cell-autonomous FGF signaling regulates anteroposterior patterning and neuronal differentiation in the mesodiencephalic dopaminergic progenitor domain. Development. 139:894-905.

Lauder JM, Bloom FE. (1974). Ontogeny of monoamine neurons in the locus coeruleus, Raphe nuclei and substantia nigra of the rat. I. Cell differentiation. J. Comp. Neurol. 155:469-481.

Laurens B, Constantinescu R, Freeman R, Gerhard A, Jellinger K, Jeromin A, Krismer F, Mollenhauer B, Schlossmacher MG, Shaw LM, Verbeek MM, Wenning GK, Winge K, Zhang J, Meissner WG. (2015). Fluid biomarkers in multiple system atrophy: A review of the MSA Biomarker Initiative. Neurobiol Dis. 80:29-41.

Le Moine C, Bloch B. (1995). D1 and D2 dopamine receptor gene expression in the rat striatum: sensitive cRNA probes demonstrate prominent segregation of D1 and D2 mRNAs in distinct neuronal populations of the dorsal and ventral striatum. Journal of Comparative Neurology. 335:418-426.

Le Moine C, Bloch B. (1996). Expression of the D3 dopamine receptor in peptidergic neurons of the nucleus accumbens: comparison with the D1 and D2 dopamine receptors. Neuroscience. 73:131-143.

Lee A, Gilbert RM. (2016). Epidemiology of Parkinson disease. Neurol Clin. 34:955-965.

Lee KW, Kim Y, Kim AM, Helmin K, Nairn AC, Greengard P. (2005). Cocaine-induced dendritic spine formation in D1 and D2 dopamine receptor-containing medium spiny neurons in nucleus accumbens. PNAS. 103:3399-3404.

Leggio GM, Salomone S, Bucolo C, Platania C, Micale V, Caraci F, Drago F. (2013). Dopamine D(3) receptor as a new pharmacological target for the treatment of depression. Eur J Pharmacol. 719:25-33.

Lepack AE, Fuchikami M, Dwyer JM, Banasr M, Duman RS. (2014). BDNF release is required for the behavioral actions of ketamine. Int J Neuropychopharm. 18:1-6.

Levant B, Cross RS, Pazdernik TL. (1998). Alterations in local cerebral glucose utilization produced by D3 dopamine receptor-selective doses of 7-OH-DPAT and nafadotride. Brain Research. 812:193-199.

Little D, Luft C, Mosaku O, Lorvellec M, Yao Z, Paillusson S, Kriston-Vizi J, Gandhi S, Abramov AY, Ketteler R, Devine MJ, Gissen P. (2018). A single cell high content assay detects mitochondrial dysfunction in iPSC-derived neurons with mutations in SNCA. Sci Rep. 8:9033.

Liu A, Niswander LA. (2005). Bone morphogenetic protein signalling and vertebrate nervous system development. Nat. Rev. Neurosci. 6:945-954.

Loh YH, Agarwal S, Park IH, Urbach A, Huo H, Heffner GC, Kim K, Miller JD, Ng K, Daley GQ. (2009). Generation of induced pluripotent stem cells from human blood. Blood. 113:5476-5479.

Lumsden A, Krumlauf R. (1996). Patterning the vertebrate neuraxis. Science. 274:1109-1115.

Malenka EJ, Nestler SE, Hyman RC. (2009). Chapter 13: Higher Cognitive Function and Behavioral Control. Molecular neuropharmacology: a foundation for clinical neuroscience (2nd ed.). New York: McGraw-Hill Medical: 318.

Marti M, Mulero L, Pardo C, Morera C, Carrio M, Laricchia-Robbio L, Esteban CR, Izpisua Belmonte JC. (2013). Characterization of pluripotent stem cells. Nat Protoc. 8:223-253.

Martin GR. (1981). Isolation of a pluripotent cell line from early mouse embryos cultured in medium conditioned by teratocarcinoma stem cells. Proc Natl Acad Sci U S A. 78:7634-7638.

Martinez-Barbera JP, Signore M, Boyl PP, Puelles E, Acampora D, Gogoi R, Schubert F, Lumsden A, Simeone A. (2001). Regionalisation of anterior neuroectoderm and its competence in responding to forebrain and midbrain inducing activities depend on mutual antagonism between OTX2 and GBX2. Development. 128:4789-4800.

Matsuo I, Kuratani S, Kimura C, Takeda N, Aizawa S. (1995). Mouse Otx2 functions in the formation and patterning of rostral head. Genes. Dev. 9:2646-2658.

McBride WJ, Murphy JM, Ikemoto S. (1999). Localization of brain reinforcement mechanisms: intracranial self-administration and intracranial place-conditioning studies. Behavioural Brain Research. 101:129-152.

McMahon AP, Bradley A. (1990). The Wnt-1 (int-1) proto-oncogene is required for development of a large region of the mouse brain. Cell. 62:1073-1085.

Meador-Woodruff JH, Mansour A, Healy DJ, Kuehn R, Zhou QY, Bunzow JR, Akil H, Civelli O, Watson SJ Jr. (1991). Comparison of the distributions of D1 and D2 dopamine receptor mRNAs in rat brain. Neuropsychopharmacol. 5:231-234.

Mendoza MC, Er EE, Blenis J. (2011). The Ras-ERK and PI3-K-mTOR pathways: cross-talk and compensation. Trends Biochem Sci. 36:320-328.

Millan MJ, Dekeyne A, Rivet J-M, Dubuffet T, Lavielle G, Brocco M. (2000). S33084, a novel, potent, selective and competitive antagonist at dopamine D3 receptors: functional and behavioral profile compared with GR218,231 and L741,626. Journal of Pharmacology and Experimental Therapeutics. 293:1063-1073.

Millan MJ, Cussac D, Milligan G, Carr C, Audinot V, Gobert A, Lejeune F, Rivet JM, Brocco M, Duqueyroix D, Nicolas JP, Boutin JA, Newman-Tancredi A. (2001). Antiparkinsonian agent piribedil displays antagonist properties at native, rat,

and cloned, human alpha(2)-adrenoceptors: cellular and functional characterization. J. Pharmacol. Exp. Ther. 297:876-887.

Millan MJ, Gobert A, Newman-Tancredi A, Lejeune F, Cussac D, Rivet JM, Audinot V, Dubuffet T, Lavielle G. (2000). S33084, a novel, potent, selective, and competitive antagonist at dopamine D(3)-receptors: I. Receptorial, electrophysiological and neurochemical profile compared with GR218,231 and L741,626. J. Pharmacol. Exp. Ther. 293: 1048-1062.

Ming G, Henley J, Tessier-Lavigne M, Song H, Poo M. (2001). Electrical activity modulates growth cone guidance by diffusible factors. Neuron. 29:441-452.

Missale C, Nash RS, Robinson SW, Jaber M, Caron MG. (1998). Dopamine receptors: from structure to function. Physiological Reviews. 78:189-225.

Morissette M, Goulet M, Grondin R, Blanchet P, Bedard PJ, Di Paolo T, Levesque D. (1998). Associative and limbic regions of monkey striatum express high levels of dopamine D3 receptors: effects of MPTP and dopamine agonist replacement therapies. European Journal of Neuroscience. 10:2565-2573.

Morizane A, Li JY, Brundin P. (2008). From bench to bed: the potential of stem cells for the treatment of Parkinson's disease. Cell Tissue Res. 331:323-336.

Mueller D, Chapman CA, Stewart J. (2006). Amphetamine induces dendritic growth in ventral tegmental area dopaminergic neurons in vivo via basic fibroblast growth factor. Neuroscience. 137:727-735.

Multiple-System Atrophy Research Collaboration. (2014). Mutations in COQ2 in familial and sporadic multiple-system atrophy. N Engl J Med. 369:233-244.

Murray AM, Hyde TM, Knable MB, Herman MM, Bigelow LB, Carter JM, Weinberger DR, Kleinman JE. (1995). Distribution of putative D4 dopamine receptors in postmortem striatum from patients with schizophrenia, Journal of Neuroscience. 15:2186-2191.

Nakatake Y, Fukui N, Iwamatsu Y, Masui S, Takahashi K, Yagi R, Yagi K, Miyazaki J, Matoba R, Ko MS, Niwa H. (2006). Klf4 cooperates with Oct3/4 and Sox2 to activate the Lefty1 core promoter in embryonic stem cells. Mol Cell Biol. 26:7772-7782.

Nestler EJ, Hope BT, Widnell KL. (1993). Drug addiction: a model for the molecular basis of neural plasticity. Neuron. 11:995-1006.

Nichols J, Zevnik B, Anastassiadis K, Niwa H, Klewe-Nebenius D, Chambers I, Scholer H, Smith A. (1998). Formation of pluripotent stem cells in the mammalian embryo depends on the POU transcription factor Oct4. Cell. 95:379-391.

Nishimura K, Sano M, Ohtaka M, Furuta B, Umemura Y, Nakajima Y, Ikehara Y, Kobayashi T, Segawa H, Takayasu S, Sato H, Motomura K, Uchida E, Kanayasu- Toyoda T, Asashima M, Nakauchi H, Yamaguchi T, Nakanishi M. (2011). Development of defective and persistent Sendai virus vector: a unique gene delivery/expression system ideal for cell reprogramming. J Biol Chem. 286:4760-4771.

O'Dowd BF, Hnatowich M, Caron MG, Lefkowitz RJ, Bouvier RJ. (1989). Palmitoylation of the human b2-adrenergic receptor: mutation of CYS 341 in the carboxy tail leads to an uncoupled, non-palmitoylated form of the receptor. Journal of Biology and Chemistry. 264:7564-7569.

O'Dowd BF. (1993). Structure of dopamine receptors. Journal of Neurochemistry. 60:804-816.

Obeso JA, Rodriguez-Oroz MC, Chana P, Lera G, Rodriguez M, Olanow CW. (2000). The evolution and origin of motor complications in Parkinson's disease. Neurology. 55:S13-S23.

Ovchinnikov Y, Abdulaev N, Bogachuk A. (1988). Two adjacent cysteine residues in the C-terminal cytoplasmic fragment of bovine rhodopsin are palmitoylated. FEBS Letters. 230:1-5.

Ozawa T, Paviour D, Quinn NP, Josephs KA, Sangha H, Kilford L, Healy DG, Wood NW, Lees AJ, Holton JL, Revesz T. (2004). The spectrum of pathological involvement of the striatonigral and olivopontocerebellar systems in multiple system atrophy: clinicopathological correlations. Brain. 127:2657-2671.

Papp B, Plath K. (2013). Epigenetics of reprogramming to induced pluripotency. Cell. 152:1324-1343.

Papp MI, Kahn JE, Lantos PL. (1989). Glial cytoplasmic inclusions in the CNS of patients with multiple system atrophy (striatonigral degeneration, olivopontocerebellar atrophy and Shy-Drager syndrome). J Neurol Sci. 94:79-100.

Park IH, Zhao R, West JA, Yabuuchi A, Huo H, Ince TA, Lerou PH, Lensch MW, Daley GQ. (2008). Reprogramming of human somatic cells to pluripotency with defined factors. Nature. 451:141-146.

Parkinson Study Group. (2002). Dopamine transporter brain imaging to assess the effects of pramipexole vs levodopa on Parkinson disease progression. JAMA. 287:1653-1661.

Pelletier SJ, Lagacé M, St-Amour I, Arsenault D, Cisbani G, Chabrat A, Fecteau S, Lévesque M, Cicchetti F. (2014). The morphological and molecular changes of brain cells exposed to direct current electric field stimulation. Int J Neuropsychopharmacol. 18:5.

Peretti CS, Gierski F, Harrois S. (2004). Cognitive skill learning in healthy older adults after 2 months of double-blind treatment with piribedil. Psychopharmacology. 176:176-182.

Pérez-Soriano A, Arnal Segura M, Botta-Orfila T, Giraldo D, Fernández M, Compta Y, Fernández-Santiago R, Ezquerra M, Tartaglia GG, Martí MJ, Catalan MSA Registry (CMSAR). (2020). Transcriptomic differences in MSA clinical variants. Sci Rep. 10:10310.

Petiti I, Salan Kenser N, Karry R, Robicsek O, Aberdam E, Muller FJ, Aberdam D, Ben-Shachar D. (2012). Induced pluripotent stem cells from hair follicles as a cellular model for neurodevelopmental disorders. Stem Cell Research. 8:134-140.

Petrovic IN, Ling H, Asi Y, Ahmed Z, Kukkle PL, Hazrati LN, Lang AE, Revesz T, Holton JL, Lees AJ. (2012). Multiple system atrophy-parkinsonism with slow progression and prolonged survival: a diagnostic catch. Mov Disord. 27:1186-1190.

Pierce RC, Kumaresan V. (2006). The mesolimbic dopamine system: the final common pathway for the reinforcing effect of drugs of abuse?. Neuroscience and Biobehavioral Reviews. 30:215-223.

Plath K, Lowry W. (2011). Progress in understanding reprogramming to the induced pluripotent state. Nat Rev Genet. 12:253-265.

Prakash N, Brodski C, Naserke T, Puelles E, Gogoi R, Hall A, Panhuysen M, Echevarria D, Sussel L, Weisenhorn DM, Martinez S, Arenas E, Simeone A, Wurst W. (2006). A Wnt1-regulated genetic network controls the identity and fate of midbrain-dopaminergic progenitors in vivo. Development. 133:89-98.

Prakash N, Wurst W. (2006). Development of dopaminergic neurons in the mammalian brain. Cellular and Molecular Life Sciences. 63:187-206.

Probst WC, Snyder LA, Schuster DI, Brosius J, Sealfon SC. (1992). Sequence alignment of the G-protein coupled receptor superfamily. DNA and Cell Biology. 11:1-20.

Puelles L, Verney C. (1998). Early neuromeric distribution of tyrosine-hydroxylase immunoreactive neurons in human embryos. J. Comp. Neurol. 394:283-308.

Re S, Dogan AA, Ben-Shachar D, Berger G, Werling AM, Walitza S, Grunblatt E. (2018). Improved Generation of Induced Pluripotent Stem Cells From Hair Derived Keratinocytes - A Tool to Study Neurodevelopmental Disorders as ADHD. Front. Cell. Neurosci. 12:321.

Reavill C, Taylor SG, Wood MD, Ashmeade T, Austin NE, Avenell KY, Boyfield I, Branch CL, Cilia J, Coldwell MC, Hadley MS, Hunter AJ, Jeffrey P, Jewitt F, Johnson CN, Jones DN, Medhurst AD, Middlemiss DN, Nash DJ, Riley GJ, Routledge C, Stemp G, Thewlis KM, Trail B, Vong AK, Hagan JJ. (2000). Pharmacological actions of a novel, high-affinity and selective

human dopamine D3 receptor antagonist, SB-277011-A. Journal of Pharmacology and Experimental Therapeutics. 294:1154-1165.

Ren C, Ding Y, Wei S, Guan L, Zhang C, Ji Y, Wang F, Yin S, Yin P. (2019). G2019S Variation in LRRK2: An Ideal Model for the Study of Parkinson's Disease?. Front Hum Neurosci. 13:306.

Ridray S, Griffon N, Mignon V, Souil E, Carboni S, Diaz J, Schwartz JC, Sokoloff P. (1998). Coexpression of dopamine D1 and D3 receptors in islands of Calleja and shell of nucleus accumbens of the rat: opposite and synergistic functional interactions, European Journal of Neuroscience. 10:1676-1686.

Robinson SW, Jarvie KR, Caron MG. (1994). High affinity agonist binding to the dopamine D3 receptor: chimeric receptors delineate a role for intracellular domains, Molecular Pharmacology. 46:352-356.

Robinson TE, Berridge KC. (2003). Addiction. Annual Review of Psychology. 54:25-53.

Robinson TE, Kolb B. (1999). Alterations in the morphology of dendrites and dendritic spines in the nucleus accumbens and prefrontal cortex following repeated treatment with amphetamine or cocaine. European Journal of Neuroscience. 11:1598-1604.

Robinson TE, Kolb B. (2004). Structural plasticity associated with exposure to drugs of abuse. Neuropharmacology. 47:33-46.

Robinton DA, Daley GQ. (2013). The promise of induced pluripotent stem cells in research and therapy. Nature. 481:295-305.

Russo SJ, Bolanos CA, Theobald DE, DeCarolis NA, Renthal W, Kumar A, Winstanley CA, Renthal NE, Wiley MD, Self DW, Russell DS, Neve RL, Eisch AJ, Nestler EJ. (2007). IRS2-Akt pathway in midbrain dopamine neurons regulates behavioral and cellular responses to opiates. Nature Neuroscience. 10:93-99.

Sanna PP, Berton F, Cammalleri M, Tallent MK, Siggins GR, Bloom FE, Francesconi W. (2000). A role for Src kinase in spontaneous epileptiform activity in the CA3 region of the hippocampus. Proc Natl Acad Sci U S A. 97:8653-8657.

Sarbassov DD, Ali SM, Kim DH, Guertin DA, Latek RR, Erdjument-Bromage H, Tempst P, Sabatini DM. (2004). Rictor, a novel binding partner of mTOR, defines a rapamycin-insensitive and raptor-independent pathway that regulates the cytoskeleton. Current Biology. 14:1296-1302.

Sarti F, Borgland SL, Kharazia VN, Bonci A. (2007). Acute cocaine exposure alters spine density and long-term potentiation in the ventral tegmental area. European Journal of Neuroscience. 26:749-756.

Schmidt U, Beyer C, Oestreicher AB, Rejsert I, Schilling K, Pilgrim C. (1996). Activation of dopaminergic D1 receptors promotes morphogenesisof developing striatal neurons. Neuroscience. 74:453-460.

Schwartz JC, Ridray S, Bordet R, Diaz J, Sokoloff P. (1998). D1/D3 receptor relationships in brain coexpression, coactivation and coregulation. Advances in Pharmacology. 42:408-411.

Searle G, Beaver JD, Comley RA, Bani M, Tziortzi A, Slifstein M Mugnaini M, Griffante C, Wilson AA, Merlo-Pich E, Houle S, Gunn R, Rabiner EA, Laruelle M. (2010). Imaging dopamine D3 receptors in the human brain with positron emission tomography, [11C]PHNO, and a selective D3 receptor antagonist. Biol Psychiatry. 68:392-399.

Seeman P, Van Tol HHM. (1994). Dopamine receptor pharmacology. Trends in Pharmacology Sciences. 15:264-270.

Seki T, Yuasa S, Oda M, Egashira T, Yae K, Kusumoto D, Nakata H, Tohyama S, Hashimoto H, Kodaira M, Okada Y, Seimiya H, Fusaki N, Hasegawa M, Fukuda K. (2010). Generation of induced pluripotent stem cells from human terminally differentiated circulating T cells. Cell Stem Cell. 7:11-14.

Sesack SR, Carr DB. (2002). Selective prefrontal cortex inputs to dopamine cells: implication for schizophrenia. Physiol. Behav. 77:513-517.

Shill HA, Stacy M. (2009). Update on ropinirole in the treatment of Parkinson's disease. Neuropsychiatr Dis Treat. 5:33-36.

Simeone A, Acampora D, Gulisano M, Stornaiuolo A, Boncinelli E. (1992). Nested expression domains of four homeobox genes in developing rostral brain. Nature. 358:687-690.

Simon DT, Kurup S, Larsson KC, Hori R, Tybrandt K, Goiny M, Jager EW, Berggren M, Canlon B, Richter-Dahlfors A. (2009). Organic electronics for precise delivery of neurotransmitters to modulate mammalian sensory function. Nat Mater. 8:742-746.

Simon H, Hornbruch A, Lumsden A. (1995). Independent assignment of antero-posterior and dorso-ventral positional values in the developing chick hind-brain. Curr. Biol. 5:205-214.

Smith AD, Bolam JP. (1990). The neural network of the basal ganglia as revealed by the study of synaptic connections of identified neurons. Trends in Neuroscience Journal. 13:259-265.

Sokoloff P, Giros B, Martres MP, Barthenet ML, Schwartz JC. (1990). Molecular cloning and characterization of a novel dopamine receptor (D3) as a target for neuroleptics. Nature. 347:146-151.

Soldner F, Hockemeyer D, Beard C, Gao Q, Bell GW, Cook EG, Hargus G, Blak A, Cooper O, Mitalipova M, Isacson O, Jaenisch R. (2009). Parkinson's disease patient-derived induced pluripotent stem cells free of viral reprogramming factors. Cell. 136:964-977.

Soliman GA, Acosta-Jaquez HA, Dunlop EA, Ekim B, Maj NE, Tee AR, Fingar DC. (2010). mTOR Ser-2481 Autophosphorylation Monitors mTORC-specific Catalytic Activity and Clarifies Rapamycin Mechanism of Action. Journal of Biological Chemistry. 285:7866-7879.

Specht LA, Pickel VM, Joh TH, Reis DJ. (1981a). Light-microscopic immunocytochemical localization of tyrosine hydroxylase in prenatal rat brain. I. Early ontogeny. J. Comp. Neurol. 199:233-253.

Specht LA, Pickel VM, Joh TH, Reis DJ. (1981b). Light-microscopic immunocytochemical localization of tyrosine hydroxylase in prenatal rat brain. II. Late ontogeny. J. Comp. Neurol. 199:255-276.

Spillantini MG, Schmidt ML, Lee VM, Trojanowski JQ, Jakes R, Goedert M. (1997). Alpha-synuclein in Lewy bodies. Nature. 388:839-840.

Stadtfeld M, Hochedlinger K. (2010). Induced pluripotency: history, mechanisms, and applications. Genes Dev. 24:2239-2263.

Stadtfeld M, Nagaya M, Utikal J, Weir G, Hochedlinger K. (2008). Induced pluripotent stem cells generated without viral integration. Science. 322:945-949.

Stefanova N, Tison F, Reindl M, Poewe W, Wenning GK. (2005). Animal models of multiple system atrophy. Trends Neurosci. 28:501-506.

Stewart E, Kobayashi NR, Higgins MJ, Quigley AF, Jamali S, Moulton SE, Kapsa RM, Wallace GG, Crook JM. (2015). Electrical stimulation using conductive polymer polypyrrole promotes differentiation of human neural stem cells: a biocompatible platform for translational neural tissue engineering. Tissue Eng Part C Methods. 21:385-393.

Sun H, Zhang F, Wang Y, Wang Z, Zhang S, Xu Y, Shi C. (2018). Generation of induced pluripotent stem cell line (ZZUi011-A) from urine sample of a normal human. Stem Cell Res. 29:28-31.

Sunahara RK, Guan HC, O'Dowd BF, Seeman P, Laurier LG, George SR, Torchia J, Van Tol HHM, Niznik HB. (1991). Cloning of the gene for a human dopamine D5 receptor with higher affinity for dopamine than D1. Nature. 350:614-619.

Takahashi J. (2020). iPS cell-based therapy for Parkinson's disease: A Kyoto trial. Regen Ther. 13:18-22.

Takahashi K, Tanabe K, Ohnuki M, Narita M, Ichisaka T, Tomoda K, Yamanaka S. (2007). Induction of pluripotent stem cells from adult human fibroblasts by defined factors. Cell. 131:861-872.

Takahashi K, Yamanaka S. (2006). Induction of pluripotent stem cells from mouse embryonic and adult fibroblast cultures by defined factors. Cell. 126:663-676.

Takahashi K, Yamanaka S. (2016). A decade of transcription factor-mediated reprogramming to pluripotency. Nat Rev Mol Cell Biol. 17:183-193.

Tang M, Miyamoto Y, Huang EJ. (2009). Multiple roles of beta-catenin in controlling the neurogenic niche for midbrain dopamine neurons. Development. 136:2027-2038.

Thomas KR, Capecchi MR. (1990). Targeted disruption of the murine int-1 proto-oncogene resulting in severe abnormalities in midbrain and cerebellar development. Nature. 346:847-850.

Thomson JA, Itskovitz-Eldor J, Shapiro SS, Waknitz MA, Swiergiel JJ, Marshall VS, Jones JM. (1998). Embryonic stem cell lines derived from human blastocysts. Science. 282:1145-1147.

Tiberi M, Jarvie KR, Silvia C, Falardeau P, Gingrich JA, Godinot N, Bertrand L, Yang-Feng TL, Fremeau RT, Caron MG. (1991). Cloning, molecular characterization and chromosomal assignment of a gene encoding a second D1 dopamine receptor subtype: differential expression pattern in rat brain compared with the D1A receptor. Proceedings of the National Academy of Sciences of the USA. 88:7491-7495.

Tieu K. (2011). A guide to neurotoxic animal models of Parkinson's disease. Cold Spring Harb Perspect Med. 1:a009316.

Toulouse A, Sullivan AM. (2008). Progress in Parkinson's disease-where do we stand? Prog. Neurobiol. 85:376-392.

Ulloa F, Briscoe J. (2007). Morphogens and the control of cell proliferation and patterning in the spinal cord. Cell Cycle. 6:2640-2649.

Valjent E, Pages C, Herve D, Girault JA, Caboche J. (2004). Addictive and non-addictive drugs induce distinct and specific patterns of ERK activation in mouse brain. European Journal of Neuroscience. 19:1826-1836.

Van Kampen JM, Eckman CB. (2006). Dopamine D3 receptor agonist delivery to a model of Parkinson’s disease restores the nigrostriatal pathway and improves locomotor behavior. Journal of Neuroscience. 26:7272-7280.

Van Tol HHM, Bunzov JR, Guan H-C, Sunahara RK, Seeman P, Niznik HB, Civelli O. (1991). Cloning of the gene for a human dopamine D4 receptor with high affinity for the antipsychotic clozapine. Nature. 350:610-614.

Vernay B, Koch M, Vaccarino F, Briscoe J, Simeone A, Kageyama R, Ang SL. (2005). Otx2 regulates subtype specification and neurogenesis in the midbrain. J. Neurosci. 25:4856-4867.

Vorel SR, Ashby CR Jr, Paul M, Liu X, Hayes R, Hagan JJ, Middlemiss DN, Stemp G, Gardner EL. (2002). Dopamine D3 receptor antagonism inhibits cocaine-seeking and cocaine-enhanced brain reward in rats. J. Neurosci. 22:9595-9603.

Wakabayashi K, Tanji K, Odagiri S, Miki Y, Mori F, Takahashi H. (2013). The Lewy body in Parkinson's disease and related neurodegenerative disorders. Mol Neurobiol. 47:495-508.

Wang H, Doering LC. (2012). Induced pluripotent stem cells to model and treat neurogenetic disorders. Neural Plasticity. 346053.

Wang M, Ling KH, Jie Tan J, Lu CB. (2020). Development and Differentiation of Midbrain Dopaminergic Neuron: From Bench to Bedside. Cells. 9:1489.

Warren L, Manos PD, Ahfeldt T, Loh YH, Li H, Lau F, Ebina W, Mandal PK, Smith ZD, Meissner A, Daley GQ, Brack AS, Collins JJ, Cowan C, Schlaeger TM, Rossi DJ. (2010). Highly efficient reprogramming to pluripotency and directed differentiation of human cells with synthetic modified mRNA. Cell Stem Cell. 7:618-630.

Wassarman KM, Lewandoski M, Campbell K, Joyner AL, Rubenstein JL, Martinez S, Martin GR. (1997). Specification of the anterior hindbrain and establishment of a normal mid/hindbrain organizer is dependent on Gbx2 gene function. Development. 124:2923-2934.

Weber M, Chang W, Breier M, Ko D, Swerdlow NR. (2008). Heritable strain differences in sensitivity to the startle gating-disruptive effects of D2 but not D3 receptor stimulation. Behav Pharmacol. 19:786-795.

Weiss HD, Marsh L. (2012). Impulse control disorders and compulsive behaviors associated with dopaminergic therapies in Parkinson disease. Neurol Clin Pract. 2:267-274.

Wernig M, Lengner CJ, Hanna J, Lodato MA, Steine E, Foreman R, Staerk J, Markoulaki S, Jaenisch R. (2008). A drug-inducible transgenic system for direct reprogramming of multiple somatic cell types. Nat Biotechnol. 26:916-924.

Whone AL, Watt RL, Stoessl AJ, Davis M, Reske S, Nahmias C, Lang AE, Rascol O, Ribeiro MJ, Remy P, Poewe WH, Hauser RA, Brooks DJ. (2003). Slower progression of Parkinson's disease with ropinirole versus levodopa: the REAL-PET study. Ann. Neurol. 54:93-101.

Wise RA, Bozarth MA. (1987). A psychomotor stimulant theory of addiction. Psychology Review. 94:469-492.

Yan Q, Rosenfeld RD, Matheson CR, Hawkins N, Lopez OT, Bennett L, Welcher AA. (1997). Expression of brain-derived neurotrophic factor protein in the adult rat central nervous system. Neuroscience. 78:431-448.

Yan Y, Yang D, Zarnowska ED, Du Z, Werbel B, Valliere C, Pearce RA, Thomson JA, Zhang S. (2005). Directed differentiation of dopaminergic neuronal subtypes from human embryonic stem cells. Stem Cells. 23:781-790.

Yang S, Boudier-Revéret M, Jin Choo Y, Cheol Chang M. (2020). Association between Chronic Pain and Alterations in the Mesolimbic Dopaminergic System. Brain Sciences. 10:701.

Ye W, Shimamura K, Rubenstein JL, Hynes MA, Rosenthal A. (1998). FGF and Shh signals control dopaminergic and serotonergic cell fate in the anterior neural plate. Cell. 93:755-766.

Yin Y, Hua H, Li M, Liu S, Kong Q, Shao T, Wang J, Luo Y, Wang Q, Luo T, Jiang Y. (2016). mTORC2 promotes type I insulin-like growth factor receptor and insulin receptor activation through the tyrosine kinase activity of mTOR. Cell Research. 26:46-65.

Yu J, Hu K, Smuga-Otto K, Tian S, Stewart R, SlukvinI I, Thomson JA. (2009). Human induced pluripotent stem cells free of vector and transgene sequences. Science. 324:797-801.

Yu J, Vodyanik MA, Smuga-Otto K, Antosiewicz-Bourget J, Frane JL, Tian S, Nie J, Jonsdottir GA, Ruotti V, Stewart R, Slukvin II, Thomson JA. (2007). Induced pluripotent stem cell lines derived from human somatic cells. Science. 318:1917-1920.

Zahm DS. (1992). Subsets of neurotensin-immunoreactive neurons revealed following antagonism of the dopamine-mediated suppression of neurotensin immunoreactivity in the rat striatum. Neuroscience. 46:335-350.

Zahoor I, Shafi A, Haq E. (2018). Pharmacological Treatment of Parkinson's Disease. In: Stoker TB, Greenland JC, editors. Parkinson's Disease: Pathogenesis and Clinical Aspects [Internet]. Brisbane (AU): Codon Publications. Chapter 7.

Zarate CA Jr, Payne JL, Singh J, Quiroz JA, Luckenbaugh DA, Denicoff KD, Charney DS, Manji HK. (2004). Pramipexole for bipolar II depression: a placebo-controlled proof of concept study. Biol. Psychiatry. 56:54-60.

Zhang X, Mi J, Wetsel WC, Wetsel WC, Davidson C, Xiong X, Chen Q, Ellinwood EH, Lee TH. (2006). PI3 kinase is involved in cocaine behavioral sensitization and its reversal with brain area specificity. Biochemical and Biophysical Research Communications. 340:1144-1150.

Zhou T, Benda C, Dunzinger S, Huang Y, Ho JC, Yang J, Wang Y, Zhang Y, Zhuang Q, Li Y, Bao X, Tse HF, Grillari J, Grillari-Voglauer R, Pei D, Esteban MA. (2012). Generation of human induced pluripotent stem cells from urine samples. Nat Protoc. 7:2080-2089.